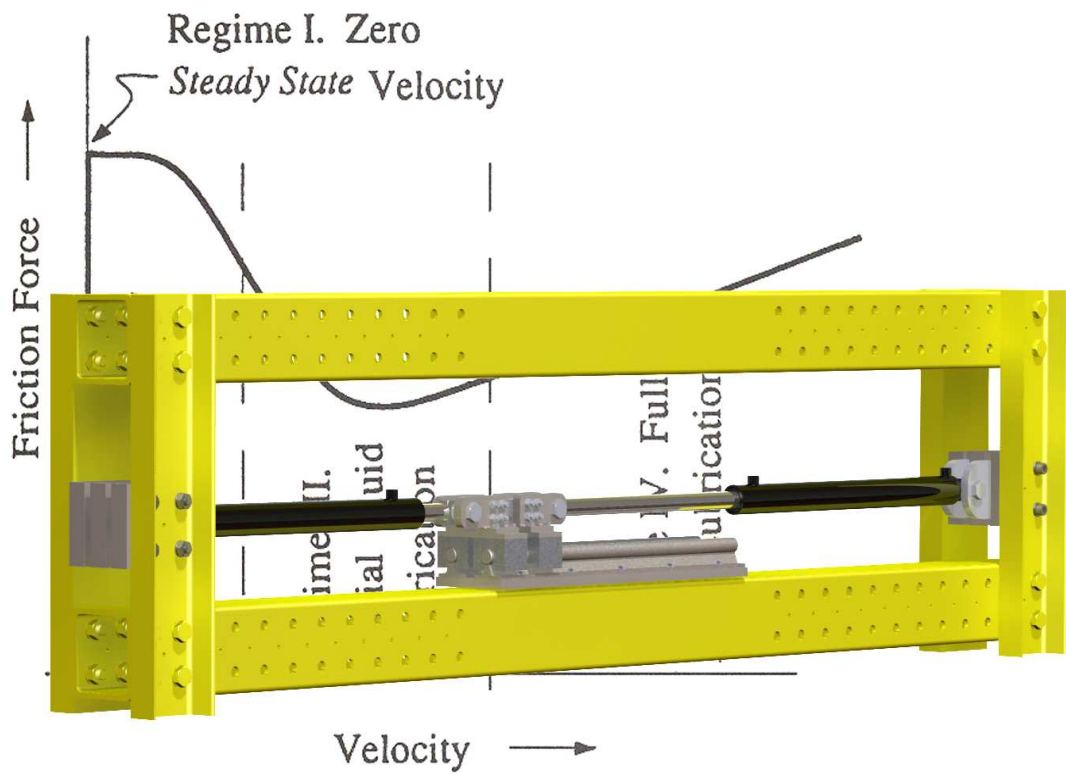


Design and Construction of a Facility for Testing Friction in Hydraulic Cylinders



Daniel Henriksen
10th Semester
Electro-Mechanical System Design
Aalborg University
Deadline: 6th January 2009



Resumé

This thesis treats the phenomenon of friction and how it affects hydraulic servo systems. A short review of the problems which friction induces in servo systems was given along with a review of the characteristics of the friction phenomena and how these can be mathematically modelled. From this review, the motivation of the thesis was clarified and the initiating problem was stated as: "What is the friction in a hydraulic cylinder?".

In order to experimentally investigate the friction in a hydraulic cylinder a suitable test facility was necessary. This test facility had to be constructed as none existed beforehand. A number of concepts were developed which suggested how the cylinder testing could be performed. A concept was chosen from which the test facility was developed. A concept called *Load-by-Cylinder* was chosen. *Load-by-Cylinder* was assessed to contribute with the greatest experimental flexibility for testing. The concept was based on using a hydraulic cylinder to provide the load acting on the cylinder to be tested. This concept results in a more complicated system, with regard to the necessary components and measurements, but the greatest advantage is a more flexible test facility with a load that can be controlled and manipulated quite accurately. From there on, a test structure was designed acting as the base of the test facility. A design of the test structure was proposed from a set of initial requirements. These requirements were related to certain parameters of the hydraulic system, and they were:

- Maximum cylinder stroke: 500 *mm*
- Maximum piston velocity: 0.5 *m/s*
- Maximum flow: 50 *l/min*
- Maximum hydraulic pressure: 200 *bar*

From these requirements a new set of requirements, which were applicable in the design of the test structure, was derived. This new set of requirements were related to the forces generated by the hydraulics, which the test structure should withstand, and a dimensional requirement of the structure with regards to cylinder lengths, strokes and diameters. In order to ensure that the design was satisfactory, a structural analysis was carried out. The analysis proved the design to be sufficient, and it was finalised in drawings and sent on to be processed in the work shop.

Next, the hydraulic system was designed. A cylinder for generating load was chosen, and a cylinder to be tested was found. Furthermore, servovalves of the kind MOOG D633, were chosen for each hydraulic subsystem (Load- and Test-subsystem). Thereafter, a fixed displacement pump was chosen which could deliver the necessary flow. This pump was configured with an appropriate pressure-relief valve achieving an ideally constant supply pressure.

Finalizing the hydraulic design, led on to the design of the experimental setup. The earlier analysis of the different concepts made it clear, what was required in the setup, for it to be capable of running the tests required for determining the friction. In order to run tests for determining friction, the motion of the test cylinder must be controlled very accurately. As mentioned, the load acting on the test cylinder is generated by another hydraulic cylinder. In order to take advantage of the load

cylinders ability to generated a wide range of forces, the output of this cylinder had to be controlled as well. This implied, that a control system had to be implemented in the experimental setup. Both determining the friction and implementing the controllers, required measuring different states in the system. The friction was not measured directly, but instead determined from measurements of the fluid pressure in the cylinder chambers, load force and acceleration of mass. In addition, the control strategy consisted of primarily feedback control loops which required measurements of velocity for the test-subsystem and force for the load-subsystem. This lead to a experimental setup consisting of a realtime PC running LabVIEW for data acquisition (input) and control signal generation (output). Pressure transducers, an accelerometer, a force sensor (loadcell) along with a position sensor (incorporated in the load cylinder) were the measuring devices of the system. An appropriate loadcell satisfying the requirements was not found, whereby a loadcell was designed for this special application. Hence, the system was now defined.

In order to make the system capable of running the required friction testing, the necessary feedback controls were designed. This was done by mathematically describing the dynamics of the system, from which a linear model was created. This model was used to design PI-controller with velocity feedback for the test-subsystem while a PI-controller with force feedback and a velocity feed-forward compensation was designed for the load-subsystem. The controllers were designed to make the systems as fast and accurate as possible. A specific requirement was to make the load-system 5-10 times faster than the test-system. Meeting this requirement, would ensure robustness of the load-system towards the velocity disturbances from the test-system. Furthermore, stability and bandwidth were analyzed using the linear model.

A friction test, with the purpose of determining the parameters of a specific friction model, should have been a part of the report. The result of the test, would have been an attempt at establishing a valid friction model of the friction in the test cylinder. Unfortunately, the design of the test structure was finalised too late in project, for it to be completed in the work shop, before deadline. Too compensate for this, setup of the test facility and execution of the experiments will be done after the deadline when the test structure has been completed. Hopefully, this will make the results available to be presented along with the presentation of the project.

Title: Design and Construction of a Facility for Testing Friction in Hydraulic Cylinders
Semester: Electro-Mechanical System Design, 10th semester
Theme: Friction and Servo Systems
Project period: 18th of September 2009 - 6th of January 2010
ECTS: 30
Supervisors: Torben O. Andersen and Henrik C. Pedersen

SYNOPSIS:

This project deals with friction in hydraulic cylinders. The friction phenomenon is reviewed in a control context. A friction test facility consisting of a test support structure, hydraulic system and a experimental setup is designed and constructed. The hydraulic system is described mathematically in preparation for modelling. At first, a model with a high degree of detail, but of a non-linear character is created. This model is linearised leading to a linear model of the system. The linear model is used in the design of an appropriate control system which enables accurate control of both the velocity of the test cylinder and the force of the load cylinder, which is required for testing. Feedback control along with a PI-controller is used on both subsystems to generate the desired performance. Furthermore, a velocity feed-forward compensation is designed for the load-servo to further enhance the performance. Because of delays, it is not possible to complete the construction of the test facility before the deadline. This means, no practical system exists for verifying models and control designs, as well as performing friction tests. Therefore, no experimental results can be presented as of this time.

Daniel Henriksen

Number printed: 4 pcs.
Number of pages: 79 pages
Appendices: 5 pages, Drawing folder + CD



Preface

This report, documents the work completed, from mid September 2009 till start January 2010, in the Master's Thesis by Daniel Henriksen during the 10th semester of the Electro-Mechanical Systems Design (EMSD) at the University of Aalborg (AAU). The Master's thesis is the final project which finishes off the ten semesters of projects and courses on the way to become a Masters of Science in Engineering.

By completing and submitting this project, I trust and hope it will qualify me to graduate from AAU with a Master's in Mechanical Engineering.

The subject of this thesis was proposed to me by my advisors, Torben O. Andersen and Henrik C. Pedersen. As will soon be apparent, the main subject of this thesis is *Friction* and *Hydraulics*. The main motivation is an investigation of friction in hydraulic cylinders. But before being capable of pursuing this idea, there had to be established a basis, a facility to work from. This circumstance widened the scope of this thesis as preliminary tasks, such as designing and constructing the necessary test facilities had to initially be completed. Therefore, the work in this thesis covers a wide number of engineering subjects which are all documented. Unfortunately, a lack of time and an incompleted test-facility before the submissions date, have meant that an actual experimental investigation of friction in hydraulic cylinders have not been completed, but almost everything in order to do so has been prepared, which is documented by this report.

The time leading up to this point has been filled with many hours and late nights of studying and working on the "project". Since I began this education back in September 2003, I have many times felt like quitting. Along with almost every semester a crisis emerged at some point, but luckily, every time things got better before my aspirations to become an engineer would be strangled. A lot sacrifices and comprimises have been made along the way, but now almost finished and looking back, I'm happy and proud that I got this far. This, I not only owe to my own determination but also to the people around me, who have helped and supported me along the way.

Therefore, I would like to thank the teachers I've had along the way who have inspired me in every kind of way, my fellow students who have helped me stay awake in class, my project group members for good discussions and laughs about everything else than engineering, the Danish Study System for the help i received to study in Hawaii at the University of Hawaii and, last but not least, my friends and family for being there.

Practical information regarding this report follows. Referencing is done using the well known *Harvard Method*. A CD containing various material accompanies the report. The CD will contain data sheets, SIMULINK and SolidWorks models, a digital version of the report and a collection of articles about *Friction* in *hydraulics* and *controls* among other things. The literature of friction is quite extensive in *Tribology* and *Controls* and a wide array of articles and studies are out there to be found.

- Daniel Henriksen, *January 2009*



Contents

1	Introduction	7
1.1	Friction modelling	8
1.2	Motivation and project description	16
1.3	Problem formulation and definition	17
1.4	Overall system requirements and definitions	17
2	Concepts for determining the friction in hydraulic cylinders	19
2.1	Issues of determining friction in hydraulic cylinders	19
2.2	Concepts	20
2.3	From concept to design - continuing work	26
3	Design of the mounting frame	29
3.1	Design proposition	30
3.2	Structural analysis of the frame	32
3.3	Final design	34
4	Hydraulic system and experimental setup	37
4.1	Hydraulic system design	37
4.2	Experimental setup	38
5	Dynamic model of the fluid-mechanical system	43
5.1	Modelling of Cylinders	44
5.2	Servo valve	46
5.3	Simulation model using SIMULINK	49

CONTENTS

6	Linear model of the system	53
6.1	Linearisation of the equations of the system	53
6.2	Block diagram and transfer functions	56
6.3	Operating point of linearisation	56
7	Control system analysis and design	61
7.1	Control strategy	62
7.2	Velocity-servo	63
7.3	Force-servo with velocity feedforward compensation	70
7.4	Stability analysis	76
7.5	Test of the controllers in the non-linear model	78
8	Conclusion	83
A	Load analysis	87
A.1	Vertical beam	87
A.2	Lower beam	89
B	Hydraulic eigenfrequency of a differential cylinder	91

Introduction

This chapter will be an introduction to this thesis. At first, a short introduction will be given to the initiating problems whereafter a review of friction in controls and modelling of friction will be carried out. At last, the thesis will be formulated and defined with respect to the previous sections.

Hydraulic actuators are used in a lot of different mechanical applications like wind mills, industrial production such as robots and processing machinery, construction machines such as cranes and excavators, just to name a few. The term *Hydraulic actuators* covers a group of components in machine design which can create a rotating or linear motion by utilizing a pressurised fluid. Actuators generating rotation are called motors while linear hydraulic actuators are called cylinders. The focus in this thesis will be on hydraulic cylinders.

Hydraulic actuators are widely applied in hydraulic servo-systems, which is a system that is made up of several individual hydraulic components such as pump, valves, actuators, sensors and the connecting elements in-between. These components are interconnected so they can perform a pre-defined task through the hydraulic transfer [Jelali and Kroll, 2003].

The biggest advantage of fluid power is the power to size and weight ratio when compared to other types of power-systems. The generation of a wide range of forces and torques in the same system makes direct drive constructions possible and thereby avoids the use of gearboxes and such, which simplifies the construction and reduces the chance of breakdown due to wear in the power transmitting components.

As with most mechanical systems, friction is a factor that has to be dealt with in hydraulics. The greatest source of friction in a hydraulic system is most often the hydraulic actuator which delivers the output. As with hydraulic cylinders the primary friction is caused by the seals (if the cylinder is not sealless) around the piston and rod. This friction leads to wear of the cylinder affecting life expectancy while at the same time complicating the process of mathematically modelling the system. For control purposes a mathematical modelling of the hydraulic servo-systems is often required which demands knowledge of the phenomena occurring and the parameters of the system. A linear system is always preferred as this makes the modelling and control analysis easier but the presence of friction creates non-linear characteristics. Thus, friction complicates the task of modelling and applying controls to the system. Furthermore, friction has great influence on the performance of a given system and leads to problems such as tracking errors, instability at low velocities, imprecise force control and undesired stick-slip motion [de Wit et al., 1995] causing limit cycles. As it is impossible to totally remove the friction, by mechanical design, in any system which has contacting surfaces controls can be used to compensate for the effects of friction. In order to do this, it is required to either know the friction directly or be able to predict it mathematically in order to design a compensation. Predicting the friction by mathematical approximations can be a difficult task, and this is where friction models are very useful. By having a good model of the friction in the servo-system, the friction forces can be estimated and compensated for, by the control. Therefore, it is important to have a good model of the friction so a satisfying performance of the system can be achieved.

As investigation of the friction phenomenon is the main motivation for this work, both the nature

1 Introduction

of the friction phenomena and ways to describe it mathematically will be further reviewed in the following sections.

1.1 Friction modelling

This section will give an introduction to the friction phenomena and present methods useful in the mathematical modelling of friction.

As mentioned earlier the derivation of a friction model, which is a good approximation of the actual friction in the system, is important in order to secure a good performance of the servo system. Different methods to model friction have been proposed in the literature. Some models are very detailed and try to capture most of the effects and properties of friction while the more classic models describe only the most characteristic properties of the frictional phenomena. Friction is a general phenomena that is always present in mechanical systems in the physical interface between two surfaces in contact [Olsson et al., 1997]. This property, results in many of the existing friction models being very general whereby they are usable on a wide variety of applications. In some cases though, a model might not be appropriate or modification is necessary in order to it be suitable.

1.1.1 Friction characteristics

The total friction in a given situation can be divided up in different types of friction which are characterized by the velocity state at which they act and their dependence of this state. Furthermore, certain phenomenons exist which characterize the nature of friction. These frictions and effects according to [Armstrong-Hélouvy, 1991] are:

Static Friction (Sticktion) The force necessary to initiate motion from rest.

Kinetic Friction Friction independent of the magnitude of velocity. Also referred to as Coulomb friction.

Viscous Friction Friction directly dependent of velocity as this friction is zero at zero velocity.

Dahl Effect A friction phenomenon which arises from the elastic deformation of bonding sites between two surfaces which are locked in static friction.

Stribeck Effect or Stribeck Friction A phenomenon occurring when using fluid lubrication where the friction is decreasing with increasing velocity at low velocities.

Break-away Force The amount of force required to overcome static friction.

In figure 1.1-1.1 three different friction models are presented. These friction models are made up of three different combinations of the above mentioned friction components.

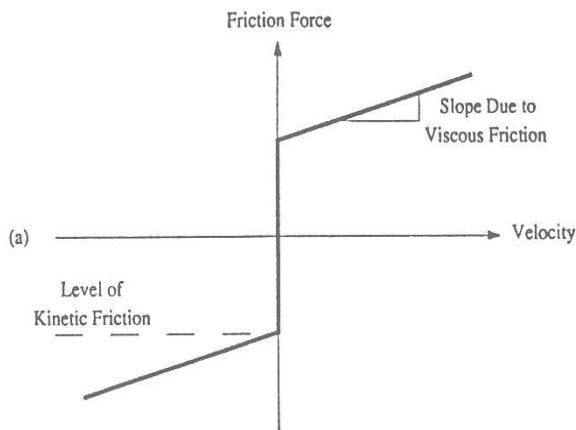


Figure 1.1: Kinetic and Viscous friction. [Armstrong-Hélouvy, 1991]

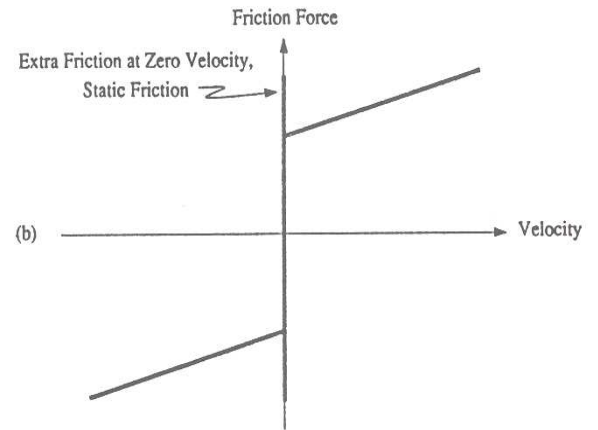


Figure 1.2: Static, Kinetic and Viscous friction combined.

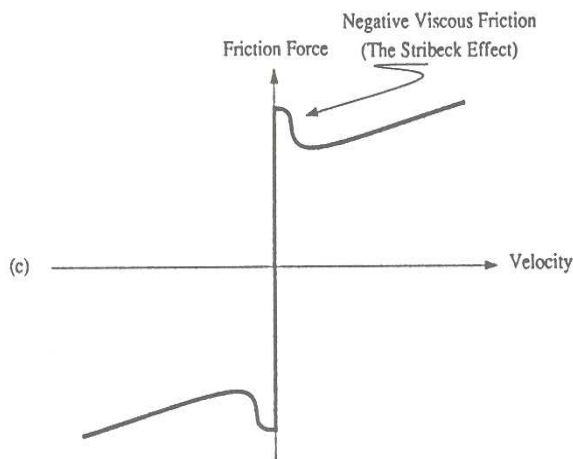


Figure 1.3: Kinetic and Viscous friction with the Stribeck friction.

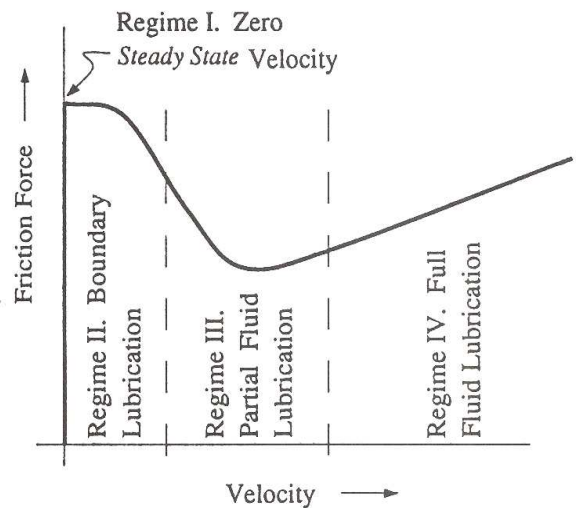


Figure 1.4: The generalized Stribeck curve illustrating frictions dependence of velocity for low velocity. [Armstrong-Hélouvy, 1991]

As seen in figure 1.1-1.3, friction is considered a function of velocity. As mentioned earlier the kinetic friction is independent of velocity and always present. On the contrary, the viscous friction is proportional to the velocity and it occurs in fluid lubricated interfaces (figure 1.1). As figure 1.2 illustrates, in some cases the break-away force, which is the force necessary to initiate motion, is larger than the force needed to sustain motion because of the static friction. The static friction and the Dahl effect are closely correlated as the Dahl effect is a consequence of the static friction and the asperities of the surfaces in the interface. Static friction is the greatest cause to stick-slip motion which is explained later. Another consequence of correlation between the Dahl effect and the static friction is position-dependence of the static friction. An in depth explanation of the Dahl effect and static friction can be found in [Armstrong-Hélouvy et al., 1994]. The Stribeck effect is illustrated in figure 1.3 which suggests that the drop from the static friction doesn't happen instantaneously

1 Introduction

whereby the friction decreases with increasing velocity for low velocities. The Stribeck curve in figure 1.4 gives a closer look at friction at low velocity and show the three moving regimes, of the four in total, which contribute to the dynamics a controller confronts as the system accelerates away from zero velocity [Armstrong-Hélouvy, 1991].

The Stribeck curve is a representation of the friction in a system which is lubricated with grease or oil, as is the case in most mechanical systems. The curve illustrates how the different regimes of lubrication change according to velocity and how this affects the friction. The lubrication regimes provides a physical explanation for the friction phenomena, but this will not be covered in depth here. For more information see [Armstrong-Hélouvy, 1991; Armstrong-Hélouvy et al., 1994]

From figure 1.1-1.4 it is apparent that all the different kinds of friction, except viscous, are discontinuous when the velocity is zero. This property along with the Stribeck effect causes non-linearity and the consequences of this, with respect to servo systems, will be discussed in the following section.

1.1.2 Friction in servo systems

Upper and lower bounds

Friction brings both positive and negative traits into a servo system. Friction can bring damping into a system which otherwise would be unstable. This damping is provided at all frequencies both under and over the bandwidth of the control. Besides playing a role in the dynamics of the system, friction affects the speed and power and thereby limiting the overall performance. Most often systems are assessed at their upper performance bounds with regards to maximum speed, maximum force and so on. Just as much as friction affects the upper bounds of performance, it affects the lower bounds, as very small displacements and corresponding low velocities can be unobtainable because of friction and its non-linear nature at low velocity. The non-linearity causes a periodic process of sticking and slipping motion called stick-slip which limits the lower bounds with regards to minimum achievable displacement and minimum sustainable velocity. [Armstrong-Hélouvy, 1991]

Hunting

Stick-slip may arise during low speed motion with any control design and another consequence of the non-linearity of friction, when using integral control, is a phenomenon called *Hunting*. Hunting is a integral-induced periodic oscillation around the reference position. According to [Tung and Wu, 2002], the static and coulomb friction form a dead zone in the system because of the earlier mentioned *break-away force*, which is the force necessary to create motion. Integral control eliminates the steady state error caused by the dead zone, but it might lead to hunting as the friction becomes larger at low velocities, as illustrated by the Stribeck curve (figure 1.4). The increased friction at low velocity might cause the mechanism to stop before reaching the desired point. As the error accumulates in the feedback control system the mechanism will start moving when the break away force is exceeded. This motion reduces the friction from the maximum static friction to a sliding level and the overdriven control input results in overshoot whereby the desired point is passed and the system has to reverse. This repeats and the stick and slide motions results in oscillations around the desired position.

Frictional Lag

So far, friction have been assumed to have a steady dependence of velocity as shown by the Stribeck curve. It has been assumed that if the velocity changes then the friction will change simultaneously. Though, experiments by [Hess and Soom, 1990] have shown that there is a lag in the change of the friction, which is designated as frictional lag. Frictional lag is illustrated in figure 1.5.

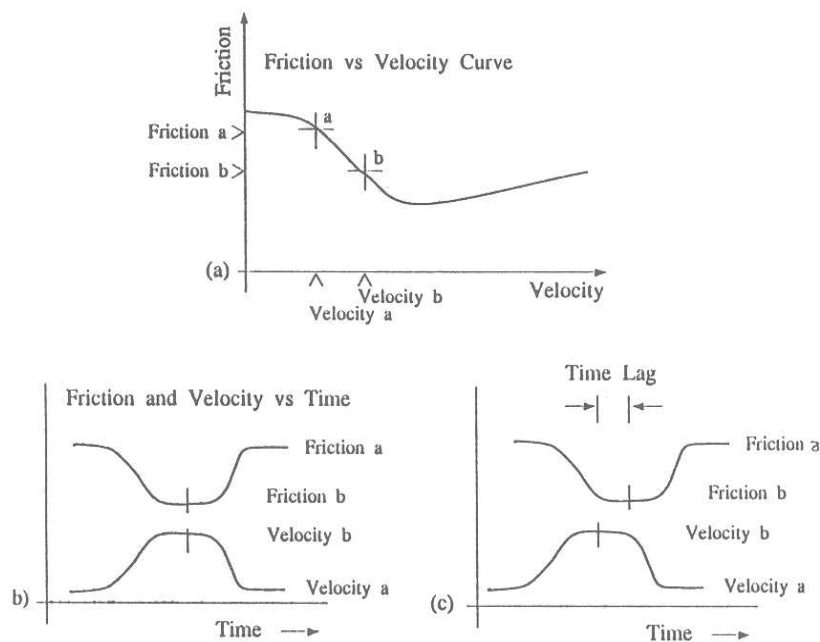


Figure 1.5: a and b) Friction as a function of velocity (the Stribeck curve) independent of time; c) The friction lags behind as the velocity changes. [Armstrong-Hélouvy, 1991]

Furthermore, frictional lag creates hysteresis, which is the separation between the friction levels during acceleration and deceleration. The hysteresis loop is shown in figure 1.6 and it is greatly affected by the oscillatory frequency, as the hysteresis is greatest when the oscillating period is short relative to the frictional lag. The existence of frictional lag and hysteresis indicates a necessity for dynamic friction models which describe these phenomenons. [Armstrong-Hélouvy, 1991; Olsson et al., 1997]

Mechanical considerations and experimental measurement of friction

The total friction in a given system may be the result of similar friction levels in interfaces between the parts which makes up the mechanical system. If that is the case, it can be impossible to separate the different contributions and an overall friction model is necessary to describe the friction in the entire mechanism. In other cases, the primary source of friction might originate from a single interface as can be the case when using a hydraulic cylinder.

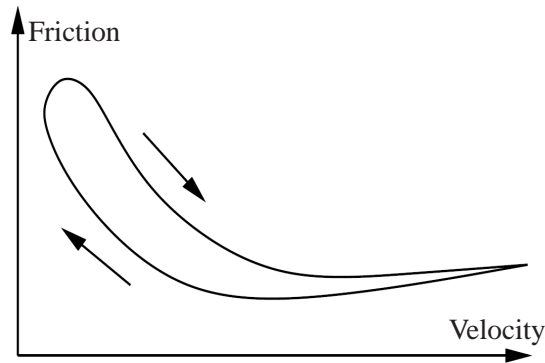


Figure 1.6: The friction-velocity hysteresis loop reported in [Hess and Soom, 1990]. The shorter the period of the oscillation the wider the loop. [Olsson et al., 1997]

Besides locating the main contributors of friction in a system before establishing the friction model, experiments are often necessary in order to determine the parameters of the model. For some systems the friction varies depending on position and direction whereby it is necessary to perform experiments in both directions and for many positions in order to increase the accuracy [Armstrong-Hélouvry, 1991].

1.1.3 Mathematical models of friction

This section will give a review of both classic and modern friction models. The purpose of the mathematical friction models is to capture and describe the effects of friction with the necessary degree of detail, for it to be a valid and useful representation. Many different friction models exist. There are the classic models which are characterized by being simple but with a minor degree of detail. Then there are the more advanced static and dynamic models which give more detailed descriptions by including the Stribeck effect and other phenomena. This section will present the classic models for the static friction, Coulomb friction and Viscous friction, and the advanced static models of *Armstrong's seven parameter model* [Armstrong-Hélouvry et al., 1994], the exponential model [Bo and Pavelescu, 1982] and the dynamic LuGre model [de Wit et al., 1995].

Classical models

The classical models of friction deal with describing the Coulomb friction, viscous friction and the static friction. A combination of these three are the most commonly used friction models in controls as they are described by simple expressions. Especially the Coulomb friction has often been used for friction compensation. The general notion for the classical friction models is that friction opposes motion. Furthermore, the Coulomb frictions magnitude is independent both the velocity, v , and surface area. The Coulomb friction is described by,

$$F_C = \mu F_N \text{sgn}(v) \quad (1.1)$$

where F_C is the Coulomb friction, F_N is the normal force and μ is the coefficient of friction. The model of (1.1) does not specify Coulomb friction for zero velocity where the friction force can be anything in the interval between $-F_C$ and F_C . Therefore the complete model for the Coulomb friction is:

$$F_C = \begin{cases} -F_C & \text{if } v > 0 \\ [-F_C, F_C] & \text{if } v = 0 \\ F_C & \text{if } v < 0 \end{cases} \quad (1.2)$$

The viscous friction is dependent of the velocity both in magnitude and direction. The expression is derived from theory of hydrodynamics and is normally given as in (1.4).

$$F_v = f_v v \quad (1.3)$$

Where F_v is the viscous friction force, f_v is the viscous friction parameter and v is the velocity.

A better fit to experimental data is sometimes found when using the expression in (1.4).

$$F_v = f_v |v|^{\delta_v} \text{sgn}(v) \quad (1.4)$$

Where δ_v depends on the geometry of the application.

The static friction occurs when at rest and is therefore clearly not a function of velocity. Instead it is modeled using the external force as shown in (1.5).

$$F_s = \begin{cases} F_{ex} & \text{if } v = 0 \text{ and } |F_{ex}| < F_s \\ F_s \text{sgn}(F_{ex}) & \text{if } v = 0 \text{ and } |F_{ex}| \geq F_s \end{cases} \quad (1.5)$$

F_S is the static friction while F_{ex} is the external force. The expressions in (1.1), (1.3) and (1.5) are the classical friction components and they are combined in different ways to establish an overall model. Any combination of these components are referred to as a classical model and the combination of all three is illustrated in figure 1.2. The classical models are simple, but not very detailed in their description as effects like the Stribeck friction, frictional lag and hysteresis, is not captured at all. This limits the models applicability at zero and low velocity where friction is recognised to be most destabilizing [de Wit et al., 1995]. In order to capture the Stribeck effect, and provide a general description, more advanced static friction models are needed. Attempts at this are presented hereafter along with the LuGre model, which is a dynamic friction model that includes rate dependent friction phenomena like frictional lag, hysteresis and varying break-away forces. [Olsson et al., 1997]

1 Introduction

Armstrong's Seven Parameter Model

Armstrong's model from [Armstrong-Hélouvy et al., 1994] is made up of two expressions, one for when in the state of sticktion, and one describing the sliding regime. The model consists of seven parameters represented in the expressions (1.6) and (1.7).

Not sliding (Pre-sliding displacement):

$$F_f(x) = -k_t x \quad (1.6)$$

Sliding (Coulomb + viscous + Stribeck curve friction with frictional memory):

$$F_f(\dot{x}, t) = - \left(F_C + F_v |\dot{x}| + F_s(\gamma, t_2) \frac{1}{1 + \left(\frac{\dot{x}(t - \tau_L)}{\dot{x}_s} \right)} \right) \text{sgn}(\dot{x}) \quad (1.7)$$

Rising static friction (friction level at breakaway):

$$F_s(\gamma, t_2) = F_{s,a} + (F_{s,\infty} - F_{s,a}) \frac{t_2}{t_2 + \gamma} \quad (1.8)$$

Where,

$F_f(\cdot)$:	the instantenous friction force
F_C :	the Coulomb friction force
F_v :	the viscous friction force
F_s :	magnitude of the Stribeck friction (frictional force at breakaway is $F_C + F_s$)
$F_{s,a}$:	magnitude of the Stribeck friction at the end of the previous sliding period
$F_{s,\infty}$:	magnitude of the Stribeck friction after a long time at rest (with a slow application of force)
k_t :	tangential stiffness of the static contact
\dot{x}_s :	characteristic velocity of the Stribeck friction
τ_L :	time constant of frictional memory
γ :	temporal parameter of the rising static friction
t_2 :	dwel time, time at zero velocity

As the model consists of two expressions, a logical element requiring another eighth parameter is presumably necessary, if the model is to be implemented. Compared to the classical models, this models captures the Stribeck effect but in contrast has a lot of parameters which must be determined or estimated. For approximate ranges for the parameters of the model see [Armstrong-Hélouvy et al., 1994].

The Exponential Model

The Exponential friction model appears often in friction literature and is mentioned by [Armstrong-Hélouvy, 1991; Bo and Pavlescu, 1982; Olsson et al., 1997; Putra, 2004] among others. The exponential model does not require much explanation as it is a straight forward empirical expression which relates friction and velocity, \dot{x} , as shown in equation (1.9).

$$F_f(\dot{x}) = F_C + (F_s - F_C)e^{-(\dot{x}/\dot{x}_s)^\delta} + F_v\dot{x} \quad (1.9)$$

Where,

$F_f(\cdot)$:	the velocity dependent friction force
F_C :	the minimum level of the Coulomb friction force
F_v :	the viscous friction parameter
F_s :	the level of the static friction
\dot{x}_s :	empirical parameter
δ :	empirical parameter

For the value of δ , Bo and Pavlescu [Bo and Pavlescu, 1982] found it ranging from 0.5-1, Armstrong [Armstrong-Hélouvy, 1991; Armstrong-Hélouvy et al., 1994] uses $\delta = 2$, while Tustin [Tustin, 1947] suggests $\delta = 1$. The exponential model is static, as it is a mathematical representation of the Stribeck curve, whereby the friction is a function of the steady state velocity. It captures the Stribeck effect, but it lacks descriptions of dynamical phenomena like frictional lag.

The LuGre Model

The LuGre model [de Wit et al., 1995] is a dynamic model which captures the Stribeck effect as well as rate dependent effects such as frictional lag, hysteresis and varying break-away forces. The LuGre model is established by assuming the contact between the surfaces of two rigid bodies to be like that of elastic bristles, as shown in figure 1.7.

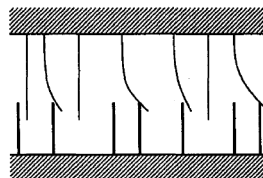


Figure 1.7: The interface of two surfaces in contact is modeled like bristles in contact to simulate the surface asperities. For simplicity the lower bristles are shown as rigid while the upper are elastic. [de Wit et al., 1995]

If the displacing force is sufficiently large a number of bristles will deflect enough to cause slipping. This phenomenon is quite random due to the irregularity of the surfaces. In the LuGre model the surface irregularities are neglected and the model is instead based on a average behaviour of the bristles. The average bristle deflection is denoted by z and modeled by equation (1.10).

1 Introduction

$$\frac{dz}{dt} = v - \frac{|v|}{g(v)}z \quad (1.10)$$

v is the relative velocity between the two surfaces. The function g is positive and depends on factors such as material properties, lubrication and temperature. g is not necessarily symmetric which makes it possible to capture direction dependent behavior. The bending of the bristles results in a friction force F , which is described by (1.11).

$$F = \sigma_0 z + \sigma_1 \frac{dz}{dt} + \sigma_2 v \quad (1.11)$$

σ_0 is the stiffness, σ_1 is a damping coefficient and σ_2 is the viscous friction parameter. The function $\sigma_0 g + \sigma_2 v$ can be determined by measuring steady state friction force when the velocity is held constant. A good approximation of the Stribeck effect is given by the parameterization of g in (1.12).

$$\sigma_0 g(v) = F_C + (F_s - F_C)e^{-(v/v_s)^2} \quad (1.12)$$

F_C is the level of the Coulomb friction, F_s is the level of the static friction and v_s is the Stribeck velocity. This makes the model characterized by the six parameters: σ_0 , σ_1 , σ_2 , F_C , F_s and v_s .

With the presentation of the LuGre model the mathematical modelling of friction has been concluded and this introduction will be finished off with the motivation, formulation and definition of the thesis.

1.2 Motivation and project description

The motivation for this project, comes from the desire to be able to design and implement better control in hydraulic servo systems which incorporates hydraulic cylinders. As mentioned earlier, hydraulic cylinders can be a great source of friction, which in most servo systems causes the performance to suffer. In the future, requirements to the performance of servo systems will only be higher with regards to performance parameters such as precision, stability and energy consumption. In order to insure the competitiveness of hydraulic servo systems every aspect is worth investigating. At the moment, friction is one of the greatest challenges when it comes too fulfilling the requirements. At present time, friction in most applications are modelled using simple classical models which provides a low degree of detail and a poor approximations. If good friction approximations can be made with friction models, either based on classic friction theory or more advanced models, then better performance parameters of the servo system might be achievable. Most friction models are derived from empirical data, whereby it is necessary to back the specific model up with thorough and extensive experimental data in order to ensure a reliable output. The consequence of this with regards to hydraulic cylinders and servo systems, is the need for a facility for **friction testing of hydraulic cylinders**. The design and construction of this facility, along with the design and analysis of a hydraulic system and experimental setup for the testing of friction in hydraulic cylinders, will be the major tasks of this project.

On a side note, the test facility could be used for other test purposes besides friction, such as life expectancy. Hydraulics is widely used in renewable energy applications such as windmills

and wave energy plants. As mentioned in [Sørensen, 2008] these kinds of applications have high operational requirements and testing would be beneficial for lifespan and friction concerns as the last mentioned induces wear which, when all comes to all, affects the lifespan.

1.3 Problem formulation and definition

As mentioned in the previous section, the main tasks of this project will be:

- Design and construction of a test facility
- Design and analysis of hydraulic system for testing
- Design of the necessary experimental setup

With these tasks in mind, the main problems constituting the thesis can be formulated as:

1. How should the facility be designed in order to perform friction tests of hydraulic cylinders?
2. What is required of the hydraulic system in order to perform friction test?
3. What is necessary in the experimental setup for performing the desired friction tests?

This project will deal with the design of an overall system which can be used to determine the friction of a hydraulic cylinder. This system will consist of a test structure for the mounting of components, a hydraulic system and an experimental setup. Every system will be designed in detail and build in reality. When designing, attempts to use existing parts will be made, and when that is not possible finished parts or parts produced in the workshop will be used instead. Finished parts will be ordered while produced parts are processed in the workshop of the *Department of Energy Technology at Aalborg University*. Each design will be analysed to ensure it meets the requirements. In addition, a linear control system will be developed according to the system requirements when testing for the purpose of modelling the friction. The control system will be based on a mathematical model of the system, and it will be analysed using linear system theory.

If time allows it, and the building of the overall system finishes before the deadline of the project, a program for data acquisition and control signal generation will be developed on the LabView system used in the experimental setup. The controls will be implemented and system runs will be performed, for model verification and tuning of controllers. Thereafter, testing will commence of the chosen cylinder, with the purpose of determining the friction parameters of the chosen friction model.

1.4 Overall system requirements and definitions

A number of requirements are specified for the system beforehand. These requirements are divided into two groups, which are *general requirements (qualitative)* and *specific requirements (quantitative)*.

1 Introduction

1.4.1 General requirements

The general requirements which the system must meet are:

1. Must be able to directly or indirectly measure the friction occurring in a cylinder
2. Must be able to test a wide variety of hydraulic cylinders
3. Must be able to control the load and load cyclus.

1.4.2 Specific requirements

The specific requirements constrains some of the general requirements. They are:

1. Maximum cylinder stroke: $500[mm]$
2. Maximum piston velocity: $0.5[m/s]$
3. Maximum flow: $50[l/min]$
4. Maximum hydraulic pressure: $200[bar]$

From these requirements, other specifications used in the design process will be derived along the way.

Concepts for determining the friction in hydraulic cylinders

2

This chapter describes the initiating development of concepts for determining the friction of a hydraulic cylinder. The issues with measuring the friction in a hydraulic cylinder will be threaded. By taking these issues into consideration a number of concepts for determining the friction will be proposed through preliminary conceptual designs. A final concept will be chosen from an evaluation of their properties with regards to a number of design correlated parameters.

2.1 Issues of determining friction in hydraulic cylinders

The actual determination of friction in a hydraulic cylinder brings up important issues which has to be considered when developing the test setup.

2.1.1 Direct measurements of friction

Friction is a phenomenon which is only noticeable when motion is induced or attempted because of the dependence upon the velocity generated by relative motion. As friction force is a consequence of relative motion, measuring it demands induced motion and circumstances which enables the acting forces to be distinguished and measured. For some types of motions and mechanisms it can be difficult to measure the friction force directly and it is instead measured indirectly by measuring other quantities. A small example can be given with the tugging of a block over a tabletop. If the motion is characterised by a constant acceleration and the setup prescribes only use of an accelerometer (to measure the acceleration of the block) and a force transducer to measure the force of which the block is being tugged with, then the friction will be measured indirectly as it is determined from the measurements of the acceleration and tugging force. If the motion was characterised by a constant velocity then the friction would be measured directly as it would be equal to the tugging force needed to maintain the velocity. In the case of constant acceleration, the friction force could have been measured directly if the setup was changed by isolating the table from external forces except the friction between block and table, and thereafter measure the displacement force acting on the table as a consequence of the friction. Still though, this setup would ideally be impossible to achieve. This emphasises, that when measuring friction it is important to carefully evaluate the setup and behaviour of the operating system before proceeding with friction tests.

This leads to the fact, that measuring the friction of a hydraulic cylinder is a difficult task. Most hydraulic cylinders are constructed such that the piston is encased in the cylinder housing which is mounted to a stiff structure. As mentioned in [Meikandan et al., 1994], the friction of a hydraulic cylinder is most often measured indirectly as it is determined from measurements of pressure in cylinder chambers, external forces and/or acceleration. In most cases measuring the friction directly, if not being impossible, complicates the test-setup, whereby this has to be taking account when developing concepts and designs of the test setup.

2.1.2 Load dependent friction

So far, friction has been viewed upon as only dependent of velocity. In some applications this is true, but in other cases where the load changes this might not be true. Hydraulic cylinders are often used in applications which leads to a varying load on the cylinder. This dependency on load is mentioned by [Bonchis et al., 1999; Dupont, 1993]. Especially [Bonchis et al., 1999] treats this with regards to hydraulic cylinders by modelling frictions dependency on the pressure and thereby indirectly the load. As friction depends on the load, and in some cases the load is varying, this calls for the need to be able to perform friction tests of cylinders for varying loads. Thereby, another requirement has been established to take into consideration when designing the test setup.

2.2 Concepts

This section presents a five different concepts for the design of a testing facility for hydraulic cylinders. A short description and illustration of each concept will be given whereafter the concepts will be compared and one will chosen to be used in the design. These concepts are characterised by the way load is applied to the cylinder in test, and how the friction is determined from the testing. [Aderikha et al., 2002; Bernzen, 1999; Bonchis et al., 1999; Krutz et al., 2002; Meikandan et al., 1994; Nissing, 2002; Yanada and Sekikawa, 2008] have been used as inspiration in the development of the following concepts.

2.2.1 #1 - Load-by-Spring

In figure 2.1 the principal idea of this setup is shown. The test cylinder is matched up against a spring. When the piston is moved it either compresses or elongates the spring which leads to a reaction force. Thus, the reaction force becomes the load on the piston rod. Depending on the compression or elongation of the spring the load varies, but it is limited by the spring constant and deflection.

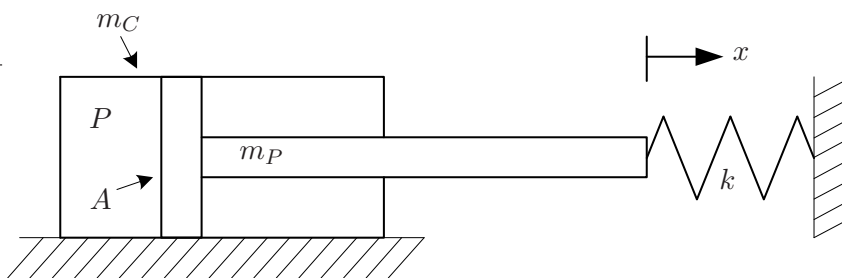


Figure 2.1: The test setup using a deflected spring as load.

From first principles it is shown that the friction force in the hydraulic cylinder can be determined using this setup. If the spring rate is linear, the load force when the spring is deflected from its equilibrium is given by:

$$F_L = k \cdot x \quad (2.1)$$

where,

F_L :	load force or spring force	([N])
k :	spring constant	([N/m])
x :	deflection of the spring from equilibrium	([m])

The pressure, P , in the chamber on the piston side creates a force on the piston, while the load force from the spring acts on the piston rod. A friction force acts on the piston and rod as well, whereby the equation of motion is given by,

$$m_P \ddot{x} = PA - F_L - F_F \Leftrightarrow \quad (2.2)$$

$$F_F = PA - kx - m\ddot{x} \quad (2.3)$$

where,

m_P :	mass of piston	([kg])
F_F :	friction force between cylinder and piston	([N])
A :	area of piston	([m ²])
\ddot{x} :	acceleration of piston and rod	([m ² /s])

As seen in equation (2.3) the friction force can be determined if the pressure, spring deflection and acceleration of piston is measured. The limitations for controlling the load etc. makes this setup not suitable when it is desired to test the cylinder under load conditions that differ from the characteristic of the spring.

2.2.2 #2 - Load-by-Mass

The most simple way to provide a load on the test cylinder is by using a fixed mass. The load will depend on the movement and orientation of the mass. For simplicity, it is easiest to move the mass translational in either a horizontal or vertical direction as shown in figure 2.2.

In the case where the mass is translated horizontally, the inertia of the mass and piston is utilized as the load. In the vertical case, both inertia and gravity of the mass and piston is used as the load. Using a fixed mass simplifies the setup, but limits the loading characteristic as the load cannot be varied during cycles, etc.

2.2.3 #3 - Load-by-Cylinder-1

This concept suggests using a hydraulic cylinder to provide the load as shown in figure 2.3 where the test-cylinder is matched up against another hydraulic cylinder.

The load cell determines the applied load to the test-cylinder, which is necessary for determining the friction. In addition, the measurements of the load cell are used to control the output of the load-cylinder. Without the load cell it would be impossible to distinguish the friction in the load-cylinder from the test cylinders friction. This is best illustrated by the equation of motion of the mechanical system. The free body diagram of the two connected pistons are shown in figure 2.4.

2 Concepts for determining the friction in hydraulic cylinders

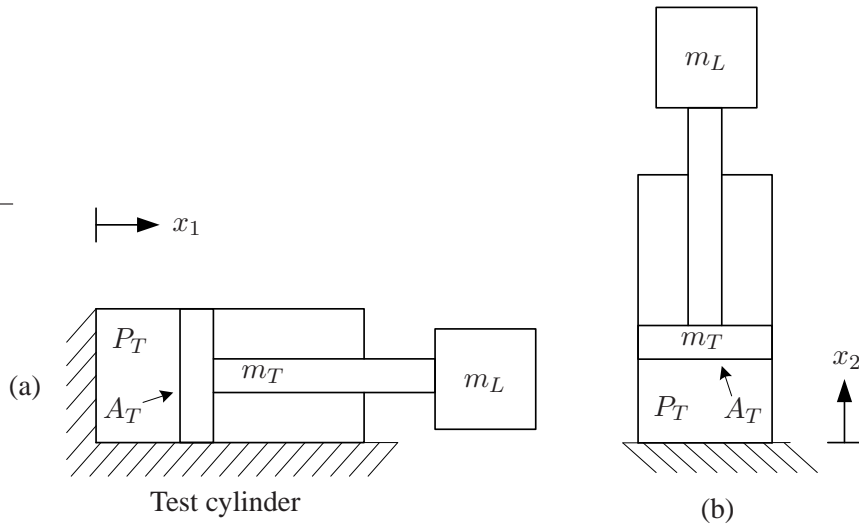


Figure 2.2: Test setup using a fixed mass translated in either a horizontal (a) or vertical direction (b).

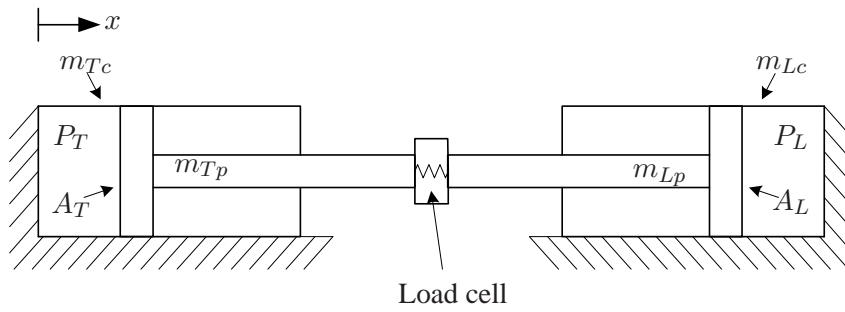


Figure 2.3: The test setup using a hydraulic cylinder to provide the load.

From the free body diagram in figure 2.4 the following equation of motion is derived:

$$(m_{Tp} + m_{Lp})\ddot{x} = P_T A_T - P_L A_L - F_{FT} - F_{FL} \Rightarrow \quad (2.4)$$

$$F_{FT} + F_{FL} = P_T A_T - P_L A_L - (m_{Tp} + m_{Lp})\ddot{x} \quad (2.5)$$

where,

m_{LP} :	mass of the piston in load-cylinder	([kg])
m_{TP} :	mass of the piston in test-cylinder	([kg])
F_{FT} :	friction force in test-cylinder	([N])
F_{FL} :	friction force in load-cylinder	([N])
P_T :	pressure in the test-cylinders piston side chamber	([Pa])
P_L :	pressure in the load-cylinders piston side chamber	([Pa])
A_T :	area of test-cylinders piston	([m ²])
A_L :	area of load-cylinders piston	([m ²])
\ddot{x} :	acceleration of test and load piston	([$\frac{m}{s^2}$])

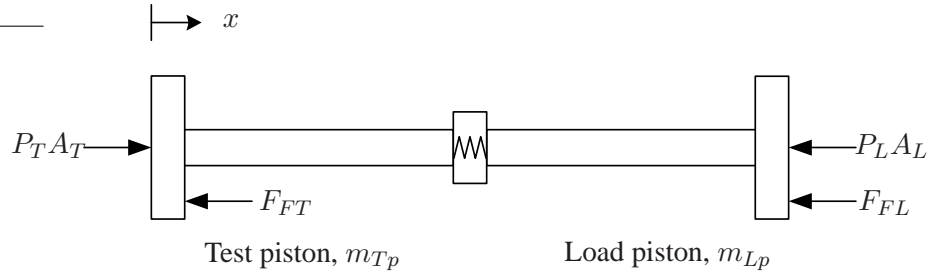


Figure 2.4: Free body diagram of the connected test- and load-pistons.

From equation (2.5) it is clear, that the friction of the test-cylinder cannot be determined from measurements of the acceleration and pressures alone. The load, F_L , measured by the load-cell, is given as,

$$F_L = P_L A_L + F_{FL} \Rightarrow \quad (2.6)$$

$$F_{FL} = F_L - P_L A_L \quad (2.7)$$

Applying (2.7) in (2.5) leads to the elimination of F_{FL} whereby the friction in the test-cylinder, F_{FT} , is expressed as:

$$F_{FT} + (F_L - P_L A_L) = P_T A_T - P_L A_L - (m_{TP} + m_{LP})\ddot{x} \Rightarrow \quad (2.8)$$

$$F_{FT} = P_T A_T - (m_{TP} + m_{LP}) - F_L \quad (2.9)$$

The loading force, F_L is generated because of the reaction force between the test and load cylinder. By measuring this force it is possible to decouple the effect of the friction in the load-cylinder and thereby determine the friction in the test-cylinder. In addition, by applying feedback control it should be possible to vary the load as desired with good precision.

2.2.4 #4 - Load-by-Cylinder-2

This concept is almost similar to #3 explained in 2.2.3. Where the concept in 2.2.3 has a load cell between the test- and load-cylinder this concept has the load cells placed behind each cylinder housing as shown in figure 2.5.

By placing the load cells behind each cylinder housing, the friction can be determined from the measurement of the pressures in the cylinder housings and the force measured by the load cell. If the force measured by the load cell is F_{LC} , then the friction in each cylinder can be expressed as the difference between the force, from the pressure acting within the cylinder, and the force measured by the load cell. Using figure 2.5, this can be expressed as the following for the test-cylinder,

$$F_{FT} = P_T A_T - F_{LC} \quad (2.10)$$

2 Concepts for determining the friction in hydraulic cylinders

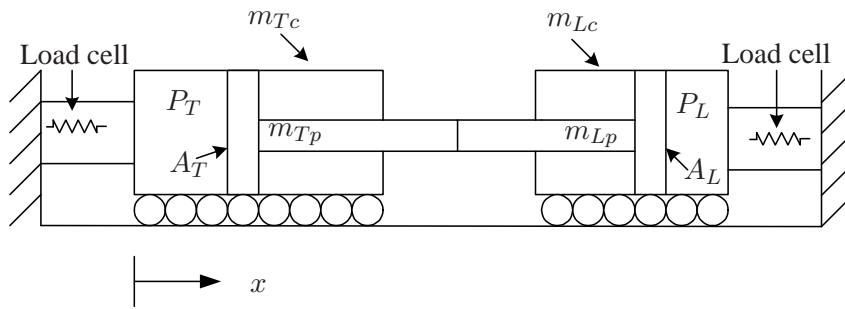


Figure 2.5: Test- and load-cylinder with load cells mounted behind the cylinder housings.

Where F_{FT} is the friction in the test-cylinder. By having a load cell behind each cylinder, makes it possible to determine the friction force of each cylinder independently of each other.

This concept brings the same advantages as in #3, as it would be possible to control the load and thereby create varying loads and cycles. Because the placement of the load cells are in the mountings of the cylinder housings, higher requirements for the design of the cylinder mountings has to be specified in order to ensure good measurements for a wide variety of cylinders.

2.2.5 #5 - Load-by-Cylinder-3

The idea of this concept comes from [Meikandan et al., 1994]. In #3 and #4 the friction was measured indirectly as it was determined from the measurements of other quantities. The idea of this concept is to design a special load-cylinder, which makes it possible to measure the friction of this cylinder directly. The direct measured friction makes it possible to avoid using load cells to measure the load in between the cylinders or behind the cylinder housings. The concept is shown in figure 2.6.

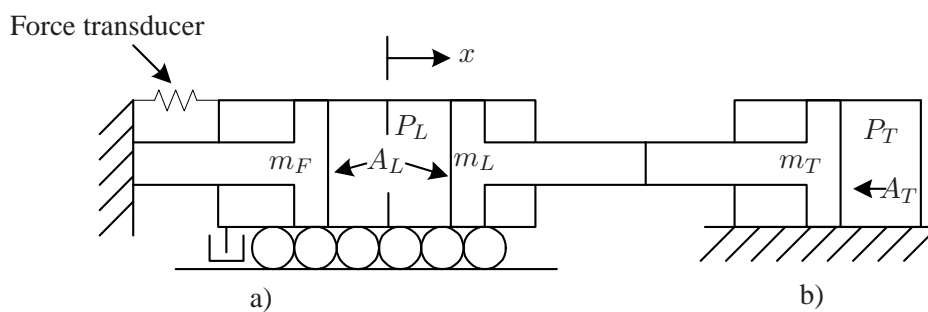


Figure 2.6: Test setup using a special load cylinder. a) Load cylinder. b) Test cylinder.

The load-cylinder is designed so there is two separate pistons inside the cylinder housing. As seen in figure 2.6 the piston, m_F , is fixed while piston, m_L is free to move. In addition, the cylinder housing is mounted in a way allowing low friction (i.e. negligible friction) movement in the horizontal direction. Furthermore, the cylinder is designed to have very low friction between the fixated piston and housing, whereby this friction can be neglected. The friction between the moving piston and the cylinder housing is not necessarily low but this friction can be measured

2 Concepts for determining the friction in hydraulic cylinders

by a suitable force transducer [Meikandan et al., 1994]. The measurement of the load-cylinders friction works like this:

When the pressure P_L builds inside the cylinder housing it forces the moving piston to move. With the movement of the piston, friction will occur between the cylinder housing and the moving piston. As the cylinder housing is free to move, the friction drags it along with the moving piston. The force displacing the cylinder is the friction and as mentioned it can be measured using a suitable force transducer.

To illustrate how this concept works, the equations for equilibrium and motion are written for the bodies of the load-cylinder. The free-body diagrams for the fixed and moving pistons and housing of the load cylinder is shown in figure 2.7.

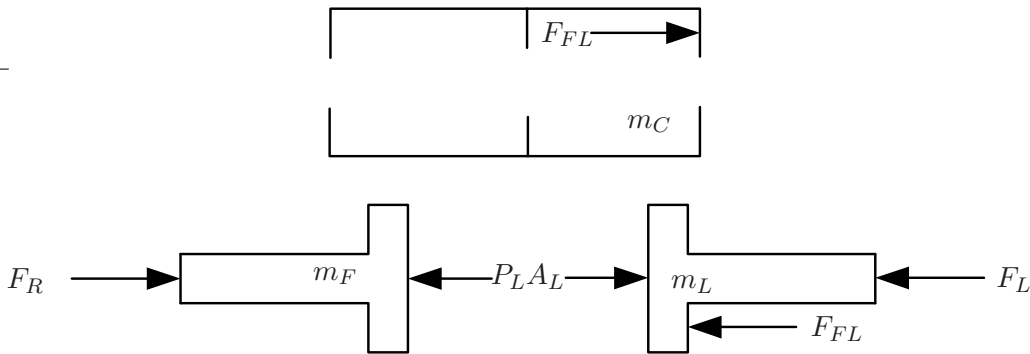


Figure 2.7: Free-body diagram for the bodies of the load-cylinder.

Using the free-body diagram in figure 2.7 the equation of motion for the cylinder housing is,

$$m_C \ddot{x}_C = F_{FL} \quad (2.11)$$

where,

m_C :	mass cylinder housing	([kg])
\ddot{x}_C :	acceleration of the cylinder housing	($[\frac{m}{s^2}]$)
F_{FL} :	friction between the cylinder housing and moving piston	([N])

As the friction force is measured by a force transducer the dynamics of the cylinder can be neglected. Using the measured friction, F_{FL} , the load on the test-cylinder is determined by writing the equation of motion for the moving piston,

$$m_L \ddot{x} = P_L A_L - F_L - F_{FL} \Rightarrow \quad (2.12)$$

$$F_L = P_L A_L - m_L \ddot{x} - F_{FL} \quad (2.13)$$

where,

m_L :	mass of the moving piston	([kg])
\ddot{x} :	acceleration of the moving piston	($[\frac{m}{s^2}]$)
P_L :	pressure in piston side chamber	([Pa])
A_L :	area of piston	($[m^2]$)

2 Concepts for determining the friction in hydraulic cylinders

If the pressures and accelerations are measured, then the friction of the test-cylinder is determined by using equation (2.13) along with the test-pistons equation of motion which results in an equation identical to (2.9).

This concept is more complex and it demands that a special cylinder is built for the purpose. The need for a special cylinder limits the setup, as a new load-cylinder has to be built if the existing cannot provide the required load. Furthermore, if neglecting the friction between the cylinder and fixed piston is not possible, the acceleration of the cylinder housing and the load of the fixed piston must be determined. This leads to more measurements and an indirect determination of the load-cylinders friction, whereby the idea of this concept collapses.

2.2.6 Choice of concept

In order to choose a concept to create a real design from, the five concepts are evaluated with regards to five correlated parameters of the design and function, which are:

Flexibility - The designs usability for a wide range of cylinders and load characteristics. High flexibility is great.

Complexibility - The complexity of the design. Low complexity is great.

Cost - The cost of realising the design. Low cost is great.

Robustness - The designs robustness towards use. High robustness is great.

Quality - The quality and precision of the designs output. High quality is great.

The five concepts will be subjectively assessed according to these parameters. Each concept will be given a score between 1 and 10 for each parameter, where 10 is great and 1 is poor. The concept with the highest score, will be chosen as the concept that will be carried over to the design phase. The result of the evaluation is shown in table 2.1.

Concept	Flexibility	Complexibility	Cost	Robustness	Quality	Total score
#1	1	7	7	8	8	31
#2	1	7	7	8	8	31
#3	10	5	5	8	7	35
#4	9	5	4	7	7	32
#5	6	2	2	7	6	23

Table 2.1: Evaluation of the concepts.

Concept #3 - *Load-by-Cylinder-1* scores highest and is thereby chosen to be used in the following design of an actual test setup.

2.3 From concept to design - continuing work

As the concept has been chosen, the real design of the test facility can be developed. The concepts were rough ideas for a real design, and is only the starting point for the design process to work

2 Concepts for determining the friction in hydraulic cylinders

from. As mentioned in section 1.3, a working test facility is one of the main objectives of this project, whereby the concept must lead to a overall system which consists of the following parts and subsystems:

- Mounting frame
- Hydraulic system
- Experimental setup

The purpose of the structure is to create a backbone for the mounting of the systems components in an way which ensures that the desired test will run. The components are the test- and load-cylinder, the servovalve and the sensing equipment. The structure creates the conditions necessary for the system to perform as required.

The hydraulic system is the collection of hydraulic components which are necessary in order make the system perform the required tests. This system must be designed, accordingly with the purpose of the friction tests, by choosing components which meets the requirements.

The experimental setup consists of the components necessary to record the performance of the system. This is done, by using the appropriate sensing devices for doing the necessary measurements and a PC for data acquisition.

The continuing work from here, is thereby creating the design of the test structure, design the hydraulic system and create an experimental setup.

2 Concepts for determining the friction in hydraulic cylinders

Design of the mounting frame

This section describes the design of the mounting frame which is the backbone of the overall system. The purpose of this structure is to be a rigid frame on which the hydraulic system is mounted. The primary concern is the mounting of the hydraulic test- and load-cylinder, as these generate great loads which must be absorbed by the mounting frame.

In section 1.4 several requirements were listed. A number of these requirements are addressed to the design of the mounting frame with regards to dimensions. The general requirements specify that it should be possible to test a wide variety of cylinders. Hydraulic cylinders come in many shapes and sizes, and the ways to mount them are numerous. Designing a mounting frame which would accept any kind of hydraulic cylinder without customisation is close to impossible. The underlying theme during the design has therefore been to make the setup as general as possible, whereby requiring little customisation in order to fit the cylinder. The earlier mentioned general requirement is constrained by the specification that the maximum stroke of the cylinders tested are 500[mm].

As the cylinders are securely fastened in the mounting frame, the forces generated by the cylinders will be directly transferred to the frame. This requires the mounting frame to possess a certain strength. The requirements do not directly specify the maximum loads of the system, but these can be derived from the specific requirements mentioned in section 1.4.2. By combining the maximum flow and velocity requirements, a maximum cylinder diameter is derived and defined. Using the maximum cylinder diameter, along with the rated system pressure of 200[bar] leads to the load acting on the mounting frame. Using the correlations between flow and velocity and the definition of pressure leads to the following cylinder diameter and load-specification:

- Maximum piston diameter: 46[mm]
- Maximum load on structure: 34[kN]

With all the requirements in mind, the following problems could be formulated:

1. What design is most flexible with regards to differences in mounting types, etc.?
2. How should the cylinders be mounted?
3. How should the cylinders be connected?
4. What dimensions are needed to ensure the necessary strength?

By analysing these questions it is possible to propose a design.

3.1 Design proposition

Analysing the requirements and problems, led to a design which was modelled in SolidWorks. From here, the design was analysed and iterations were made in order to optimise the design. The primary objective of the mounting frame, was to securely fasten and connect the hydraulic cylinders during testing. Investigation and analysis was therefore carried out with regards to existing cylinder- and mounting types and ways to connect the cylinders.

Cylinder types

Many different types of hydraulic cylinders exists, and they can overall be divided into two major groups,

- Differential cylinders
- Symmetric cylinders

Differential (asymmetric) cylinders are characterised by having a rod side and piston side, whereby there is only a rod extending from one end of the cylinder-housing. The symmetric cylinder on the other hand have two rod sides as the rod goes all the way through the cylinder. The rod can thereby extend from both ends of the cylinder-housing. The mounting frame must allow for both differential and symmetric cylinders to be tested, whereby space must be given to the for rod through the symmetric cylinder.

Mounting of cylinders

The easiest way to mount the cylinders, is to use the existing mounting method. A wide variety of mounting methods are used on hydraulic cylinders. A well known way to to mount cylinders is by using a clevis or eye located in both ends of the cylinder. Other mounting types are trunions, lugs, flanges and more, whereby it is necessary to create a flexible mounting system which can be changed according to the mountings of the cylinder to be tested.

Connection of cylinders

The ends of the test- and load-cylinder has to be connected for them to be matched up against each other. For the connection to be satisfying, it must be able to transfer the forces between the cylinders appropriately so the cylinders are loaded as specified to avoid buckling and misalignments. The forces must be transferred in a way which maintains the force and doesn't interfere with measurements.

3.1.1 Initial design

By taking the above considerations into account an initial design was created. This, was further developed, and the result is the design illustrated in figure 3.1.

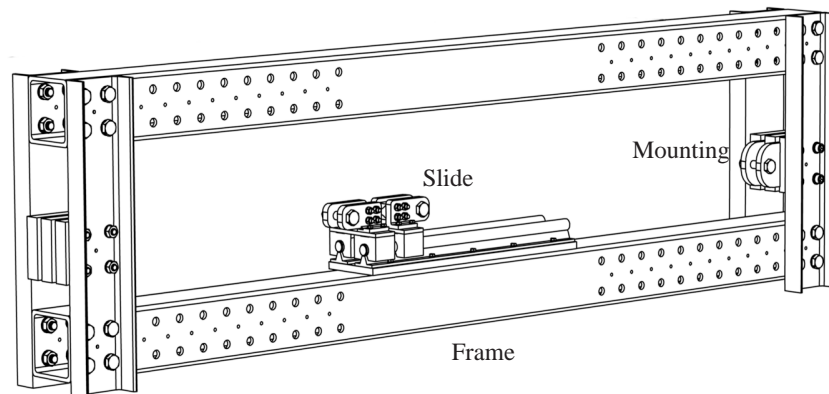


Figure 3.1: The design of the entire mounting frame showing the slide, frame and cylinder attachments.

The design consists of a frame, a slide and cylinder attachments at each end. A description of each is given as follows.

Frame

The frame consists of two horizontal TPS beams S355 J2H 160x160x10 and four vertical UNP S355 J2+AR 160x65 beams which are bolted together with preloaded M20 bolts in each end to create the structure of the frame. The bolted connections, along with the displaced holes along the length of the horizontal beam, allows for the configuration of the frame to be changed depending on the stroke of the cylinders. Furthermore, holes are drilled in the vertical beams for the attachments mounting the cylinders. The overall dimensions of the frame are derived from an assessment cylinder sizes. From empirical studies it is assumed that a hydraulic cylinder with a stroke of 500[mm] has a total length of 800[mm] when the rod is fully retracted. In addition, it is assumed that a cylinder with a 50[mm] piston diameter, has a 100-120[mm] outside diameter. These assumptions will not be true for every cylinder, but in many cases they will be valid.

Slide

The slide in figure 3.2, serves the purpose of connecting and guiding the two cylinders to avoid misalignment. In addition, the load cell from 4.2.2 is integrated into the slide in between where the two cylinders are connected. The slide is based on two sets of linear ball bearing guides, on which eye-brackets are bolted for mounting of the cylinders. The linear guides are placed on a level machined plate which is bolted to the lower beam of the frame. On each guide runs two linear ball bearing which are connected through the strain-element of the load cell.

Mountings

The mountings or attachments are used to fasten the cylinders securely to the frame. In this project two differential cylinders mounted through eyes in both ends are used. To make the mounting more general, it is made out of 3 spacer plates and 2 mounting plates which act like

3 Design of the mounting frame



Figure 3.2: The slide through which the load and test-cylinder is connected.

lamellas as shown in figure 3.3. These plates are bolted together between the vertical beams with preloaded M16 bolts.

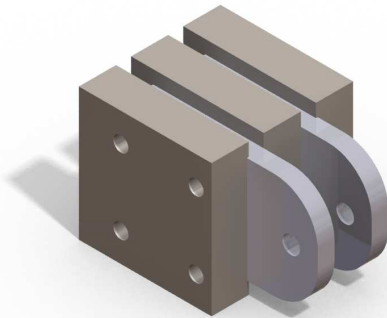


Figure 3.3: The mountings through which the hydraulic cylinders are mounted to the frame.

Design criteria

For the design to be valid for construction, the following criterias must be met:

- The design must be strong enough to withstand the maximum load of $34[kN]$.
- The design must withstand 10^7 load cycles.

The design is validated by doing a structural analysis.

3.2 Structural analysis of the frame

The structural analysis is carried out to make sure the design is sufficient, according to the requirements. The analysis deals with determining the forces acting on the elements in the design.

When the normal and shear forces along with the bending moment are known, these will be used to determine the stresses in the structure using the classic formulas from [Gere, 2002; Norton, 2006]. Furthermore, [DS, 1998] has been used for the code of practice in the use of structural steel.

The loads acting on the structure is calculated by doing a load analysis. This load analysis can be found in appendix A. The following elements have been checked with regards to structural strength. Calculations have been performed by hand using the classic formulas as mentioned. To verify these calculations, FEM-calculations have been carried out using SolidWorks Simulation (CosmosWorks). The beams of the frame are made of steel S355 with a yield strength of 355MPa . According to [DS, 1998], the yield strength of the material has to be divided by 1.17 before being compared with the effective Von Mises stress. The results of the structural analysis will be summed up in the following.

3.2.1 Vertical beam

The vertical beam is analysed with regards to shear stresses and bending moments. The nominal Von Mises stress is used as the criteria towards yielding and the point of the highest stress in the beam is shown in figure 3.4.

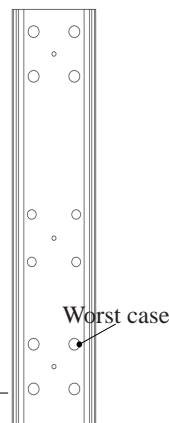


Figure 3.4: The point of the critical stress in the vertical beam.

In the illustrated point, the maximum Von Mises stress is:

$$\sigma_{nom} = 74.5\text{MPa} \quad (3.1)$$

The stress in this point is used to determine the frames fatigue strength. As there are no welds in frame, the elements can be treated as machine elements. Calculating the fatigue strength of the vertical beam by drawing a Woehler diagram shows that the structure will have infinite life against the required load.

3.2.2 Lower beam

The stress in the lower beam is due to normal force and bending moment. The maximum tensile stress is found at the outer fibres on the underside of the beam as shown in figure 3.5.

3 Design of the mounting frame

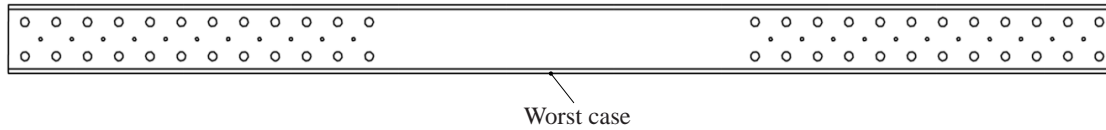


Figure 3.5: The point of the highest stress in the lower beam.

The maximum stress in this element is found to be:

$$\sigma_{max} = 17.26MPa \quad (3.2)$$

Furthermore, the elongation, δ , of the beam due to normal forces are:

$$\delta = 0.046mm \quad (3.3)$$

It is assessed, that this elongation is not large enough to have an influence on there measurements which have to performed within the frame.

3.2.3 Bolted connections

The bolted connections in the real structure will be preloaded to improve the fatigue strength. In the static calculations the bolts have been assumed as not being preloaded. This assumption leads to pure shear loading of the bolts. This assumption is very conservative and calculations showed that the bolted connections are strong enough to resist the maximum loads in static loading without being preloaded. As this structure will experience many load cycles, the bolted connection will be preloaded up to 75% of their proof strength to improve fatigue strength.

3.3 Final design

The structural analysis showed that the structure had sufficient static and fatigue strength to withstand the required loads. The design was therefore finalised by making the technical drawings necessary for it to be manufactured by the work shop. The final design is illustrated in figure 3.6.

The drawings of the parts of the structure can be found on the attached CD.

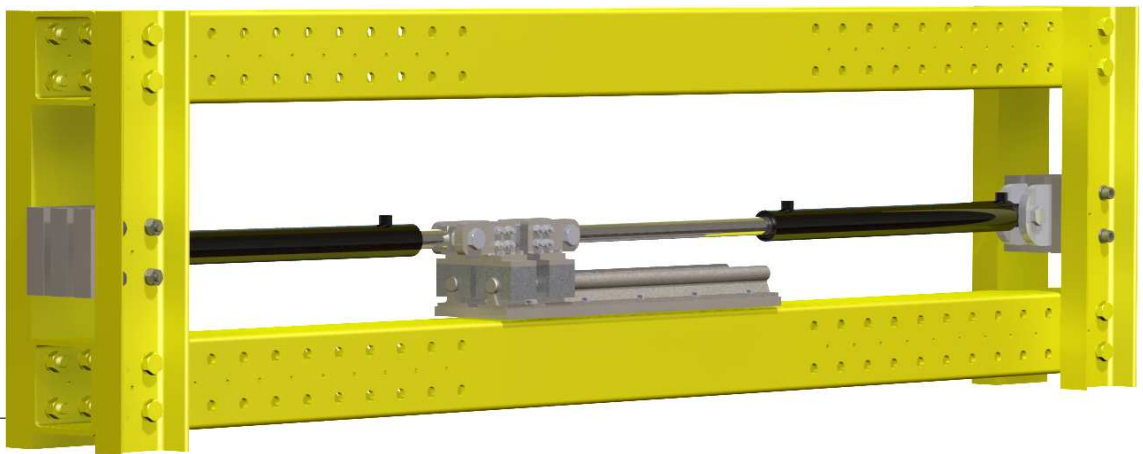


Figure 3.6: The point of the highest stress in the lower beam.

3 Design of the mounting frame

Hydraulic system and experimental setup

4

This chapter gives an introduction to the hydraulic system and the experimental setup with regards to components and transducers.

4.1 Hydraulic system design

This section describes the design of the hydraulic system with regards to the chosen components. All of the components have been found in the hydraulics lab.

Specifications for the hydraulic system are given in section 1.4.2.

4.1.1 Hydraulic components

The following components are chosen to be used in the hydraulic system:

The datasheets of the test-cylinder and servovalve are found on the attached cd. The test-cylinder is bigger than the systems rated cylinder size, which is 46mm . The maximum velocity of the chosen test-cylinder is 0.3 m/s which results in a flow of 56 l/min . This exceeds the rated flow of the system, which is 50 l/min pr. cylinder, but as the load-cylinder is smaller than rated, it should be possible to run the test-cylinder at maximum velocity if a suited pump station is specified. A pressure relief valve and a pump station will be specified, when the overall system is constructed, as these are not important in the following analysis of the hydraulic system.

4.1.2 Hydraulic system diagram

The configuration of the hydraulic system is shown in figure 4.1.

Component	Type
Test-cylinder:	LJM NH30-1-SD-63/30x-100S
Load-cylinder:	Hydra Tech 8054202 Cyl 40/25x400 Regal CC
Servovalve:	MOOG D633-313B
Pressure relief valve:	Unspecified
Pump station:	Unspecified

Table 4.1: Components of the hydraulic system.

4 Hydraulic system and experimental setup

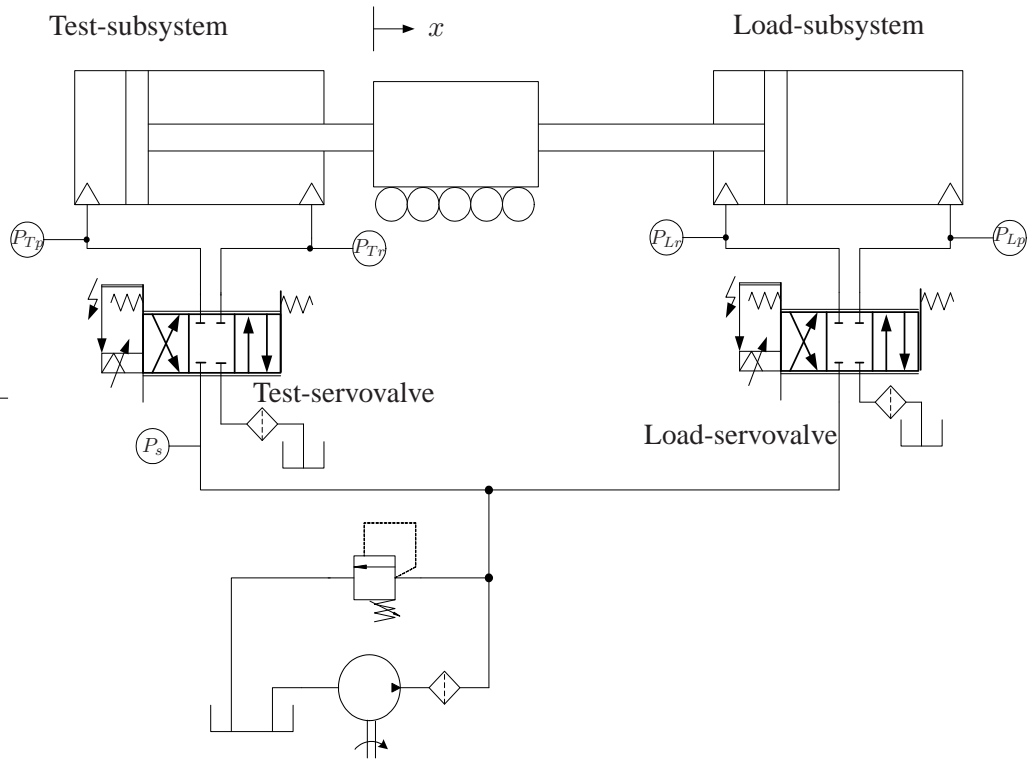


Figure 4.1: Hydraulic systems diagram.

State	Sort	Transducer type	Make
Acceleration	Piezoelectric Accelerometer	471	Brüel & Kjær
Pressure	Pressure transducers	SCP/SCPT	Parker

Table 4.2: Commercial transducers used in the experimental setup. See data sheets on the attached cd.

4.2 Experimental setup

This section gives an introduction to the experimental setup of the system. This is a proposal to the setup, as a lack of time made it necessary to downgrade the actual arrangement of the experimental setup. As this is a proposal, the experimental setup will not be designed in detail, but suggestions will be given of the components of the system.

4.2.1 Commercial transducers

The experimental setup, is the part of the system which measures the required states. As mentioned in chapter 2, the chosen concept from which the test facility is designed requires measurements of the acceleration, pressure and load. Furthermore, friction measurements requires the position to be known. Transducers are therefore chosen which can perform satisfying measurements of the states of the system. Commercial transducers are used for measuring the acceleration and the pressures. The transducers are in tab:

The load-cylinder in table 4.1 has a built in position transducer, which will measure the position of the pistons. Using a commercially available load cell was looked in to, but it was not possible to find a suitable load cell which could measure the required range of loads, whereby it was chosen to design a custom load cell for the system.

Mounting of accelerometer and pressure transducers

The mounting of the pressure transducers must be as close to the cylinder-chambers as possible, to minimise the loss of pressure between the transducer and the cylinder-chamber. The accelerometer will be mounted on the centerslide, which connects the two cylinders.

4.2.2 Load Cell

The load cell is used to measure the load of the test-cylinder. This load is generated by the load-cylinder whereby the load-cell is mounted in between the cylinders on the centerslide. To have a steady setup, with a load cell that can measure the whole range of loads necessary with good accuracy is required. The requirements to the load cell are:

- Range of [-34,34]kN
- Must be able to measure tensile and compressive axial loads.

The basic idea of the load cell, is a well-defined element which is mounted with a certain strain gauge configuration. When the cell is loaded axially the strain gauges measures the strain of the element, from which the axial load can be calculated. The strain element is illustrated in figure 4.2.

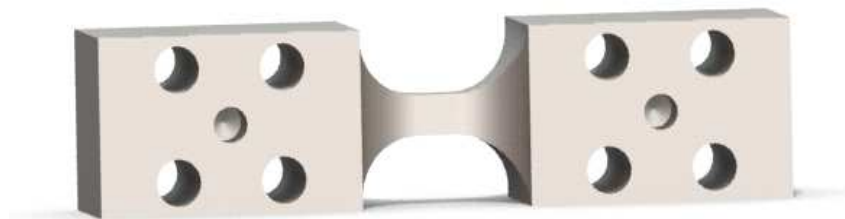


Figure 4.2: The strain-element of the load cell.

The narrowing section of the strain-element in figure 4.2 will be the area of interest when dimensioning the strain- element, as the cross-sectional area of the narrow section determines how much it is strained.

The factors determining the the dimensions of the strain element are the maximum load and minimum load, yield strength of the applied material and the desired measurement resolution. The load cell is required to measure a wide range of loads and even measurements of small loads must be done with good accuracy, if possible. Strain gauges can measure strains as small 1×10^{-6} and this is decisive for the resolution of the load cell [Gere, 2002]. The wide range of the load cell, limits its resolution, whereby it might not be possible to design a load cell which is precise

4 Hydraulic system and experimental setup

enough for all loading-application within the defined range. Using the expressions for normal stress and strain from [Gere, 2002] yields the cross-sectional area of the strain-elements narrow section (strain-section):

$$A_s = \frac{P_{res}}{E \cdot \varepsilon_{min}} \quad (4.1)$$

Where,

P_{res} :	load cell resolution	([N])
A_s :	cross-sectional area of strain-section	([m ²])
E :	E-moduli of the material	([GPa])
ε_{min} :	minimum measurable strain	([GPa])

To avoid overloading, the stress of load-cell must not exceed $\frac{2}{3}$ of the materials yield strength:

$$\sigma_{max} \leq \frac{2}{3}\sigma_y, \quad \sigma_{max} = \frac{P_{max}}{A_s} \quad (4.2)$$

$$(4.3)$$

Where,

σ_{max} :	maximum normal stress in the strain-element	([MPa])
σ_y :	yield strength of material	([MPa])
P_{max} :	maximum load	([MPa])

To ensure the strain-section against buckling under a compressive load, the critical load is calculated as [Gere, 2002]:

$$P_{cr} = \frac{4\pi^2 EI}{L^2} \quad (4.4)$$

Where,

P_{cr} :	critical load for buckling	([N])
I :	moment of inertia	([m ²])
L :	length of strain-section	([GPa])

The material is TOOLOX44, a high strength steel (see data sheet on CD) for which $\sigma_y = 1300$ [MPa]. Other values are, $P_{max} = 34$ [kN], $\varepsilon_{min} = 1 \times 10^{-6}$ and $E = 200$ [GPa]. Using (4.1)-(4.4) and assuming the cross-section must be square and $L = \sqrt{A_s}$ leads to the results in table 4.3.

As seen in table 4.3, a higher resolution (smaller P_{res}) of the load cell demands a smaller cross-sectional area of the strain-section. In addition, it is seen that it is impossible, with the used material, to design a load cell with a high resolution that covers the whole range of application. Therefore different load cells are necessary depending on the applicable load range. As a starting

$P_{res} [N]$	$A_s [m^2]$	$L [mm]$	$\sigma_{max} [MPa]$	$P_{cr} [kN]$
1	0.000005	2.2	6800	3184.6
5	0.000025	5	1360	16449.3
20	0.0001	10	340	65797.3

Table 4.3: Dimensions of the load-cell with respect to resolution.

point, a load cell has been designed which can be used in the required load range. This load cell has a strain-section length $L = 9[mm]$ which leads to a resolution of $17[N]$, and it meets the requirement stated in (4.3). It leaves plenty of room for mounting of the strain gauges but it might not have a high enough resolution, whereby a different would have to be designed.

Mounting of strain gauges

The strain gages are mounting on the strain-element using a full bridge arrangement. The full bridge is very advantageous when axial loads have to be measured, as it eliminates the contribution by bending. The load cell and fixture are designed to avoid bending of the strain-element, but should it occur for some reason, then it will not affect the measurements.

4.2.3 Data acquisition

For data acquisition and generating control signals the plan is to use a realtime PC running LabVIEW.

4 Hydraulic system and experimental setup

Dynamic model of the fluid-mechanical system

5

This chapter will describe the mathematical modelling of the dynamics of the system in question. At first the modelling detail with regards to the system will be defined by bounding the region of importance in order to establish a sufficient model. Thereafter the assumptions preceding the mathematical descriptions will be mentioned and finally the mathematical models will be presented.

The purpose of this model is to describe the dynamics of the system and how these dynamics affects the output when a specific input is given. Further on, this model will be linearized and the linearized model will be used to evaluate system behaviour with regards to stability and design specific closed-loop controllers.

The dynamic part of the system consists of two interconnected hydraulic cylinders which are mounted in a rigid frame. The cylinders are controlled by two servovalves, one for each cylinder, which controls the fluid flow supplied to the cylinders. The fluid is supplied by a hydraulic pump, and by designing the hydraulic system appropriately the supply pressure is kept almost constant by using a pump which at all times can deliver the demanded flow. This reduces the dynamics within the system which has a real influence on the output whereby the modelling required to create a sufficient model is reduced. For this system it will be necessary to describe the dynamics and properties of the servovalve and cylinder with regards to flow, pressure and force..

The overall system contains two subsystems which are defined by the hydraulic cylinder. The test-cylinder and the connected components is called the *Test-subsystem* while the load-cylinder and connected components is called the *Load-subsystem*.

The following assumptions have been made in order to simplify the modelling of the system:

1. The frame and cylinder mountings are completely rigid.
2. The supply pressure is constant.
3. No leakage flow is present in the cylinders or valves.
4. Constant Bulk Modulus.
5. Tank pressure is constant.

In figure 5.1 an illustration of the parts in the system, which have to be described mathematically, are shown. The designations indicated by figure 5.1 will be used to set up the equations for the system.

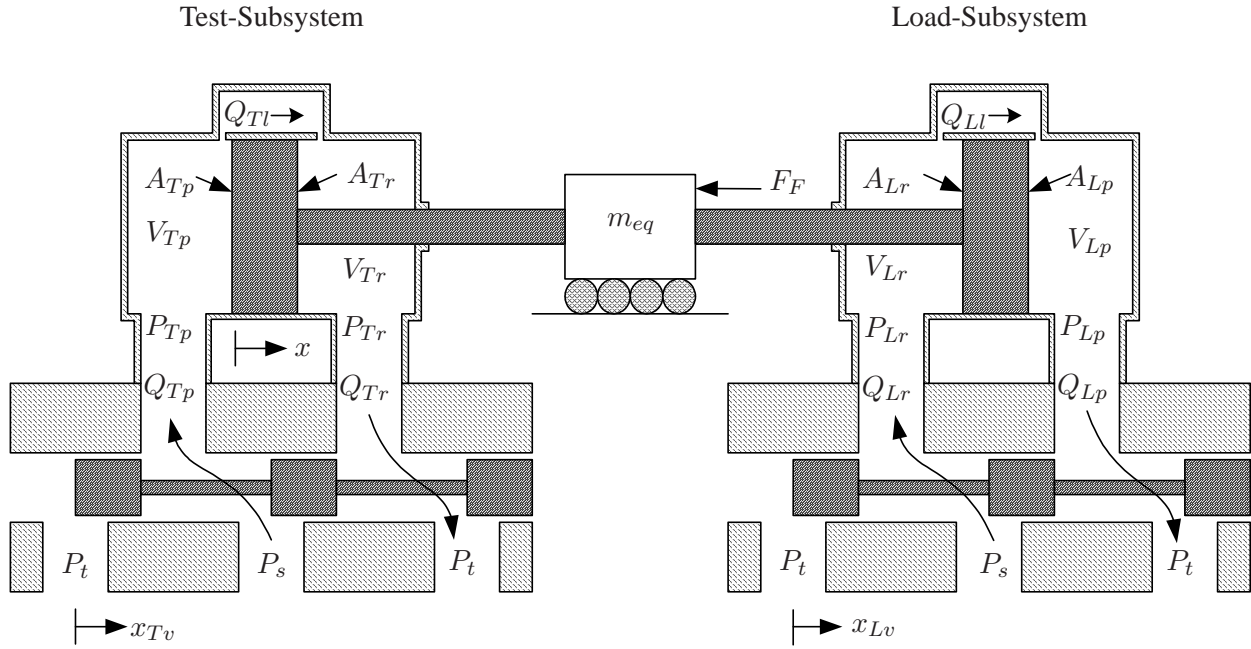


Figure 5.1: Illustration of the connected servovalve and cylinder, with leakage flow, of each subsystem. Models will be set up for the servovalve and cylinder.

5.1 Modelling of Cylinders

Modelling of the cylinders refer to determining the pressures in the cylinder chambers along with describing the motion of the pistons. The pressures are expressed via the flow continuity equations while the motion of the system is given by Newtons 2. law of motion.

5.1.1 Continuity flow for the cylinders

Test-subsystem

Changes in the control volumen and the compressibility flow for the test-cylinder is expressed by the flow continuity equations given by (5.1) and (5.2).

$$Q_{Tp} - Q_{Tl} = \frac{dV_{Tp}}{dt} + \frac{V_{Tp}}{\beta} \frac{dP_{Tp}}{dt} ; V_{Tp} = V_{Tp0} + A_{Tp}x \quad (5.1)$$

$$Q_{Tl} - Q_{Tr} = \frac{dV_{Tr}}{dt} + \frac{V_{Tr}}{\beta} \frac{dP_{Tr}}{dt} ; V_{Tr} = V_{Tr0} - A_{Tr}x \quad (5.2)$$

Where,

Q_{Tp} :	flow into the test-cylinder on the piston side	$([m^3/s])$
Q_{Tl} :	leakage flow over the cylinder piston	$([m^3/s])$
Q_{Tr} :	flow out of the test-cylinder on the rod side	$([m^3/s])$
V_{Tp} :	volume on the piston side	$([m^3])$
V_{Tr} :	volume on the rod side	$([m^3])$
V_{Tp0} :	initial volume on the piston side	$([m^3])$
V_{Tr0} :	initial volume on the rod side	$([m^3])$
A_{Tp} :	piston area	$([m^2])$
A_{Tr} :	rodside piston area	$([m^2])$
P_{Tp} :	pressure acting in the piston side chamber	$([m^3])$
P_{Tr} :	pressure acting in the rod side chamber	$([m^3])$
x :	displacement of the piston from the initial position	$([m])$
\dot{x} :	velocity of piston	$([m/s])$
β :	bulk modulus of the fluid	$([bar])$

By neglecting the leakage flow, Q_{Tl} , the pressure gradient of the rod- and pistonside can be expressed from (5.1) and (5.2) which is done in (5.3) and (5.4)

$$\dot{P}_{Tp} = \frac{\beta}{V_{Tp0} + A_{Tp}x} (Q_{Tp} - A_{Tp}\dot{x}) \quad (5.3)$$

$$\dot{P}_{Tr} = \frac{\beta}{V_{Tr0} - A_{Tr}x} (A_{Tr}\dot{x} - Q_{Tr}) \quad (5.4)$$

Load-subsystem

The load-subsystem is modelled in the same way as the test-subsystem besides a few small differences because of cylinder orientation. The equations are given in (5.5) and (5.6).

$$Q_{Lr} - Q_{Ll} = \frac{dV_{Lr}}{dt} + \frac{V_{Lr}}{\beta} \frac{dP_{Lr}}{dt}; \quad V_{Lr} = V_{Lr0} + A_{Lr}x \quad (5.5)$$

$$Q_{Ll} - Q_{Lp} = \frac{dV_{Lp}}{dt} + \frac{V_{Lp}}{\beta} \frac{dP_{Lp}}{dt}; \quad V_{Lp} = V_{Lp0} - A_{Lp}x \quad (5.6)$$

Where,

Q_{Lp} :	flow into the test-cylinder on the piston side	$([m^3/s])$
Q_{Ll} :	leakage flow over the cylinder piston	$([m^3/s])$
Q_{Lr} :	flow out of the test-cylinder on the rod side	$([m^3/s])$
V_{Lp} :	volume on the piston side	$([m^3])$
V_{Lr} :	volume on the rod side	$([m^3])$
V_{Lp0} :	initial volume on the piston side	$([m^3])$
V_{Lr0} :	initial volume on the rod side	$([m^3])$
A_{Lp} :	piston area	$([m^2])$
A_{Lr} :	rodside piston area	$([m^2])$
P_{Lp} :	pressure acting in the piston side chamber	$([m^3])$
P_{Lr} :	pressure acting in the rod side chamber	$([m^3])$

5 Dynamic model of the fluid-mechanical system

Hence, the pressure gradients in the load-subsystem are:

$$\dot{P}_{Lr} = \frac{\beta}{V_{Lr0} + A_{Lr}x} (Q_{Lr} - A_{Lr}\dot{x}) \quad (5.7)$$

$$\dot{P}_{Lp} = \frac{\beta}{V_{Lp0} - A_{Lp}x} (A_{Lp}\dot{x} - Q_{Lp}) \quad (5.8)$$

5.1.2 Equation of motion of Test- and Load-cylinder

The systems equation of motion is given by Newtons 2. law of motion from the forces acting on the interconnected pistons:

$$m_{eq}\ddot{x} = P_{Tp}A_{Tp} + P_{Lr}A_{Lr} - P_{Tr}A_{Tr} - P_{Lp}A_{Lp} - F_F \text{sign}(\dot{x}) \quad (5.9)$$

Where,

F_F :	the total friction in the system	$([m^3/s])$
\ddot{x} :	acceleration of masses	$([m/s^2])$
m_{eq} :	total mass of the moving bodies	$([kg])$

Friction model

A simple friction model will initially be applied. It will be based on the classical friction models of section 1.1.3 and consist of the viscous friction and the Coulomb friction. The friction model will be expressed as:

$$F_F = (f_{Tv} + f_{Lv}) |\dot{x}| + (F_{TC} + F_{LC}) \quad (5.10)$$

f_{Tv} :	the viscous friction parameter of the test-cylinder	$([Ns/m])$
f_{Lv} :	the viscous friction parameter of the load-cylinder	$([Ns/m])$
F_{TC} :	the Coulomb friction of the test-cylinder	$([N])$
F_{LC} :	the Coulomb friction of the load-cylinder	$([N])$

Equation (5.10) concludes the modelling of the cylinder.

5.2 Servo valve

As mentioned, both subsystems utilise a MOOG D633 servo valve. The flow through the orifices in the servo valve are determined from the valve-input, which is equivalent to a displacement of the valve spool, and the pressure drop over the valve. The input is a +/-10VDC voltage (10V corresponds to 100% valve opening) where a positive voltage corresponds to a displacement in the

positive direction and vice versa.

For both subsystems, the modelling of the servovalve is almost similar and the following expressions are therefore written in a general manner. The only variation in the modelling is a reversed configuration of the equations in (5.11)- (5.14) with regards to the sign of u_v when modelling the load-servovalve.

For an input voltage $u_v > 0$ the static flow through the valve is given as:

$$Q_p = K_T \cdot u_v \cdot \sqrt{\frac{2}{\rho} \cdot (P_s - P_p)} \quad (5.11)$$

$$Q_r = K_T \cdot u_v \cdot \sqrt{\frac{2}{\rho} \cdot (P_r - P_t)} \quad (5.12)$$

When $u_v < 0$ the flow is given as:

$$Q_p = K_T \cdot u_v \cdot \sqrt{\frac{2}{\rho} \cdot (P_p - P_t)} \quad (5.13)$$

$$Q_r = K_T \cdot u_v \cdot \sqrt{\frac{2}{\rho} \cdot (P_s - P_r)} \quad (5.14)$$

where,

Q_p :	flow at the inlet orifice of the valve	$([m^3/s])$
Q_r :	flow at the exit orifice of the valve	$([m^3/s])$
K_T :	static valve gain	$([-])$
u_v :	input voltage to the servovalve	$([V])$
ρ :	density of the oil	$([kg/m^3])$
P_s :	supply pressure	$([Pa])$
P_t :	tank pressure	$([Pa])$
P_p :	pressure acting between the orifice, and the piston side	$([Pa])$
P_r :	pressure acting between the orifice, and rod side	$([Pa])$

The equations in (5.11) and (5.13) are static models for the flow through the valve. The valve gain, K_T is calculated from the rated flow, which is found in the data sheet for MOOG D633. This data sheet can be found on the attached CD. The data sheet contains the valve flow diagram illustrated in figure 5.2. The data sheet states that the rated pressure drop is $\Delta p_N = 35bar$ per metering land for the rated flow $Q_N = 40l/min$ (figure 5.2) at 100% command signal (i.e. 10 VDC = 100% valve opening).

Applying these values in equation (5.11), and the valve gain K_T is found to be:

$$K_T = \frac{Q_N}{U_{100\%} \sqrt{\frac{2\Delta p_N}{\rho}}} \quad (5.15)$$

$$K_T = \frac{(40l/min) \cdot \left(\frac{1m^3 \cdot min}{60000l \cdot s}\right)}{10V \sqrt{\frac{2 \cdot 70 \cdot 10^5 Pa}{870kg/m^3}}} = 7.43 \cdot 10^{-7} \frac{m^2}{V} \quad (5.16)$$

5 Dynamic model of the fluid-mechanical system

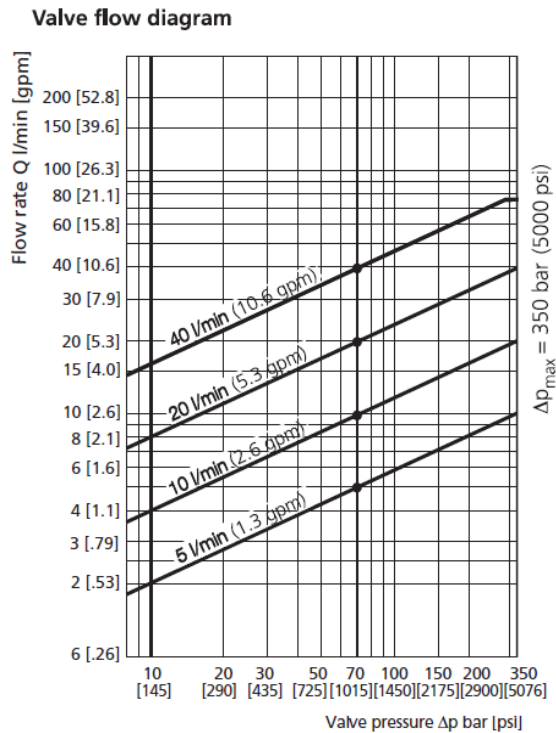


Figure 5.2: Valve flow diagram from the data sheet of the MOOG D633 servovalve. [MOOG-Controls]

The dynamics of the servovalve is determined from its frequency response which is also to be found in the data sheet [MOOG-Controls]. The frequency response is shown in figure 5.3.

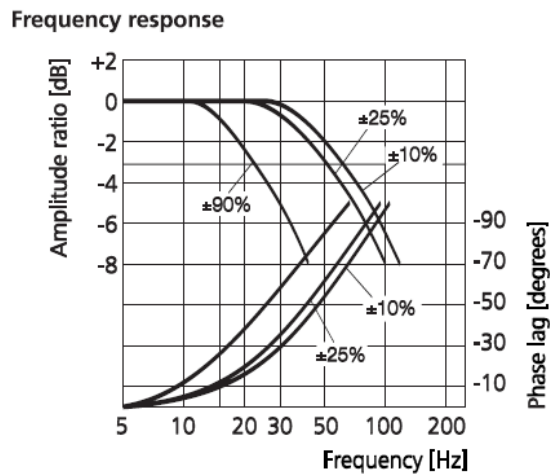


Figure 5.3: Valve flow diagram from the data sheet of the MOOG D633 servovalve. [MOOG-Controls]

The frequency response indicates that the dynamics can be estimated by using a second order transfer function. Signals used, are considered small in the $\pm 10\%$ range. For performing the estimation, the transfer function of a second-order system is considered:

$$G(s) = \frac{K}{\frac{1}{\omega_n^2}s^2 + \frac{2\zeta}{\omega_n}s + 1} \quad (5.17)$$

Where,

K :	gain	([-])
ζ :	damping of the system dynamics	([-])
ω_n :	eigenfrequency of the system dynamics	([rad/s])

From figure 5.3 it is clearly seen that the gain is $K = 1$ as the amplitude is zero for low frequencies. Furthermore, the lack of a resonans peak indicates that the damping is in the interval $0.7 \leq \zeta \leq 1$. ζ is estimated to be 1, which is also the most conservative, with regards to fast performance. The eigenfrequency of the system is found as the frequency at -90 degrees phase lag. As seen in figure 5.3 the eigenfrequency is approximately $\omega_n = 2 \frac{rad}{Hz \cdot s} \cdot 90Hz$. The second order model for the dynamics of the servovalve is thereby given as:

$$G_v(s) = \frac{1}{\frac{1}{565}s^2 + \frac{2}{565}s + 1} \quad (5.18)$$

This concludes the mathetically modelling of the system. This model is highly non-linear as several of its equation are non-linear. In chapter 6, a linear model will be created by linearising this non-linear model. Though, before that will happen, the non-linear version will be implemented in SIMULINK in order to carry out simulations.

5.3 Simulation model using SIMULINK

The mathematical expressions from section 5.1 and 5.2 are implemented in SIMULINK in order to create a simulation model. The simulation model is illustrated in figure 5.4 with voltage-input (U) of the servovalves and the different outputs right from flow (Q) to position (x) and velocity (\dot{x}). The implementation is straight forward and will not be described further here, but the SIMULINK and MatLAB files of model can be found on the attached CD.

5.3.1 Model verification

Delays in finalising the design resulted in the construction of the test facility, not being completed before the deadline of the project. A consequence of this, was the lack of actual sampled data from the experimental setup which could be used for verifying the models validity. Furthermore, the lack of a test facility and experimental data meant that identification of system parameters, such as friction (the main subject of this project), was not possible. The parameters needed to be identified for modelling are instead estimated by a qualified guess, and these guesses are used until the real system, is up and running. To replace a real verification, an assessment of the models validity will be carried out based on the general behaviour of the model and the aforementioned estimated parameters.

5 Dynamic model of the fluid-mechanical system

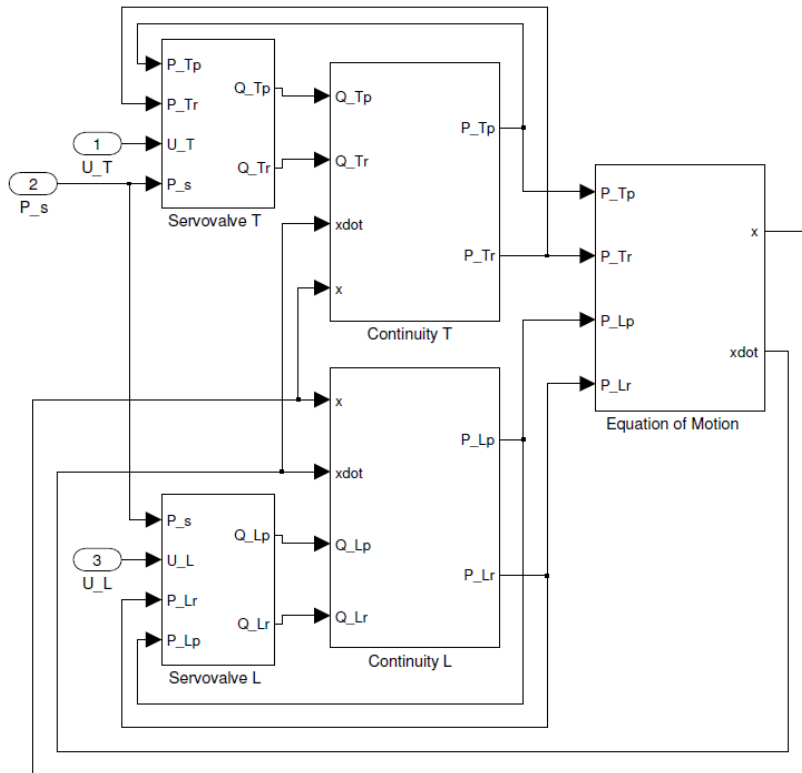


Figure 5.4: SIMULINK model of the fluid-mechanical system.

Model behaviour and scenarios

The model will be assessed by running the simulations for certain scenarios with the aim of showing specific system properties such as pressure buildup and flow.

The simulations will be run with a constant input so the model will reach a recognisable steady state. The scenarios will be defined by the applied inputs. The following scenarios will be run:

Pressure buildup To test the models capability to simulate the buildup of pressure, simulations are run where the input of either the test or load-subsystem is zero while the other input is held at a constant non-zero value.

Flow and piston velocity To verify the relation between flow and piston velocity in steady state, simulations are run where both subsystems receive the same input. The pressure in the load-subsystem is set to the tank pressure to minimise the load on the test-cylinder.

By comparing the behaviour of the models output with what is expected from the mathematical expressions, an indication will be given of the models of the validity. In no way will this verify the model as a valid representation of the real system, but it will show if the mathematical expressions have been implemented correct.

Pressure buildup

As mentioned, simulations are run where the input of either the test or load-subsystem is zero while the other input is held at a constant non-zero value. Doing this, imitates that one of the servovalves are closed while a flow is led through the other open servovalve. The flow into the open cylinder will initiate motion of the connected pistons whereby pressure will start building pressure in the cylinder which chambers are cut of by the closed servovalve. This pressure keeps rising until equilibrium of the forces in the cylinders are reached, whereafter the motion stops. A simulation run is shown in figure 5.5 where a constant input is given to the servovalve of the test-cylinder while the servovalve of the load-cylinder is closed.

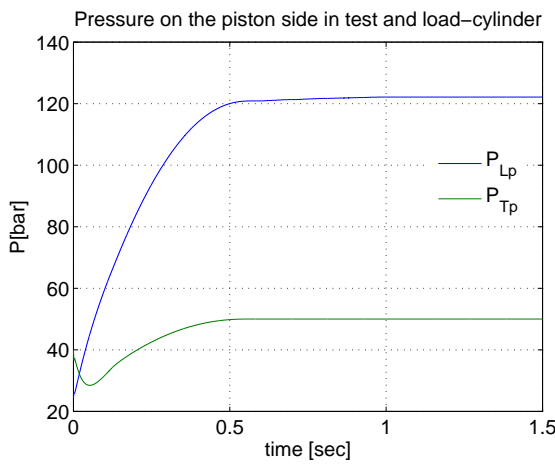


Figure 5.5: As the piston is moved by the test-cylinder, pressure builds up on the piston side of the cut-off load-cylinder. ($P_s = 50bar$)

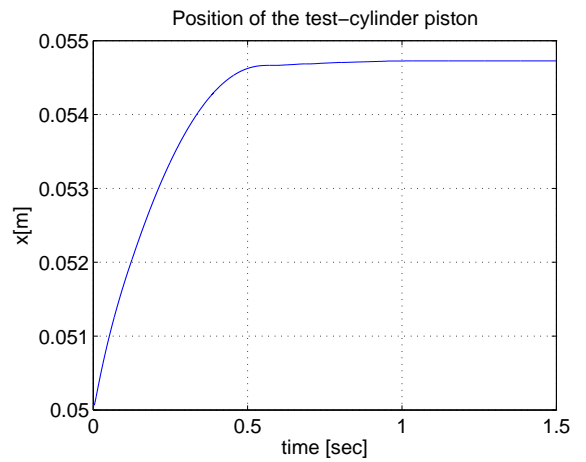


Figure 5.6: The position keeps changing until the piston side pressures in both cylinder creates equilibrium.

As seen from figure 5.5, the pressure builds as expected in the piston side chamber of the load-cylinder. Furthermore, the piston position becomes stationary after a short amount of time due to equilibrium of the forces in the cylinders as given by:

$$P_{Lp}A_{Lp} = P_{Tp}A_{Tp} \quad (5.19)$$

$$P_{Lp} = \frac{A_{Tp}}{A_{Lp}} P_{Tp} \quad (5.20)$$

The area of the pistons are $A_{Tp} = 0.0031m^2$ and $A_{Lp} = 0.0013m^2$. Using equation (5.20) and the steady-state value of P_{Tp} , P_{Lp} is calculated as:

$$P_{Lp} = 2.48 \cdot 50bar \quad (5.21)$$

$$= 124bar \quad (5.22)$$

The calculations shows agreement with the model, and taking the behaviour of the model into account it is assessed that the continuity and equation of motion is modelled in a correct manner.

5 Dynamic model of the fluid-mechanical system

Flow and piston velocity

This case investigates the validity of the servovalves and the correlation between flow and piston velocity used in the continuity equations. When the pressure reaches a steady-state, the correlation between flow and piston velocity is given as:

$$\dot{P}_p = \frac{\beta}{V_{p0} - A_p x} (A_p \dot{x} - Q_p) = 0 \Rightarrow \quad (5.23)$$

$$Q_p = A_p \dot{x} \quad (5.24)$$

The servovalves are given a constant input of $U = 1V$ while the supply pressure is kept at $P_s = 50bar$. The results of the simulation are shown in figure 5.7 and figure 5.8.

Flow into the piston side chamber of the test and load-cylinder.

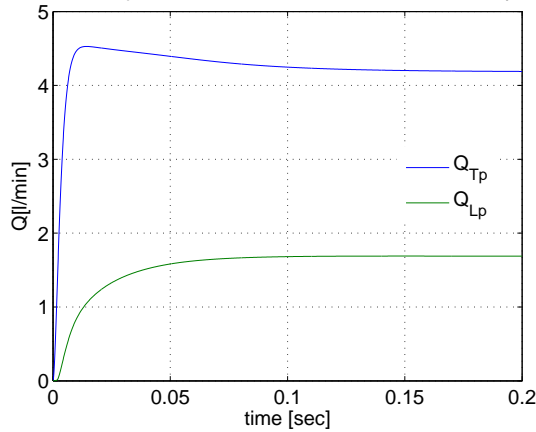


Figure 5.7: The flows Q_{Tp} and Q_{Lp} for the input $U = 1V$ to the servovalves.

Velocity of the cylinder pistons

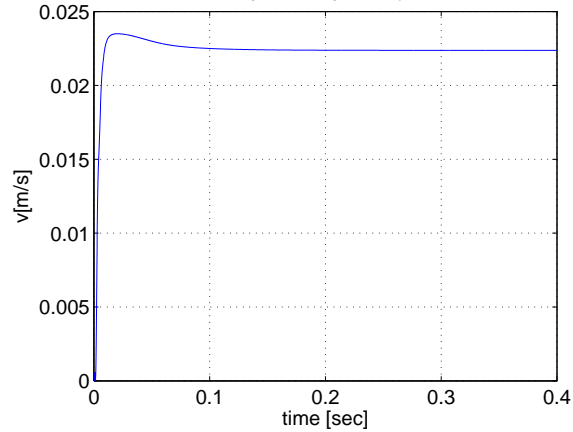


Figure 5.8: The velocity of the pistons from the flow given by the servovalves.

Using the steady-state value of $v = \dot{x} = 0.0225m/s$ from figure 5.8 in (5.24), yields the following steady-state flows:

$$Q_{Tp} = 4.2l/min \quad (5.25)$$

$$Q_{Lp} = 1.8l/min \quad (5.26)$$

As seen, the simulation results show agreement with the steady-state considerations, and it is assessed that the model works as intended and that validation will be obtainable when measurements from the real system are available.

Linear model of the system

This chapter describes the creation of the *Linear model*. The description will contain the linearisation of the equations from chapter 5. The linearised equations will be Laplace-transformed and used to create the block diagram from which the transfer functions of the linear system will be derived. Along with the linearisation will follow an assessment of the operating point around which the linearisation of the systems equations will be done. Furthermore, a comparison between the output of the linear and non-linear mode will be made in order to show agreement between the two models.

6.1 Linearisation of the equations of the system

This section will deal with the linearisation of the equations for the linear model. First the equations of the test-subsystem will be treated whereafter the load-subsystem will be linearised. A T in the subscripts refers to the Test-subsystem and a L refers to the Load-subsystem.

6.1.1 Test-subsystem

The following set of equations from chapter 5 will be linearised.

$$\dot{P}_{Tp} = \frac{\beta}{V_{Tp0} + A_{Tp}x} (Q_{Tp} - A_{Tp}\dot{x}) \quad (6.1)$$

$$\dot{P}_{Tr} = \frac{\beta}{V_{Tr0} - A_{Tr}x} (A_{Tr}\dot{x} - Q_{Tr}) \quad (6.2)$$

$$Q_{Tp} = K_T \cdot U_{vT} \cdot \sqrt{\frac{2}{\rho} \cdot (P_s - P_{Tp})} \quad (6.3)$$

$$Q_{Tr} = K_T \cdot U_{vT} \cdot \sqrt{\frac{2}{\rho} \cdot (P_{Tr} - P_t)} \quad (6.4)$$

First off, equation (6.1) and (6.2) are linearised by neglecting the control volumes dependence of the position (x) of the piston. Doing this, can be justified by the assumption that $V_{Tp0} \gg A_{Tp}x$ and $V_{Tr0} \gg A_{Tr}x$ as x is only a small displacement difference around the operating point (small signals). Using lower case letters to imply differences from the operational point instead of absolute values (i.e. $q_{Tp} = Q_{Tp} - \bar{Q}_{Tp}$ - small signal variable), the linearised equations are:

$$\dot{p}_{Tp} = \frac{\beta}{V_{Tp0}} (q_{Tp} - A_{Tp}\dot{x}) \quad (6.5)$$

$$\dot{p}_{Tr} = \frac{\beta}{V_{Tr0}} (A_{Tr}\dot{x} - q_{Tr}) \quad (6.6)$$

6 Linear model of the system

Equations (6.3) and (6.4) are linearised by using Taylor series expansion for a system with two inputs and one output, $Q = f(u, P)$. By Taylor series equations (6.3) and (6.4) are written as:

$$Q_{Tp} - \bar{Q}_{Tp} = K_{vTp}(U_{vT} - \bar{U}_{vT}) + K_{pTp}(P_{Tp} - \bar{P}_{Tp}) \quad (6.7)$$

$$Q_{Tr} - \bar{Q}_{Tr} = K_{vTr}(U_{vT} - \bar{U}_{vT}) + K_{pTr}(P_{Tr} - \bar{P}_{Tr}) \quad (6.8)$$

where,

\bar{Q}_{Tp} :	operating point of the flow on the cylinders piston side	$([m^3/s])$
\bar{Q}_{Tr} :	operating point of the flow on the cylinders rod side	$([m^3/s])$
K_{vTp} :	flow-input piston side	$([m^3/V \cdot s])$
K_{pTp} :	flow-pressure gain piston side	$([m^5/N \cdot s])$
K_{vTr} :	flow-input gain rod side	$([m^3/V \cdot s])$
K_{pTr} :	flow-pressure gain rod side	$([m^5/N \cdot s])$
\bar{U}_{vT} :	operating point of the servovalves input voltage	$([V])$
\bar{P}_{Tp} :	operating point of the piston side pressure	$([Pa])$
\bar{P}_{Tr} :	operating point of the rod side pressure	$([Pa])$

K_{vTp} , K_{pTp} , K_{vTr} and K_{pTr} are given by:

$$K_{vTp} = \left. \frac{\partial Q_{Tp}}{\partial U_{vT}} \right|_{U_{vT}=\bar{U}_{vT}, P_{Tp}=\bar{P}_{Tp}} \quad K_{vTr} = \left. \frac{\partial Q_{Tr}}{\partial U_{vT}} \right|_{U_{vT}=\bar{U}_{vT}, P_{Tr}=\bar{P}_{Tr}} \quad (6.9)$$

$$K_{pTp} = \left. \frac{\partial Q_{Tp}}{\partial P_{Tp}} \right|_{U_{vT}=\bar{U}_{vT}, P_{Tp}=\bar{P}_{Tp}} \quad K_{pTr} = \left. \frac{\partial Q_{Tr}}{\partial P_{Tr}} \right|_{U_{vT}=\bar{U}_{vT}, P_{Tr}=\bar{P}_{Tr}} \quad (6.10)$$

Using (6.9) and (6.10) the expressions for the linearisation gains are:

$$K_{vTp} = K_T \sqrt{\frac{2}{\rho}(P_s - \bar{P}_{Tp})} \quad K_{vTr} = K_T \sqrt{\frac{2}{\rho}(\bar{P}_{Tr} - P_t)} \quad (6.11)$$

$$K_{pTp} = \frac{-K_T \bar{U}_{vT}}{\sqrt{2\rho(P_s - \bar{P}_{Tp})}} \quad K_{pTr} = \frac{K_T \bar{U}_{vT}}{\sqrt{2\rho(\bar{P}_{Tr} - P_t)}} \quad (6.12)$$

Writing (6.7) and (6.8) with small-signal variables completes the linearisation of the test-subsystem:

$$q_{Tp} = K_{vTp} \cdot u_{vT} + K_{pTp} \cdot p_{Tp} \quad (6.13)$$

$$q_{Tr} = K_{vTr} \cdot u_{vT} + K_{pTr} \cdot p_{Tr} \quad (6.14)$$

6.1.2 Load-subsystem

The load-subsystem is linearised in the same manner as the test-subsystem. The equations to be linearised are:

$$\dot{P}_{Lr} = \frac{\beta}{V_{Lr0} + A_{Lr}\dot{x}}(Q_{Lr} - A_{Lr}\dot{x}) \quad (6.15)$$

$$\dot{P}_{Lp} = \frac{\beta}{V_{Lp0} - A_{Lp}\dot{x}}(A_{Lp}\dot{x} - Q_{Lp}) \quad (6.16)$$

$$Q_{Lr} = K_T \cdot U_{vL} \cdot \sqrt{\frac{2}{\rho} \cdot (P_s - P_{Lr})} \quad (6.17)$$

$$Q_{Lp} = K_T \cdot U_{vL} \cdot \sqrt{\frac{2}{\rho} \cdot (P_{Lp} - P_t)} \quad (6.18)$$

The linearised equations of (6.15), (6.16), (6.17) and (6.18) with small-signal variables are:

$$\dot{p}_{Lr} = \frac{\beta}{V_{Lr0}}(q_{Lr} - A_{Lr}\dot{x}) \quad (6.19)$$

$$\dot{p}_{Lp} = \frac{\beta}{V_{Lp0}}(A_{Lp}\dot{x} - q_{Lp}) \quad (6.20)$$

$$q_{Lr} = K_{vLr} \cdot u_{vL} + K_{pLr} \cdot p_{Lr} \quad (6.21)$$

$$q_{Lp} = K_{vLp} \cdot u_{vL} + K_{pLp} \cdot p_{Lp} \quad (6.22)$$

Where,

$$K_{vLr} = K_T \sqrt{\frac{2}{\rho} (P_s - \bar{P}_{Lr})} \quad K_{vLp} = K_T \sqrt{\frac{2}{\rho} (\bar{P}_{Lp} - P_t)} \quad (6.23)$$

$$K_{pLr} = \frac{-K_T \bar{U}_{vL}}{\sqrt{2\rho(P_s - \bar{P}_{Lr})}} \quad K_{pLp} = \frac{K_T \bar{U}_{vL}}{\sqrt{2\rho(\bar{P}_{Lp} - P_t)}} \quad (6.24)$$

6.1.3 Linearised equation of motion

The equation of motion (5.9) will be linearised by neglecting the static contributions of the Coulomb friction as, only changing variables are considered in the linear model. Thus, the equation of motion becomes:

$$m_{eq}\ddot{x} = P_{Tp}A_{Tp} + P_{Lr}A_{Lr} - P_{Tr}A_{Tr} - P_{Lp}A_{Lp} - f_{eq}\dot{x} \quad (6.25)$$

Where, $f_{eq} = f_{Tv} + f_{Lv}$ is the equivalent viscous friction parameter of both cylinders. The equations of the linear model are thereby determined.

6.2 Block diagram and transfer functions

6.2.1 Laplace transform of the linear model

Before constructing the block diagram, the linear model will be laplace transformed from the time domain to the frequency domain. Laplace transforming the set of equations for the test-subsystem and suitably arranging them, gives:

$$P_{Tp}(s) = \frac{\beta}{V_{Tp0} \cdot s} (Q_{Tp}(s) - A_{Tp} \cdot s \cdot X(s)) \quad (6.26)$$

$$P_{Tr}(s) = \frac{\beta}{V_{Tr0} \cdot s} (A_{Tr} \cdot s \cdot X(s) - Q_{Tr}(s)) \quad (6.27)$$

$$Q_{Tp}(s) = K_{vTp} \cdot U_{vT}(s) + K_{pTp} \cdot P_{Tp}(s) \quad (6.28)$$

$$Q_{Tr}(s) = K_{vTr} \cdot U_{vT}(s) + K_{pTr} \cdot P_{Tr}(s) \quad (6.29)$$

The set of Laplace transformed equations for the load-subsystem are:

$$P_{Lr}(s) = \frac{\beta}{V_{Lr0} \cdot s} (Q_{Lr}(s) - A_{Lr} \cdot s \cdot X(s)) \quad (6.30)$$

$$P_{Lp}(s) = \frac{\beta}{V_{Lp0} \cdot s} (A_{Lp} \cdot s \cdot X(s) - Q_{Lp}(s)) \quad (6.31)$$

$$Q_{Lr}(s) = K_{vLr} \cdot U_{vL}(s) + K_{pLr} \cdot P_{Lr}(s) \quad (6.32)$$

$$Q_{Lp}(s) = K_{vLp} \cdot U_{vL}(s) + K_{pLp} \cdot P_{Lp}(s) \quad (6.33)$$

The Laplace transform of the equation of motion are:

$$m_{eq} \cdot s^2 \cdot X(s) = P_{Tp}(s)A_{Tp} + P_{Lr}(s)A_{Lr} - P_{Tr}(s)A_{Tr} - P_{Lp}(s)A_{Lp} - f_{eq} \cdot s \cdot X(s) \Rightarrow \quad (6.34)$$

$$s \cdot X(s) = \frac{1}{(m_{eq} \cdot s + f_{eq})} (P_{Tp}(s)A_{Tp} + P_{Lr}(s)A_{Lr} - P_{Tr}(s)A_{Tr} - P_{Lp}(s)A_{Lp}) \quad (6.35)$$

The linearised and Laplace transformed equations from (6.26) to (6.35) will be used to construct the block diagram of the system. The block diagram representing the linear model is shown in figure 6.1.

The block diagram will be used later in chapter 7 in the linear analysis and controller design.

6.3 Operating point of linearisation

This chapter will deal with determining the operating point of the linearisation. As the linear model is only valid within close proximity of the operating point, choosing the right operating point is

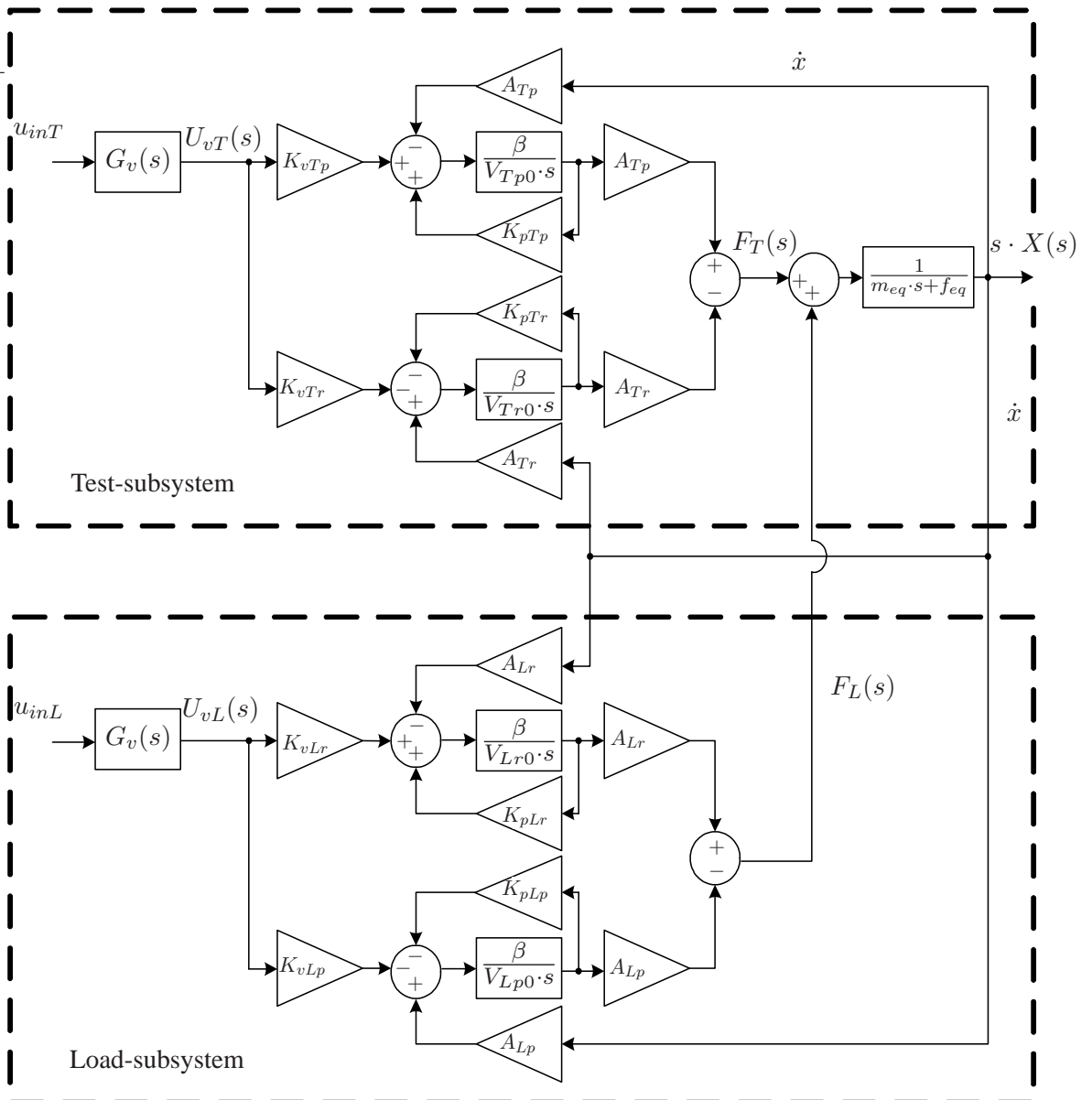


Figure 6.1: Block diagram of the linear model with valve-dynamics. The inputs are the voltage-signals (u_{inT} and u_{inL}) to the servovalves and the output is the velocity of the masses ($V(s)$).

very important. The right operating point is found as the most critical point of operation, i.e. a worst case scenario, with regards to system performance. If the system performance is satisfying around the most critical point of operation it is most likely that performance will be satisfying for all points of operation. The operating point will be chosen by assessing the eigenfrequencies of the hydraulic cylinders and the effect of valve-input on the systems relative stability.

6 Linear model of the system

6.3.1 Minimum eigenfrequency of cylinders

When the cylinders are operating at their minimum eigenfrequency they are most likely to cause resonans in the system and thereby instability. The operating points of the cylinders are therefore chosen to be where their eigenfrequencies are minimum.

The eigenfrequencies of the double-acting differential cylinders, of the system, is given by (6.36)(derived in appendix B).

$$\omega_n = \sqrt{\frac{k_h}{m_{eq}}} \quad (6.36)$$

$$(6.37)$$

Where k_h is given by:

$$k_h = \beta \left(\frac{A_R^2}{V_R} + \frac{A_P^2}{V_P} \right) \quad (6.38)$$

$$(6.39)$$

Where,

A_P :	area of piston	$([m^3/s])$
A_R :	area of piston on the rod side	$([m^3/s])$
V_P :	volume on the piston side	$([m^3/s])$
V_R :	volume on the rod side	$([m^3])$
β :	bulk modulus	$([m^3])$

As the volumes are dependent of the displacement (x) of the piston, this makes the eigenfrequency dependent of the piston position as well. By using (6.36) the eigenfrequencies for the entire stroke of the test- and load-cylinder is calculated and plotted in figure 6.2 and figure 6.3.

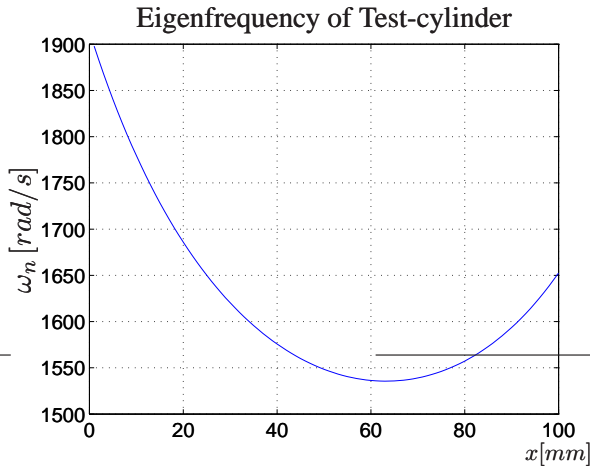


Figure 6.2: The eigenfrequency of the test-cylinder with regards to piston displacement.

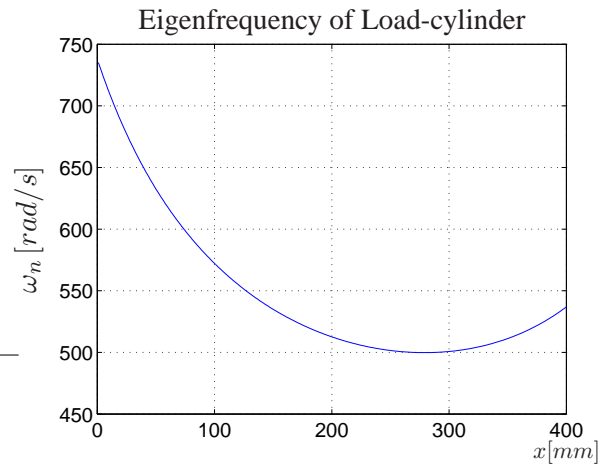


Figure 6.3: The eigenfrequency of the load-cylinder with regards to piston displacement.

As seen in figure 6.2 and figure 6.3 the minimum eigenfrequency of the test and load-cylinder is respectively $\omega_{nT} = 1536 \text{ rad/s} @ x_T = 62 \text{ mm}$ and $\omega_{nL} = 500 \text{ rad/s} @ x_L = 276 \text{ mm}$.

6.3.2 Effect of Valve-input on the relative stability

To determine the operating point of the servovalve the effect on the systems relative stability, by the servovalves input u_{in} , is studied. The study is done by determining the systems gain- and phase margins for values of the input in the interval of $[0 - 10]V$. By doing this, it is possible to determine for which value, of the servovalves input, the system will be least stable. In figure 6.4 and figure 6.5 the gain- and phase margin for the test- and loadsubsystem is shown for different values of the servovalve input.

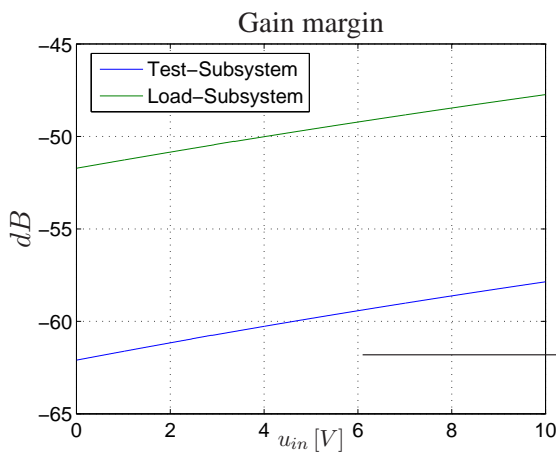


Figure 6.4: The gain margin of the test- and load-subsystem for differing values of the servovalve input, u_{in} .

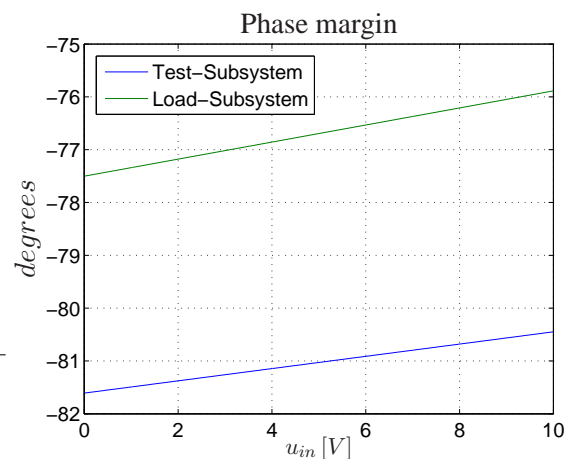


Figure 6.5: The phase margin of the test- and load-subsystem for differing values of the servovalve input, u_{in} .

6 Linear model of the system

First off, figure 6.4 and figure 6.5 shows that both subsystems are unstable as the gain and phase margins are all negative for all values of u_{in} . However, the values of the pressures which has been used in the calculation are purely fictive. With regards to determining the operating point of the servovalve, figure 6.4 and figure 6.5 show that the smaller the value of u_{in} , the further away from stability the system moves as the gain and phase margin become even more negative. This means, that the critical operating point of the servovalves is a small value of the input-signal which physically corresponds to a small displacement of the valve spool. As there is a limit for how small a signal the valve will be fed, $u_{in} = 0.01 V$ will be chosen as the operating point of the servovalves.

This concludes the determination of the operating point of the linearisation.

Control system analysis and design

7

This chapter treats the analysis and design of the control system for the test facility. The measurement of friction parameters specifies a number of requirements depending on the configuration of system which performs the tests. First off, [Armstrong-Hélouvy, 1991] recommends the implementation of a stiff velocity-servo as the system must be able to perform a range of constant velocity motion tests where the friction is measured. In addition, studying the stick-slip phenomenon requires the system to perform quasi-constant velocity motions where the commanded velocity is reduced ever slightly until it reaches the point where stick-slip motion can be observed. Furthermore, a force-servo must be implemented in the load-subsystem in order to precisely control the load which is applied to the cylinder undergoing test. Another objective of the constellation of a feedback controlled load-cylinder is the option of creating specific load cycles or loading curves. This property, along with the velocity-servo creates the possibility for the test-cylinder to be subjected to test conditions and cycles which imitates its actual operating conditions.

The controllers must be designed according to certain requirements, but for this system it will be impossible to specify a set of specific requirements which the system must meet at all times for all cylinders. Different test cylinders, causes different systems which demands different controllers. In addition, operating conditions of the hydraulic cylinders differ widely as one cylinder might operate doing high cycles with velocities around 0.5 m/s while a another cylinder might be doing small position adjustments with low velocity close to zero. The operating conditions determines the cylinders motion profile which is closely related to the friction profile of the cylinder. This underlines the need of planning friction testing and modelling according to the operating conditions of the test subject in order to get the best experimental data and modelling results. This leads to the fact, that one control design is not sufficient to test different cylinders for different conditions. Every cylinder test must be carefully assessed with reference to the operation of the cylinder, and from this assessment a set of specific controller requirements can be defined.

A set of general requirements to the system are as follows:

General requirements to the velocity-servo and test-subsystem

- Maintain constant velocity
- Perform quasi-constant velocity reduction
- System performance as fast as possible
- Achieve specified velocities from $0 - 0.5\text{ m/s}$

General requirements to the force-servo and load-subsystem

- Achieve the specified force
- 5-10 times faster than the velocity servo

7 Control system analysis and design

As mentioned above, these general requirements can be further specified by assessing the actual configuration of cylinders and their operating conditions. This will lead to a performance specification in terms of transient response and steady-state requirements from which the controller can be developed. As mentioned section 4.1, the test cylinder used in this project is a LJM NH-30S with the following data:

- Stroke: $s_T = 100 \text{ mm}$
- Piston diameter: $D_T = 63 \text{ mm}$
- Rod diameter: $d_T = 30 \text{ mm}$
- Maximum operating velocity: $v_{max} = 0.3 \text{ m/s}$
- Maximum operating pressure: $P_{max} = 250 \text{ bar}$

The manufacturer classifies this cylinder as robust and for use in the hydraulic of ships and such. From these data, more precise performance specification are defined.

Unlike a motor, the distance and thereby the time a hydraulic cylinder has to reach a given velocity is limited by its stroke. For testing friction, it is necessary run the cylinder at a constant velocity which requires the system to accelerate within a distance that allows this velocity to kept for most of the cylinders stroke. To express this requirement in a more precise manner with a numerical value, it is assessed, beforehand, that if maximum 20% of the the cylinders stroke is used for acceleration, such the velocity can be kept constant for 80% of the stroke, then this will be sufficient for testing. For the specific cylinder, this means that the system must be able to reach the maximum velocity of 0.3 m/s within 0.066 seconds. The most important transient-response specification is therefore, that the settling time, $t_{s,2\%}$, is no larger than 0.066 seconds. Other transient-response specifications, such as rise time and maximum overshoot are less important as friction tests of hydraulic cylinders require a fast occuring steady. The steady-state requirements are more or less given by the general requirements. The general requirements specify zero steady state error for step inputs for both the velocity servo and force servo. The last general requirement states that the force-servo needs to be 5-10 times faster than the velocity-servo for it to compensate fast to track the velocity. This requires the force-servo bandwidth (ω_{BL}) to be 5-10 times higher than that of the velocity servo.

The specific requirements for designing the control system is thereby defined and they are:

- A maximum settling time, $t_{s,2\%} = 0.066 \text{ s}$ of the velocity-servo.
- No steady state errors for step inputs of the velocity- and force servo's.
- Force servo bandwidth (ω_{BL}) 5-10 times higher than the bandwidth (ω_{BT}) of the velocity servo.

7.1 Control strategy

Based on the performance requirements and system types a strategy for the design of the control system will be made.

By analysing the linear model derived in chapter 6 the control system will be designed. The approach of the analysis will be to disconnect the load-subsystem from the test-subsystem, as shown in figure 7.1, and instead apply a disturbance for each system. The disturbance of load-subsystem will be the velocity, while the disturbance of the test-subsystem will be the force generated by the pressures in the load-cylinder. The analysis will show that both subsystems, to be controlled, are of type 0 which results in a steady-state error for a step inputs. To remove the steady-state error, *feedback with a PI-controller* are designed for both subsystems using the frequency responses. Values for the parameters of the PI-controllers are proposed by using Ziegler-Nichols rules for tuning PI-Controllers. In order to meet the performance specifications these values are modified if necessary. Furthermore, a velocity-feedforward compensation, for the load-subsystems force-servo will be designed, to compensate for the velocity disturbance applied by the test-subsystem. These control designs do not affect the bandwidth of the system directly, but if the bandwidth requirement are not met, other controllers such as *Lead-compensation* may be proposed and analysed.

Finally, the relative stability of the controlled system will be analysed using frequency response whereafter the control designs will be implemented in the non-linear model for verification.

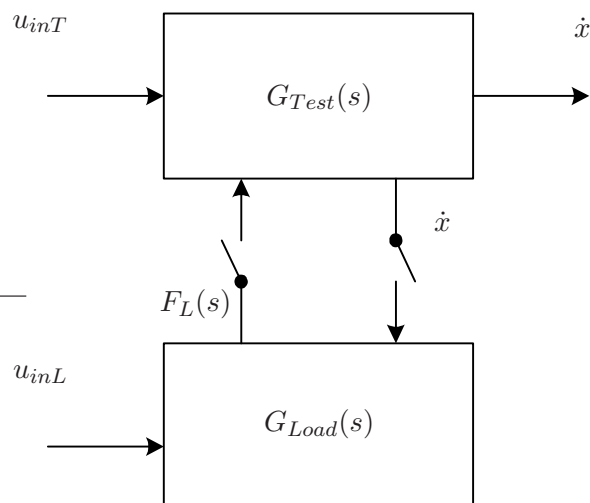


Figure 7.1: Illustration of the disconnection.

7.2 Velocity-servo

The development of the velocity servo is based on the block diagram of figure 6.1. The open-loop transfer function of the test-subsystem will be determined from the block diagram, whereafter the system will be modified with regards to feedback and controller.

7.2.1 Open-loop transfer function of the test-subsystem

The block diagram of the disconnected test-subsystem is shown in figure 7.2.

By closing the inner loops, the diagram is reduced as shown in figure 7.3.

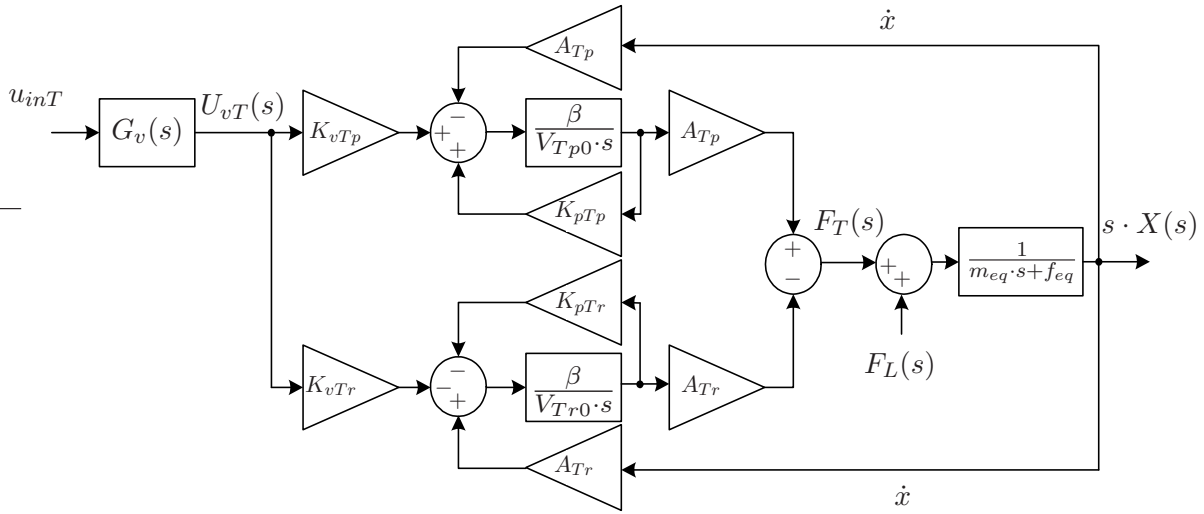


Figure 7.2: Block diagram of the disconnected test-subsystem.

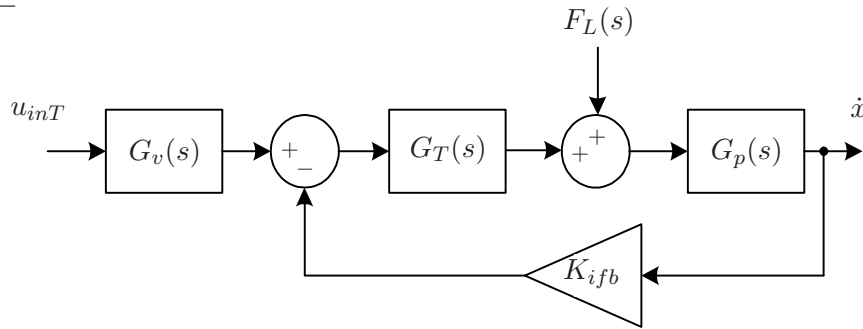


Figure 7.3: Reduced block diagram of the test-subsystem.

$G_v(s)$, in figure 7.3, is the valve-dynamics given by equation (5.18) and $G_T(s)$ is given by (7.1):

$$G_T(s) = \frac{K_{Tp}(T_{Tr}s + 1) + K_{Tr}(T_{Tp}s + 1)}{(T_{Tp}s + 1)(T_{Tr}s + 1)} \quad (7.1)$$

Where,

$$K_{Tp} = \frac{-K_{vTp}A_{Tp}}{K_{pTp}} \quad T_{Tp} = \frac{-V_{Tp0}}{\beta K_{pTp}} \quad (7.2)$$

$$K_{Tr} = \frac{K_{vTr}A_{Tr}}{K_{pTr}} \quad T_{Tr} = \frac{V_{Tr0}}{\beta K_{pTr}} \quad (7.3)$$

While,

$$G_p(s) = \frac{1}{m_{eq} \cdot s + f_{eq}} \quad K_{ifb} = \frac{A_{Tp}K_{vTr} + A_{Tr}K_{vTp}}{K_{vTp} \cdot K_{vTr}} \quad (7.4)$$

Closing the K_{ifb} -loop, and the overall open-loop transfer function, G_{Tol} , of the test-subsystem becomes:

$$G_{Tol}(s) = G_v(s) \cdot G_T(s) \cdot G_{pcl}(s) \quad (7.5)$$

Where, $G_{pcl}(s)$, is the closed-loop transfer function of the $G_T(s)$ - $G_p(s)$ - K_{ifb} -loop:

$$G_{pcl}(s) = \frac{G_p(s)}{1 + G_p(s)K_{ifb}G_T(s)} \quad (7.6)$$

As none of the transfer functions making up the overall transfer function has a free integrator ($\frac{1}{s}$), this will be a type 0 system. This leads to a steady-state error for a step-input to the unity-feedback system, whereby the system would not meet the specified requirements. For this particular system, the static position error constant, K_{ss} , is given by:

$$K_{ss} = \lim_{s \rightarrow 0} G_{Tol}(s) = \frac{K_{Tp} + K_{Tr}}{f_{eq} + K_{ifb}(K_{Tp} + K_{Tr})} \quad (7.7)$$

This leads to the following steady-state error of the unity-feedback system when given a unit-step input:

$$e_{ss} = \frac{1}{1 + K_{ss}} = 0.9785 \quad (7.8)$$

Clearly, the system exhibits a very poor performance towards steady-state operation and therefore is a controller necessary to improve the performance of the system. It has been chosen to implement a PI-controller, as the integral parts (I) primary advantage is to remove steady-state errors, while the proportional part (P) can be used to improve the response time.

7.2.2 PI-Controller with velocity feedback

Introducing feedback of the piston velocity and a controller to the test-subsystem, results in the modifications shown in figure 7.4.

$G_{Tc}(s)$ is a PI-controller which can be written as in (7.9):

$$G_{Tc} = K_P \left(1 + \frac{1}{T_I s} \right) \quad (7.9)$$

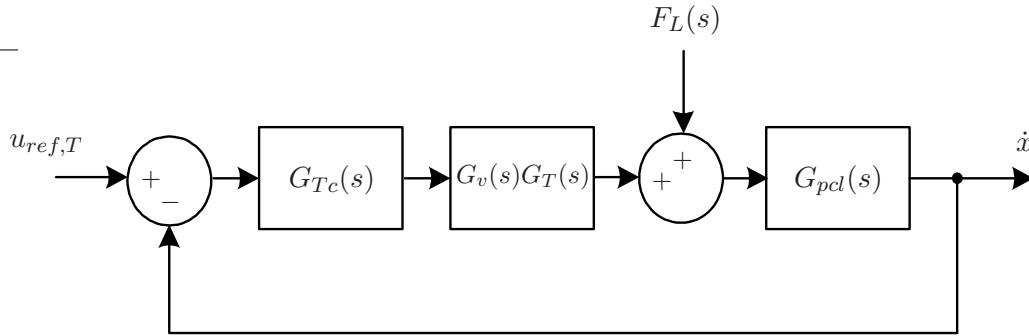


Figure 7.4: The test-subsystem with feedback control. $G_{Tc}(s)$ is the controller.

Tuning of controller parameters

For the PI-controller to be implemented, the parameters K_P and T_I needs to be determined. These are found using the second method of Ziegler-Nichols tuning rules, based on the critical gain K_{cr} and the critical period P_{cr} . The critical gain and critical period is found from the root-locus plot of $G_{TOL}(s)$ at the points where the plot crosses the imaginary axis. The root-locus plot of $G_{TOL}(s)$ is shown in figure 7.5.

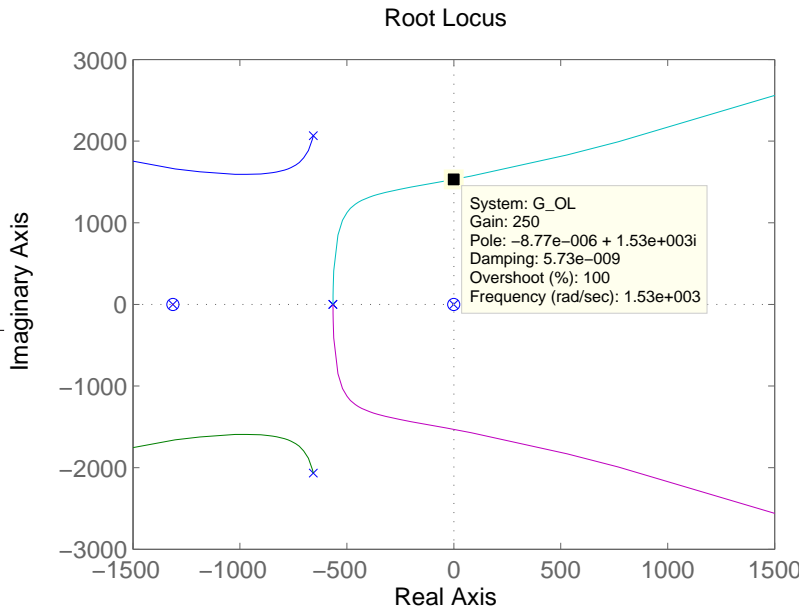


Figure 7.5: The Root-locus plot of $G_{TOL}(s)$, showing the point of where the critical gain and critical period is found.

As seen, the critical gain is found to be $K_{cr} = 250$, while the critical period is $P_{cr} = \frac{2\pi}{\omega_{cr}} = 0.0041s$. For a PI-controller, Ziegler-Nichols tuning rules are stated as:

Type of controller	K_P	T_I	T_D
PI	$0.45K_{cr}$	$\frac{1}{1.2}P_{cr}$	0

Whereby the values recommended by Ziegler-Nichols are:

$$K_P = 112.5 \qquad T_I = 0.0034 \qquad (7.10)$$

A step response of the system with and without the PI-controller implemented is shown in figure 7.6 and figure 7.7.

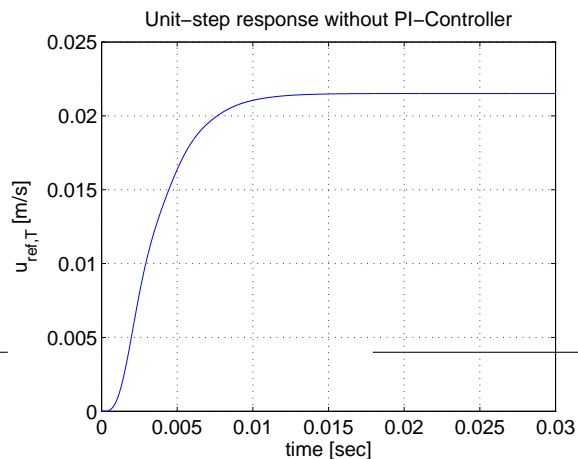


Figure 7.6: Unit-step response of the system with unit-feedback. The large steady error is very distinct.

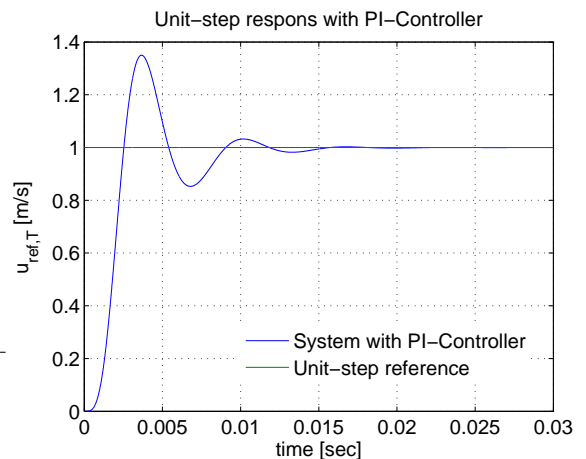


Figure 7.7: Unit-step response of the system with PI-controller using the parameters found from K_{cr} and P_{cr} .

As seen from figure 7.7, the PI-controller removes the steady-state error as expected. But, at the same time it introduces an maximum overshoot of 35% while the settling time is $t_{s,2\%} = 0.0110s$. The performance specifications do not specify any direct requirements to the allowable overshoot, but fine tuning the values in (7.10) may give an even better response, with less overshoot and a faster settling time. Manipulating the value of K_P within the range of $[50, 130]$, changes the unit-step response as illustrated by figure 7.8.

From figure 7.8 its clear that a higher value of K_P results in a faster response but with more overshoot, while the respons of lower value is slower with less overshoot. The best way to evaluate the responses in figure 7.8, is to compare the settling time of each, as the fastest respons doesn't necessarily lead to the shortest settling time. Analysing the settling time of each respons, leads to $t_{s,2\%} = 0.0099s$ for $K_p = 90$, as the shortest of all.

The controller can further be tuned by manipulating the value of T_i , which is illustrated in figure 7.9.

By manipulating the value of T_I , it is illustrated how the low-pass filter characteristics of the PI-controllers integral part influences the system. As seen in figure 7.9, higher values of T_I reduces overshoot but leads to a slower system as the high frequencies are more damped as the corner frequency has been decreased. Furthermore, a lower value of the integral time T_I leads to more overshoot as a lower value of T_I increases the integral gain which is given as $K_I = \frac{K_P}{T_I}$. The shortest settling time is found for $T_I = 0.0036$ which leads to a settling time $t_{s,2\%} = 0.0099s$ and a maximum overshoot $M_P = 19.94\%$ when $K_P = 90$.

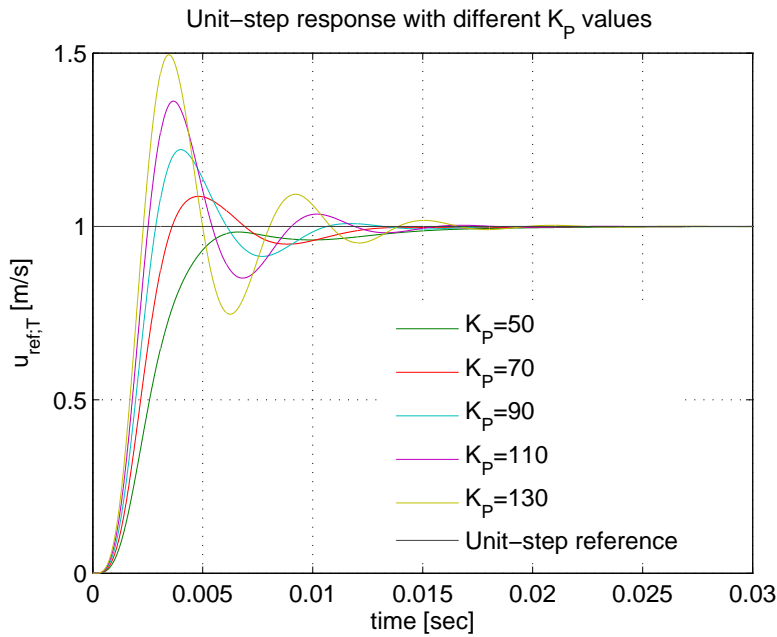


Figure 7.8: The step respons for different values of K_p in the range [50, 130].

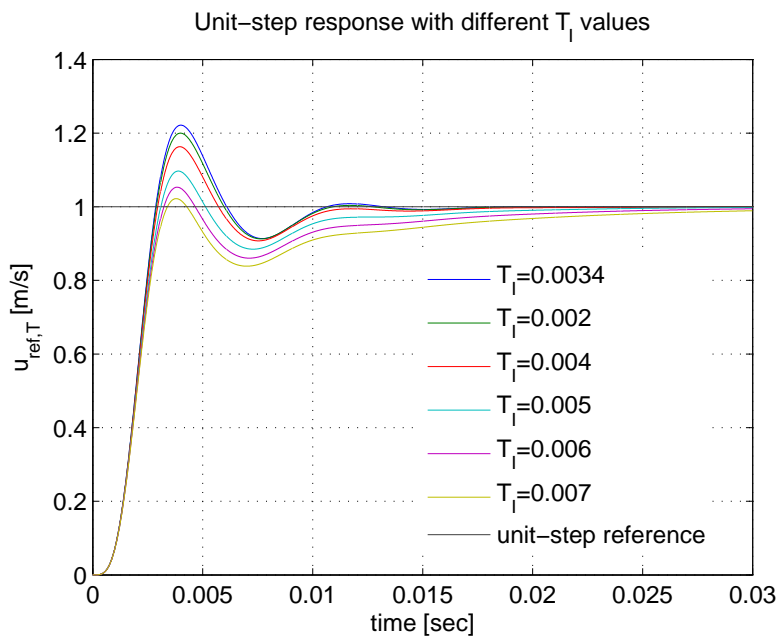


Figure 7.9: The step respons for different values of T_i in the range [0.002, 0.007].

Table 7.1 sums up the results of the fine tuning while figure 7.10 shows the step-response of the controlled system with modified values. The fine tuning of the Ziegler-Nichols values shows an improvement by decreasing the settling time $t_{s,2\%}$ and maximum overshoot M_P , but a longer rise time t_r indicates a slower respons.

Parameters	K_P	T_I	$t_{s,2\%}$	M_P	t_r
Ziegler-Nichols	112.5	0.0033s	0.0136s	39.05%	0.0013s
Modified	90	0.0036s	0.0099s	19.94%	0.0016s

Table 7.1: The fine tuning of the Ziegler-Nichols values shows an improvement in the settling time $t_{s,2\%}$ and maximum overshoot M_P while the longer rise time t_r indicates a slower response.

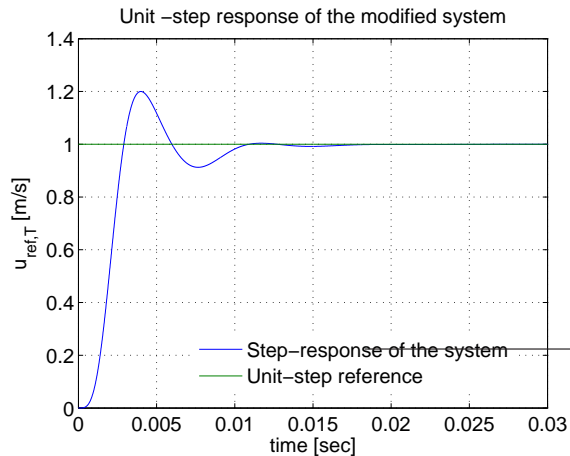


Figure 7.10: Unit-step response of the controlled system, with the modified PI-controller values.

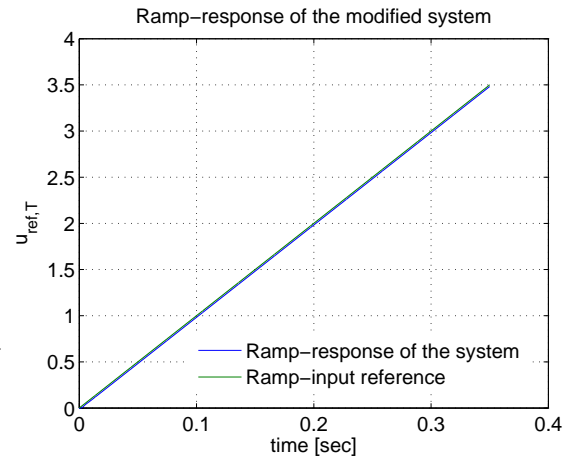


Figure 7.11: Ramp-response for a ramp-input of $u_{ref} = 10 \frac{m}{s^2} t$ to the system with modified controller values.

In figure 7.11 a ramp-response from the system is illustrated. It shows a steady-state error, which is expected as the uncontrolled system is of type 0, whereby the PI-controlled system will still exhibit a steady-state error towards ramp-inputs. Though, this control system has been designed according to a step-input, as this is the type of input the real system will receive in the preliminary tests.

This concludes the design of the control system for the test-subsystem. Analysis showed that a PI-controller could eliminate the steady state error when the system was given a step-input. In addition, the values of the PI-controller were chosen such that the system has a settling time which met the requirements, as it was shorter than the specified settling time. Besides shortening the settling time, the fine tuning of the values of the controller led to reducing the maximum overshoot to 19.94%.

Bandwidth of the test-subsystem

Before the analysis of the load-subsystem begins, the bandwidth of the modified test-subsystem will be determined from the frequency response of the closed-loop transfer function.

The bandwidth of the system is found at the frequency where the magnitude of the closed-loop system is $-3dB$. From figure 7.12 this frequency, and thereby the bandwidth of the test-subsystem, is found to be $\omega_{BT} = 217 Hz$.

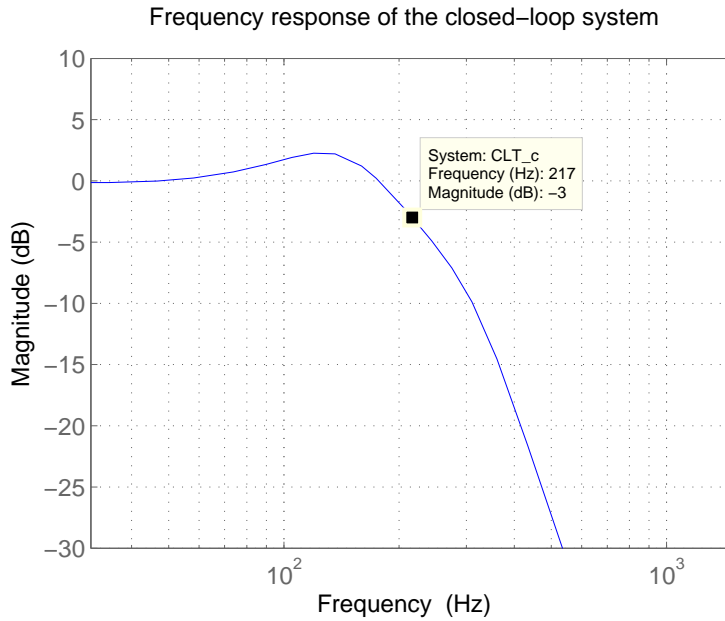


Figure 7.12: Frequency response of the magnitude of the closed-loop system. The bandwidth is found at $-3dB$.

7.3 Force-servo with velocity feedforward compensation

The approach to the control system analysis of the load-subsystem is similar to that of the test-subsystem. The analysis will be based on the block diagram in figure 6.1. From this block diagram, the open-loop transfer function of the load-subsystem will be determined, whereafter the control system analysis can begin.

7.3.1 Open-loop transfer function of the load-subsystem

The block diagram of the load-subsystem, from which the transfer function is derived, is shown in figure 7.13.

Closing the inner loops reduces the block diagram to figure 7.14, where $V(s)$ is the velocity from the test-subsystem which acts as a disturbance in the load-subsystem and $F_L(s)$ is the force-output.

$G_L(s)$ is the plant of the load-subsystem and it is given by (7.11):

$$G_L(s) = \frac{K_{Lr}(T_{Lp}s + 1) + K_{Lp}(T_{Lr}s + 1)}{(T_{Lr}s + 1)(T_{Lp}s + 1)} \quad (7.11)$$

Where,

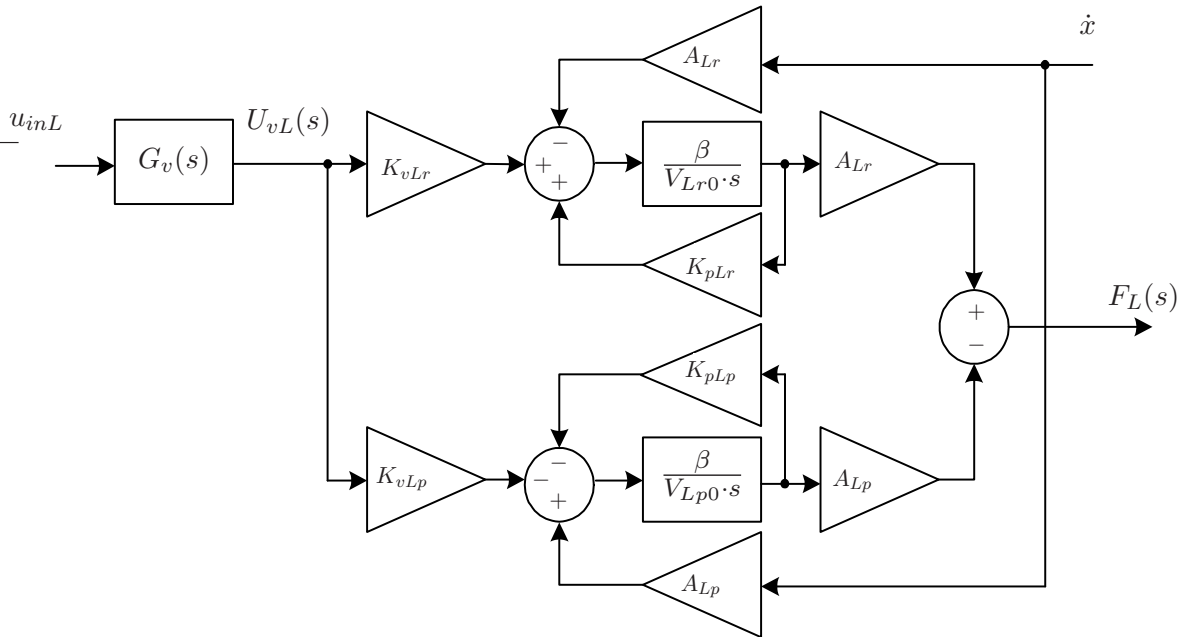


Figure 7.13: Block diagram of the disconnected load-subsystem.

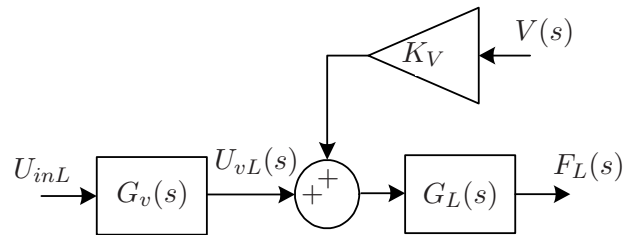


Figure 7.14: Reduced block diagram of the load-subsystem.

$$K_{Lr} = \frac{-K_{vLr}A_{Lr}}{K_{pLr}} \quad T_{Lr} = \frac{-V_{Lr0}}{\beta K_{pLr}} \quad (7.12)$$

$$K_{Lp} = \frac{K_{vLp}A_{Lp}}{K_{pLp}} \quad T_{Lp} = \frac{V_{Lp0}}{\beta K_{pLp}} \quad (7.13)$$

K_V is the disturbance gain and it is expressed as follows:

$$K_V = \frac{A_{Lp}K_{vLr} - A_{Lr}K_{vLp}}{K_{vLp}K_{vLr}} \quad (7.14)$$

The open-loop transfer function of the system is given by (7.15).

$$G_{Lol}(s) = G_v(s) \cdot G_L(s) \quad (7.15)$$

7 Control system analysis and design

As it was the case with the test-subsystem, this system is a type 0 system as well. For a unit-step input this system will exhibit a static position error of the unity-feedback system. The steady-state error of the unity-feedback system when given a step-input is therefore:

$$e_{ss} = \lim_{s \rightarrow 0} \frac{s}{1 + G_{Lol}(s)} \frac{1}{s} = \frac{1}{1 + K_{Lp} + K_{Lr}} \quad (7.16)$$

$$= 6.2 \cdot 10^{-7} \quad (7.17)$$

The steady-state error of this system is very small, which indicates a very large gain on the system and possible a unstable system. Once again, a PI-controller will be implemented in order to acheive a satisfying performance.

7.3.2 PI-Controller with force feedback

Implementing feedback of the measured cylinder force and a PI-Controller modifies the block diagram of the system, as illustrated in figure 7.15.

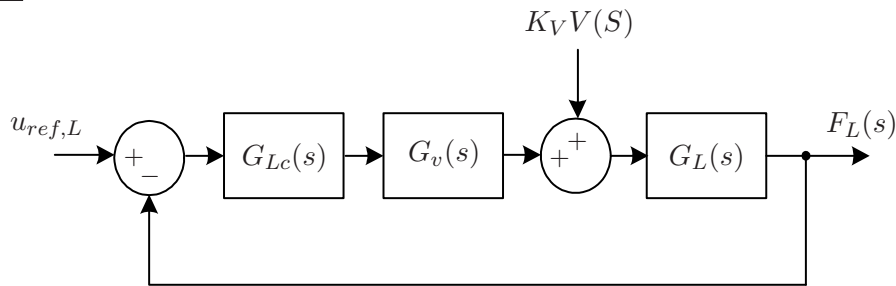


Figure 7.15: The load-subsystem with feedback control. $G_{Lc}(s)$ is the PI-controller.

7.3.3 Tuning of controller parameters

The PI-Controllers parameters, integral time T_I and proportional gain will be tuned using the same method as in 7.2.2. The critical gain K_{cr} and critical period P_{cr} is found from the root-locus plot of $G_{Lol}(s)$ in figure 7.16.

From figure 7.16 the critical gain is $K_{cr} = 0.00364$ while the critical period is $P_{cr} = \frac{2\pi}{562}s$. Applying Ziegler-Nichols second method tuning rules leads to the following proportional gain and integral time:

$$K_P = 0.00168 \quad T_I = 0.0093s \quad (7.18)$$

The step-respons of the load-subsystem with the PI-controller is illustrated in figure 7.17.

The step response in figure 7.17 for the load-subsystem with PI-control using values determined from Ziegler-Nichols shows a response which exhibits 94.3% overshoot and a settling time

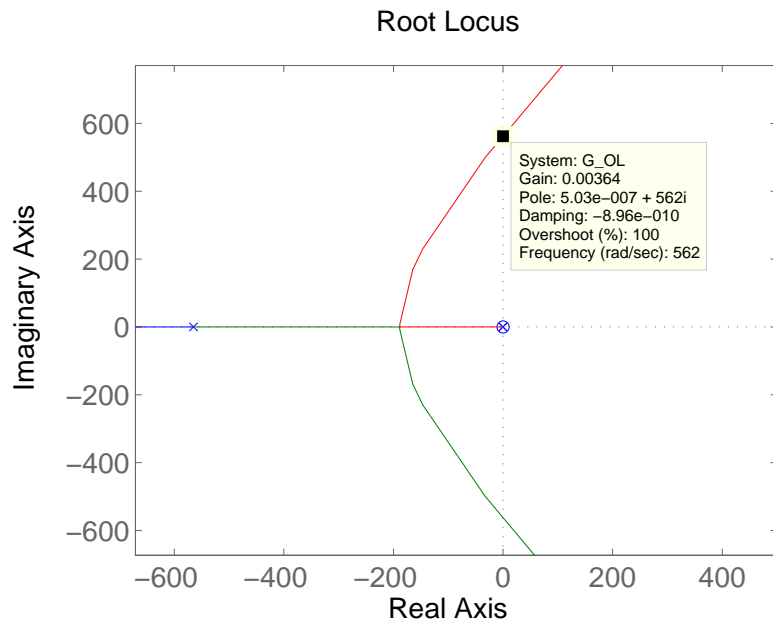


Figure 7.16: Root-locus plot of $G_{Lol}(s)$ showing the critical gain and period.

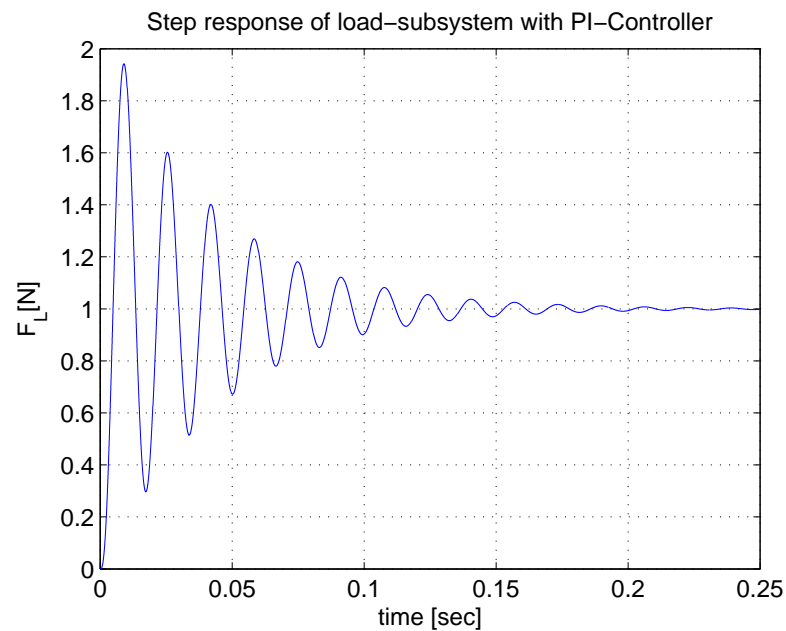


Figure 7.17: The step response of the load-subsystem with PI-Control implemented.

of $t_{s,2\%} = 0.166$. In addition the response shows decreasing oscillations. By fine tuning the controller parameters like in 7.3.2 a step response of the system with modified controller parameters are found, as seen in figure 7.18.

For the system in figure 7.18, $K_P = 0.0006$ and $T_I = 0.0161$. These values are found by iteration according to the settling time. The maximum overshoot is $M_P = 45.5\%$ and the settling time is

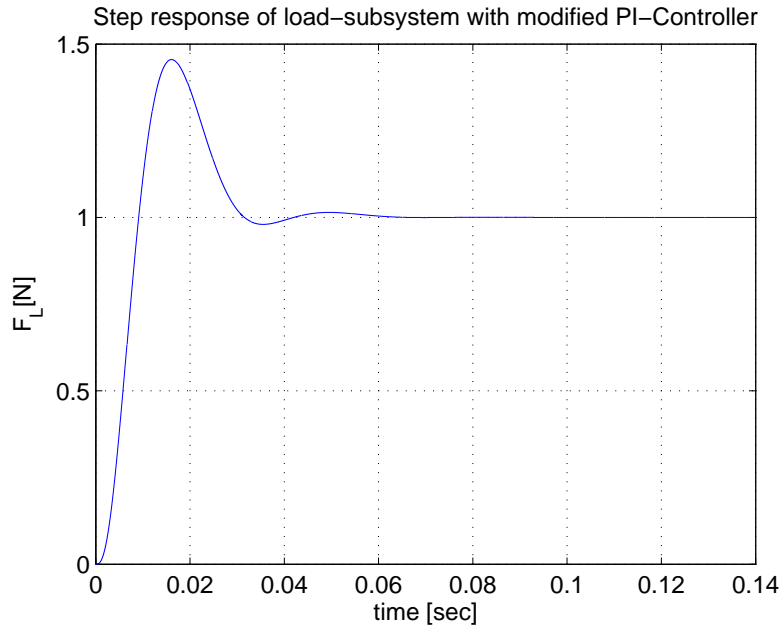


Figure 7.18: The step response of the load-subsystem using PI-Controller with modified values.

Parameters	K_P	T_I	$t_{s,2\%}$	M_P	t_r
Ziegler-Nichols	0.00168	0.0093s	0.1658s	94.3%	0.0029s
Modified	0.0006	0.0161s	0.0301s	45.5%	0.0058s

Table 7.2: The fine tuning improved the settling time $t_{s,2\%}$ and maximum overshoot M_P while the longer rise time t_r indicates a slower response.

$t_{s,2\%} = 0.0301s$, which is an improvement over the response given by the initial parameters found using Ziegler-Nichols. The values are compared in table 7.2.

To assist the PI-Controller, feedforward of the velocity will now be analysed.

7.3.4 Velocity feedforward compensation

Velocity feedforward is another control scheme which will be implemented in the force servo. Velocity feed forward helps to reduce the error in the system by estimating the disturbance and feeding it forward. Velocity feedforward implemented in the block diagram of the load-subsystem as shown in figure 7.19.

$G_{ff}(s)$ is found by analysing the signals in the block diagram. The input $m(s)$ to the plant, $G_L(s)$ of the load-subsystem consist of the actuating signal $a(s)$ and the disturbance:

$$m(s) = a(s) + K_V \dot{x} \tag{7.19}$$

The actuating signal $a(s)$ is given by:

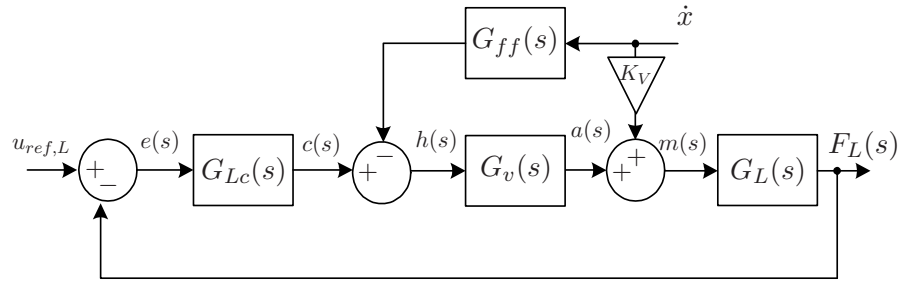


Figure 7.19: The load-subsystem with velocity feedforward implemented.

$$a(s) = G_v(s) \cdot h(s) \quad (7.20)$$

Where $h(s)$ is,

$$h(s) = c(s) - G_{ff}(s)\dot{x} \quad (7.21)$$

By combining (7.19), (7.20) and (7.21) the input to the plant can be written as:

$$m(s) = G_v(s)(C(s) - G_{ff}(s)\dot{x}) + K_v\dot{x} \quad (7.22)$$

From (7.22) it is seen that if $G_{ff}(s)$ is chosen as,

$$G_{ff}(s) = \frac{K_V}{G_v(s)} \quad (7.23)$$

leads to the disturbance being removed from the input signal to plant, as:

$$m(s) = G_v(s)c(s) \quad (7.24)$$

Ideally, this will be the case if the velocity \dot{x} and $G_{ff}(s)$ is known exactly.

Though, it isn't possible to directly implement $G_{ff}(s)$ on the form given in (7.23) [Rasmussen, 1996] as the system would have more zeros than poles. An approximate solution is to take the static DC-gain of the expression in (7.23) and neglect the dynamics. As the gain of the valve-dynamics is 1, the feedforward gain therefore becomes:

$$G_{ff} = K_v \quad (7.25)$$

The velocity feedforward will be implemented in the non-linear model and tested in section 7.5.

7.3.5 Bandwidth of the load-subsystem

The bandwidth of the modified load-subsystem is found from the frequency response of the closed-loop system.

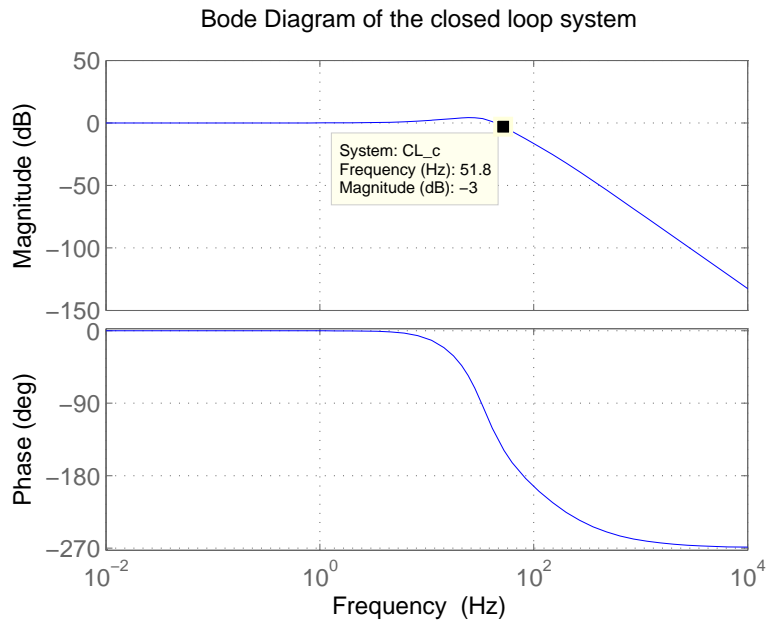


Figure 7.20: Bode plot of the PI-Controlled closed loop system.

As seen from figure 7.20, the bandwidth of the load-subsystem with the designed PI-controller is $\omega_{BL} = 51.8Hz$. The bandwidth of the test-subsystem was earlier found to be $217Hz$. In the beginning of the chapter it was listed as a requirement that load-subsystem should be 5-10 times faster than the test-subsystem which was expressed by their bandwidths. When designing the controller for the load-subsystem, it was attempted to make the bandwidth as high as possible while still having a reasonable step response with regards to maximum overshoot and settling time. The reason for the high bandwidth of the test-subsystem, is due to the small amount of mass in the system.

7.4 Stability analysis

In this section the stability of the closed-loop systems of the velocity servo and force servo will be checked. The relative stability will be investigated from the gain and phase margin of the two systems open-loop frequency responses. For a satisfying performance the gain margin (GM) must be greater than $6dB$ while the phase margin must be between 30° and 60° [Ogata, 2001].

7.4.1 Stability of test-subsystem

The open-loop frequency response of the load-subsystem is shown in figure 7.21. The margins are as required whereby the closed-loop system is stable.

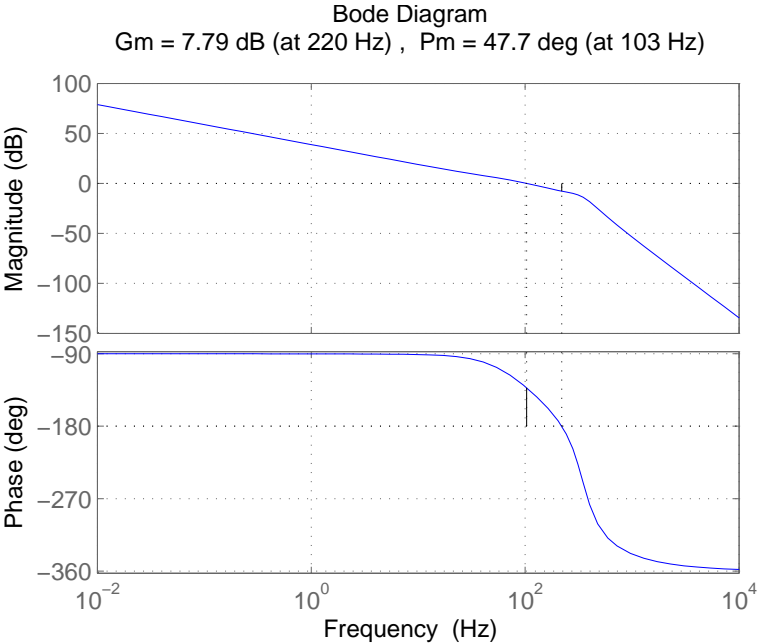


Figure 7.21: Bode plot of the open-loop test-subsystem.

7.4.2 Stability of load-subsystem

The open-loop frequency response of the load-subsystem is shown in figure 7.22.

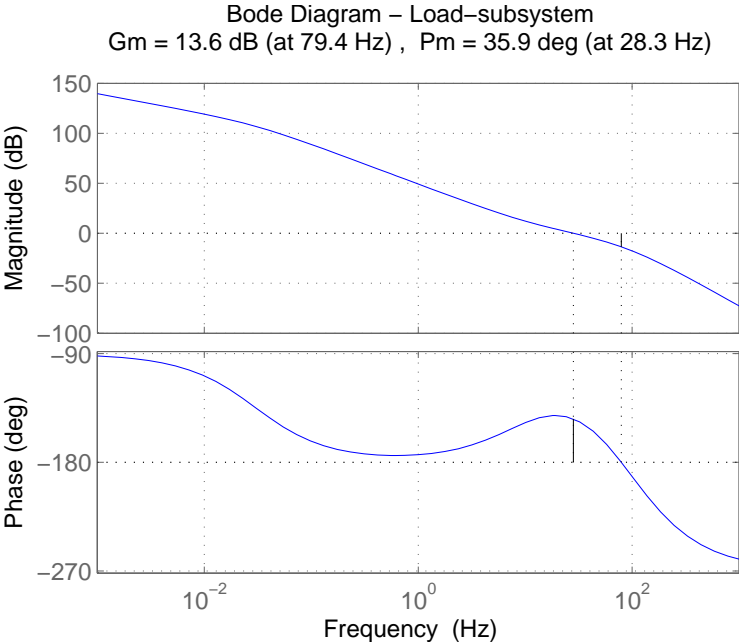


Figure 7.22: Bode plot of the open-loop load-subsystem.

As seen the margins meet the stability requirements, whereby the closed-loop system is stable.

7.5 Test of the controllers in the non-linear model

This section will present the results of implementing the designed controllers in the non-linear model. The controllers will be tested with regards to the requirements stated in the beginning of this chapter.

The PI-controller of the test-subsystem is tested by subjecting the system for a step reference. The load-system is given a constant reference which it has to follow in order to keep the load on the test-cylinder konstant. The PI-controllers will be tested for a high and low reference value. The maximum velocity of the test-cylinder is $0.3m/s$ while the low velocity is chosen to be $0.01m/s$. The maximum rated load of the load-cylinder is $25kN$ while a load of $10kN$ is chosen as the low value.

7.5.1 Velocity servo

In figure 7.23 and figure 7.24 the system is given a step input reference of $0.3m/s$ for a load of $10N$ and $25kN$. The response with the small load is characterised by a settling time $t_{s,2\%} = 0.02s$, which is faster than required. Furthermore, as required, the response shows no sign of a steady-state error. For the load of $25kN$ the system shows signs of saturation as there is a significant steady-state error of $0.0098m/s$. The PI-Controller should remove the steady-state error, but if the system saturates this will not happen.

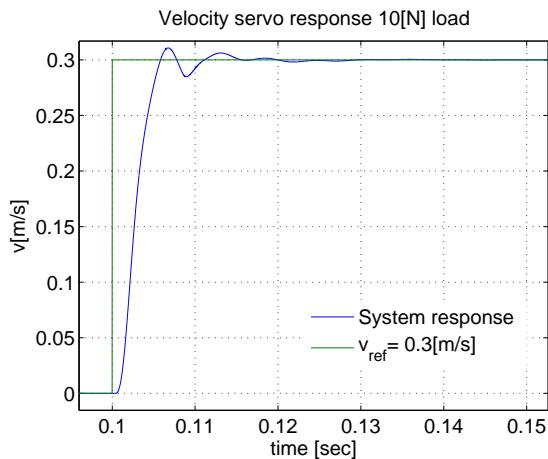


Figure 7.23: Reference step of $0.3m/s$ and a load $F_L = 10N$.

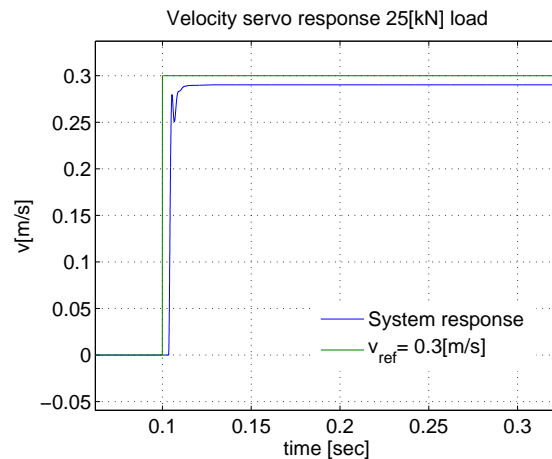


Figure 7.24: Reference step of $0.3m/s$ and a load $F_L = 25kN$.

The PI-Controller must be able to give good performance at both high and low velocities. For a step reference of $0.01m/s$ the response of the system is shown in figure 7.25 and figure 7.26 for a load of $10N$ and $25kN$ respectively. From both responses the settling time is $t_{s,2\%} = 0.06s$ and there is no steady state error. Furthermore, it is seen that the system exhibits a much greater overshoot when the load is great, but the settling time remains the same which is most important.

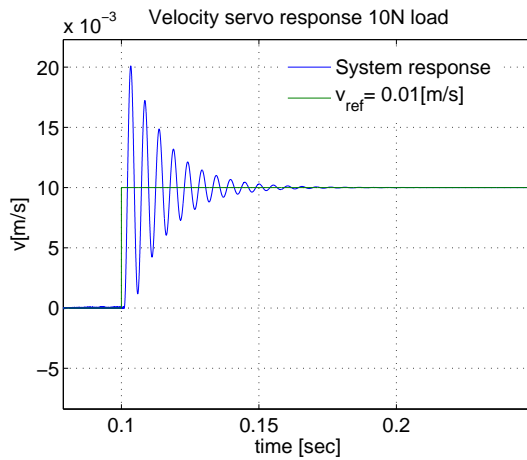


Figure 7.25: Reference step of 0.01m/s and a load $F_L = 10\text{N}$.

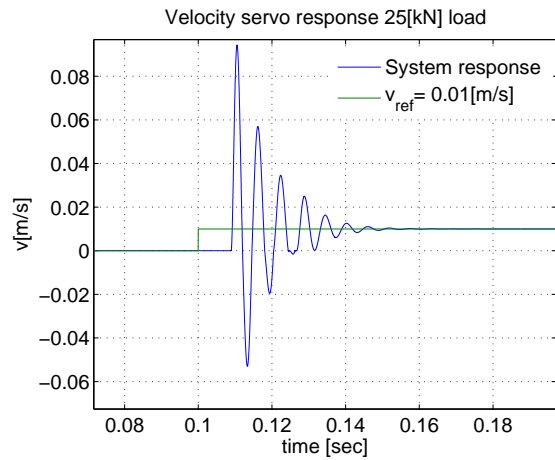


Figure 7.26: Reference step of 0.01m/s and a load $F_L = 25\text{kN}$.

7.5.2 Force servo

The performance of the force servo is tested with and without velocity feedforward. First, the servo is tested without the feedforward for a velocity step to the test-subsystem at 0.1s . In figure 7.27 and figure 7.28 the load-subsystems response is shown for a step of -10[N] at a velocity of 0.01[m/s] and 0.3[m/s] respectively. The response in figure 7.27 shows a settling time of $t_{s,2\%} = 0.097\text{s}$ and no steady state error. The response in figure 7.28 shows a settling time of $t_{s,2\%} = 0.212\text{s}$ and a slowly decreasing error of less than 2%. In addition, it is clear that the force servo has difficulties keeping up with the velocity servo especially at greater speeds.

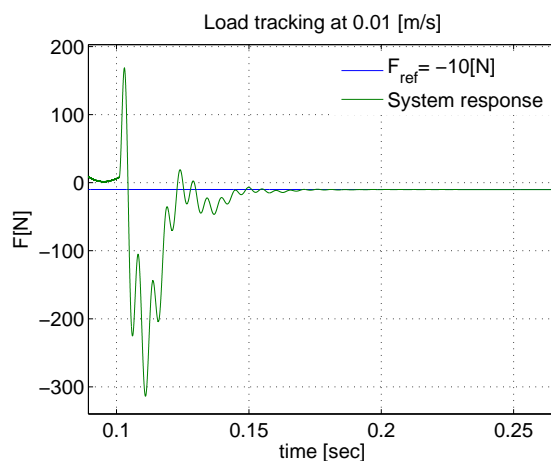


Figure 7.27: Reference step of -10N .

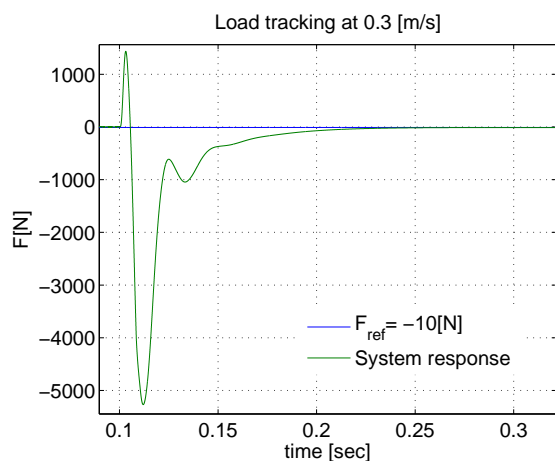


Figure 7.28: Reference step of -10N .

For a tracking reference of -25[kN] the load-subsystem gives the responses shown in figure 7.29 and figure 7.30 for velocities of 0.01[m/s] and 0.3[m/s] respectively. In figure 7.29 the response shows a settling time of $t_{s,2\%} = 0.02\text{s}$ and a steady-state error of 100[N] . In figure 7.30 the steady-state error is very large at 2100[N] whereby the settling time can't be properly defined.

7 Control system analysis and design

The steady-state errors for when the load is great indicates that there is saturation in the system, or else the PI-Controller would remove the errors with time.

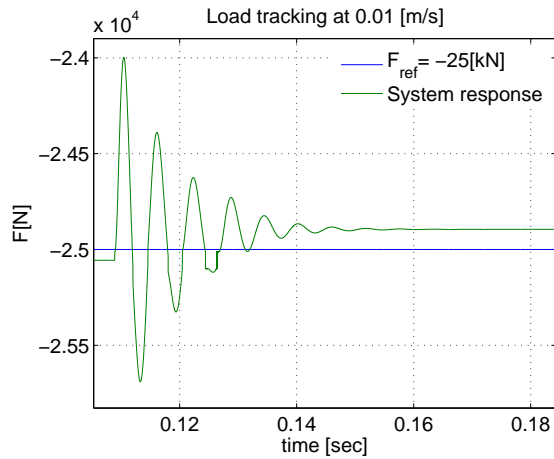


Figure 7.29: Reference step of -25 kN.

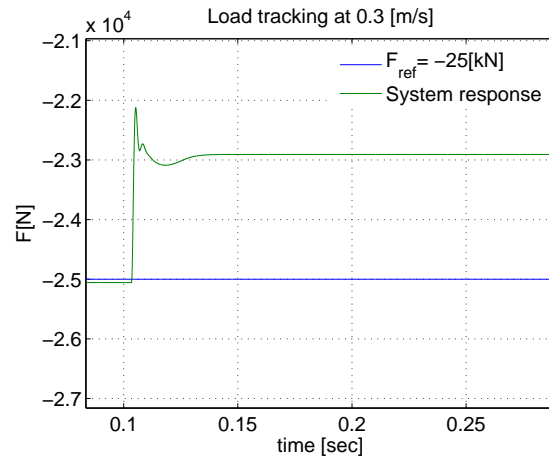


Figure 7.30: Reference step of -25 kN.

7.5.3 Velocity feedforward

Finally, the effect of the velocity feedforward (vff) will be shown by comparing it to the responses without the feedforward implemented. Responses of the system for high and low values of velocity and load, is shown in figure 7.31-7.34. As seen, implementing the velocity feedforward improves the system ability to track the reference more or less. The best improvements are found at low speed and load, where the system is far its saturation limits.

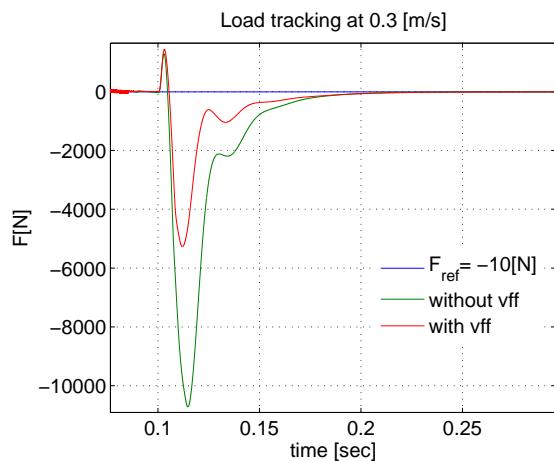


Figure 7.31: Reference step of -10 [N].

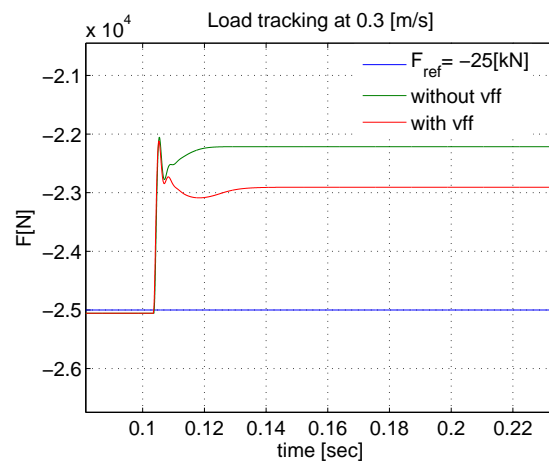


Figure 7.32: Reference step of -25 [kN].

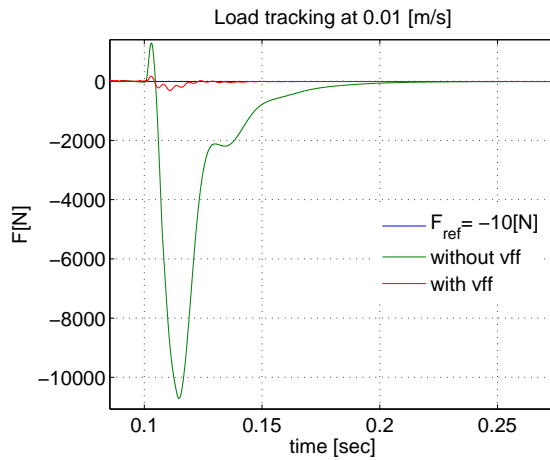


Figure 7.33: Reference step of $-10[N]$.

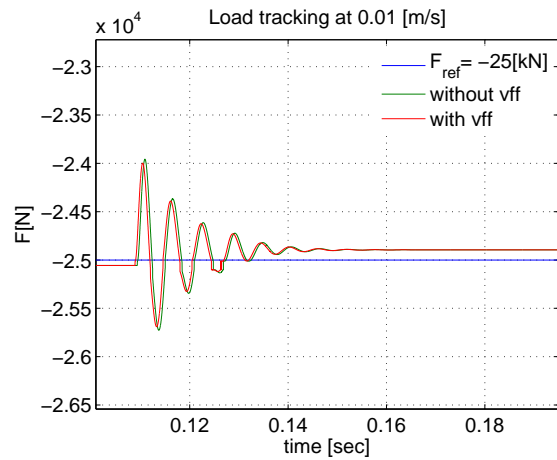


Figure 7.34: Reference step of $-25kN$.

7.5.4 Summary and suggestions

By analysing the linear model it was possible to design a control system for test and load-subsystem. Before the design proceeded, requirements to the performance of the control systems were specified. As the preliminary friction test will be carried out for constant velocities and loads, it was chosen to make the settling time and steady state errors the primary design parameters. A control strategy was made, which stated that PI-Control was to be implemented in both subsystems. In addition, a velocity feedforward compensation should be designed to help reduce the velocity disturbance in the load-subsystem. The controllers were designed and implemented in the non-linear model in order to test the design. The tests were carried out in both ends of the performance spectrum as both great and small loads and velocities were tested. The velocity servo of the test-subsystem showed satisfying performance for all cases except high velocity and load, where the system meets its saturation limits. Already before implementation of the force servo, this was not meeting the requirements. Even though the PI-controller had been tuned as well as possible by optimisation of the parameters, it was not possible to make the force servo 5-10 times faster than the velocity servo. This showed in the tests, as the force servo was too slow compared to tracking the changes of the test-subsystem. This meant that the required forces were not achieved or achieved at too slow a rate, which can be seen in the response plots. On the bright side, the implementation of velocity feedforward in the force servo improved the performance, where the biggest improvements were found at low velocities and loads. As is, the performance of the load-subsystem is not satisfying whereby the system must be further analysed and a different control system designed. Propositions for improving the performance of the load-subsystem are to use Lead-control for improving the bandwidth, using a bigger cylinder with regards to piston area in the load-subsystem and develop the feedforward to include dynamics.

Conclusion

Friction and hydraulics were the main topics of this project. Both of the topics are closely related in mechanical engineering and it is well known that friction exists in almost any hydraulic application. Especially, the operation of hydraulic cylinders are prone to be subject to a great deal of friction, which harms the overall performance of the application.

As an introduction to the project, friction in general was reviewed. Among other things, the art of mathematically modelling friction was treated. This was done, as the use of control systems along with modelling of friction can enhance the performance of a friction inflicted system, if performed appropriately. This introductory analysis, led to defining the problems of the project.

It was decided to investigate the friction in hydraulic cylinders by performing friction tests. The result of the tests should lead to the parameters of a chosen friction model. In order to do this, an appropriate testing facility was necessary and therefore this had to be designed as preparation for running tests.

Based on the specified requirements, five conceptual ideas for a test setup was developed. The concepts were compared and #3 *Load-by-Cylinder* was chosen to be carried on to the design phase. This concept utilised the idea of matching two hydraulic cylinders against each other, where one would be the test-cylinder while the other would be designated as the load-cylinder. The primary advantages of this concept was the variable load which could be generated by the load cylinder. This property was assessed to lead to the most flexible test setup.

Realising this concept, required the design of a hydraulic servo system and an experimental setup for measuring the states of the system. Furthermore, a load bearing structure consisting of a mounting frame had to be designed. The primary objective of the mounting frame was to establish a secure fixation of the cylinders used for testing. Especially the fixation of the cylinders required many considerations, as the use of a wide variety of cylinders was required of the structure. After analysing mounting types of cylinders, and dimensional requirements a design was proposed. In order for this design to be constructed, its validity as a load bearing structure had to be analysed. A structural analysis was carried out, and it verified that the structure could withstand the acting loads. The design was thereafter completed in detail and finalised in drawings, whereafter it was sent to be constructed in the work shop.

For the concept of a *load-by-Cylinder* to be realised it would be necessary to implement a control system. The objective of the control system was to ensure the specified velocity and load is maintained during testing. In order to design the control system, it was necessary to mathematically model the system. A non-linear dynamical model based on fluid-mechanical considerations was derived for the system. In order to verify the validity of the model, simulations would have to be compared with measurements performed on the real system. Unfortunately, the construction of the mounting frame was delayed, whereby it was not completed before the deadline of the project. This meant the model could not be validated with empirical measurements. Instead, the behaviour of the model was assessed and it was found to be realistic.

From there on, the model was linearised in order to establish a linear model. The linear model was used to analyse the system with the purpose of designing the beforementioned control system. The

8 Conclusion

control strategy was to create a velocity servo based on a PI-controller with velocity feedback. Furthermore, a force servo would be designed for controlling the load. The force servo would utilise a PI-controller like the velocity servo, and a velocity feedforward compensation in order to reduce the velocity disturbances coming from the velocity servo. This strategy led to the overall system being split up in two subsystems designated load and test. The two subsystems would initially be connected, but in order to design the controllers, a disconnection would be carried out. This disconnection meant, that the load-subsystem would have a velocity disturbance while the test-subsystem would experience a force disturbance. By doing this, a PI-controller for each subsystem was developed according to the requirements. The requirements were based on the tasks of the system. It was decided that the preliminary friction tests should be carried out with constant velocities along the stroke of the test-cylinder while the load-cylinder should maintain a constant load. For the specific cylinders this led to a maximum settling time of $t_{s,2\%} = 0.066[s]$ so the maximum velocity could be reached within a distance less than 20% of the stroke. In addition, no steady-state error was allowed. Furthermore, it was required of the force servo to 5-10 times faster than the velocity servo. With these requirements in mind, initial PI-controller parameters were found by using Ziegler-Nichols tuning rules. The initial parameters were fine tuned and the final values of the PI-controllers along with the bandwidth of each system were:

Subsystem	Proportional gain	Integral time	Bandwidth
Test	90	0.0036[s]	217[Hz]
Load	0.0006	0.0161[s]	51.8[Hz]

As seen, it was not possible with the use of the mentioned control to meet the bandwidth requirement. The remaining requirements were met in the linear analysis and in order to test the controllers, implementation in the non-linear model was carried out. Testing the controllers in both ends of the performance spectrum showed that the velocity servo had a satisfying performance while the force servo was less satisfying. The results showed that the force servo was too slow for the system to track the force reference precise enough when the velocity was changing. The implementation of velocity feedforward in the load-subsystem improved the the performance, but not enough for it to be satisfying. The force servo needs redesign for the requirements to be met and suggestions with regards to improving the performance were given.

Bibliography

- V.N. Aderikha, V.A. Shapovalov, Yu.M. Pleskachevskii, V.V. Zagorskii, A.F. Verbitskii, and S.M. Pilipenko. Evaluation of efficiency of hydraulic cylinder seals by results of comparative bench tests. *Journal of Friction and Wear*, 23(4):p. 1–5, 2002.
- Brian Armstrong-Hélouvry. *Control of Machines With Friction*. Kluwer Academic Publishers, 1. edition, 1991. ISBN: 0-7923-9133-0.
- Brian Armstrong-Hélouvry, Pierre Dupont, and Carlos Canudas de Wit. A survey of models, analysis tools and compensation methods for the control of machines with friction. *Automatica*, 30(7):p. 1083–1138, 1994.
- Werner Bernzen. *Zur Regelung elastischer Roboter mit Hydrostatischen Antrieben*. VDI Verlag GmbH, 1999. Fortschritt-Berichte VDI Reihe 8 Nr. 788. ISBN: 3-18-378808-x.
- L.C. Bo and D. Pavelescu. The friction-speed relation and its influence on the critical velocity of the stick-slip motion. *Wear*, 82(3):p. 277–289, 1982.
- Adrian Bonchis, Peter I. Corke, and David C. Rye. A pressure-based, velocity independent, friction model for asymmetric hydraulic cylinders. *1999 IEEE International Conference on Robotics and Automation*, pages p. 1746–1751, 1999.
- C. Canudas de Wit, H. Olsson, K.J. Åström, and P. Lischinsky. A new model for control of systems with friction. *IEEE TRANSACTIONS ON AUTOMATIC CONTROL*, 40(3):p. 419–425, 1995.
- DS. *DS412 - Norm for stålkonstruktioner*. Dansk Standard, 3. edition, 1998.
- Pierre E. Dupont. The effect of friction on the forward dynamics problem. *The International Journal of Robotics Research*, 12(3):p. 164–179, 1993.
- James M. Gere. *Mechanics of Materials*. Nelson Thornes, 5. edition, 2002. ISBN: 0-7487-6675-8.
- D.P. Hess and A. Soom. Friction a a lubricated line contact operating at oscillating sliding velocities. *Journal of Tribology*, 112:p. 147–152, 1990.
- Mohieddine Jelali and Andreas Kroll. *Hydraulic Servo-systems - Modelling, Identification and Control*. Springer, 1. edition, 2003. ISBN: 1-85233-692-7.
- Jill E. Krutz, David F. Thompson, Gary W. Krutz, and Randall J. Allemang. Design of a hydraulic actuator test stand for non-linear analysis of hydraulic actuator systems. *Automation Technology for Off-Road Equipment, Proceedings of the July 26-27, 2002 Conference*, pages p. 169–183, 2002.

BIBLIOGRAPHY

- N. Meikandan, R. Raman, and M. Singaperumal. Experimental study of friction in hydraulic actuators with sealed pistons. *Wear*, 176:p. 131–135, 1994.
- MOOG-Controls. *D633 and D634 Series Direct Drive Servo-Proportional Control Valves with integrated 24 V Electronics ISO 4401 Size 03 and 05*. Data Sheet.
- Dirk Nissing. *Identifikation, Regelung und Beobachterausslegung für Elastische Grosshandhabungs-systeme*. VDI Verlag GmbH, 2002. Fortschritt-Berichte VDI Reihe 8 Nr. 939. ISBN: 3-18-393908-8.
- R. L. Norton. *Machine Design, An Integrated Approach*. Pearson Prentice Hall, 3. edition, 2006. ISBN: 0-13-148190-8.
- K. Ogata. *Modern Control Engineering*. Prentice Hall, 4. edition, 2001. ISBN: 0-13-043245-8.
- H. Olsson, K.J. Åström, C. Canudas de Wit, M. Gäfvert, and P. Lischinsky. Friction models and friction compensation. 1997.
- Devi Putra. *Control of Limit Cycling in Frictional Mechanical Systems*. PhD thesis, Technische Universiteit Eindhoven, 2004. ISBN: 90-386-2636-3.
- Peter Windfeld Rasmussen. *Hydraulik ståbi*. Teknisk forlag A/S, 1. edition, 1996. ISBN-13: 87-571-1325-4.
- Eskil Sørensen. Hydraulikcylinder klarer 160 millioner slag. *Ingeniøren*, june 2008. <http://ing.dk/artikel/88723-hydraulikcylinder-klarere-160-millioner-slag?highlight=vindm%F8lle+hydraulik>.
- Pi-Cheng Tung and Ruh-Hua Wu. Studies of stick-slip friction, presliding displacement, and hunting. *Journal of Dynamic Systems, Measurement, and Control*, 124:p. 111–117, 2002.
- A. Tustin. The effects of backlash and of speed-dependent friction on the stability of closed-cycle control systems. *IEEE Journal*, 94(2A):p. 143–151, 1947.
- Hideki Yanada and Yuta Sekikawa. Modeling of dynamic behaviors of friction. *Mechatronics*, 18:p. 330–339, 2008.

Load analysis

A

The objective of the load-analysis is to determine the forces acting on the elements of the frame. In figure A.1 it is shown how the forces, F_L , from the hydraulic cylinder are acting on the frame.

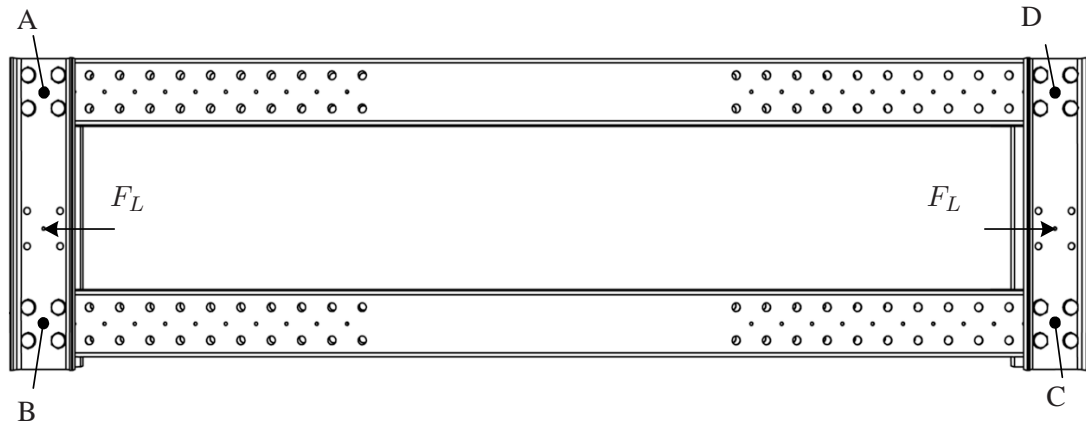


Figure A.1: The frame with the applied cylinder forces.

As the frame is symmetric and equally loaded the same forces and moments will occur in point A and D which is also true for point B and C. This simplifies the analysis as it is only necessary to determine the reaction forces and moments of point A and B. Furthermore, this means the vertical beams are loaded similar whereby their results are equal. In addition, calculations for the vertical beam will show that the lower beam, which is identical to the upper beam, is loaded considerably more whereby analysis will only be carried out for the lower beam. The gravity contribution will be neglected as this is small compared to the forces applied by the hydraulic system.

A.1 Vertical beam

The vertical beam is modelled as a statically indeterminate, as shown in figure A.2.

From [Gere, 2002] the reaction forces and moments are given as in (A.2) where $L_1 = a + b$.

$$M_A = \frac{Pab^2}{L_1^2} \qquad R_A = \frac{Pb^2(L + 2a)}{L_1^3} \qquad (\text{A.1})$$

$$M_B = \frac{Pa^2b}{L_1^2} \qquad R_B = \frac{Pa^2(L + 2b)}{L_1^3} \qquad (\text{A.2})$$

As it is assumed that the total load of $34[kN]$ from the cylinder is equally shared between the two vertical beams in each end then: $P = 17000[N]$, $a = 0.33[m]$ and $b = 0.23[m]$. These values leads to:

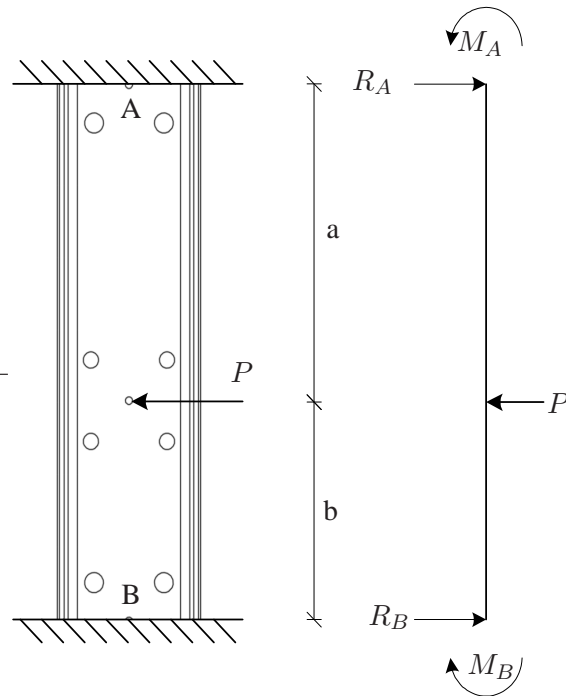


Figure A.2: Model and free-body diagram of the vertical beam.

$$M_A = 950Nm \qquad R_A = 6250N \qquad (A.3)$$

$$M_B = 1360Nm \qquad R_B = 10750N \qquad (A.4)$$

The shear force and bending moment can be found from the free-body diagram in figure A.2 and the reaction moments and forces. If y is the distance from point B to a another point along the beam, then the shear force($V(y)$) and bending moment ($M(y)$) along the beam is given as:

For $0 < y < b$:

$$V(y) = R_B \qquad (A.5)$$

$$M(y) = R_B y - M_B \qquad (A.6)$$

For $0 < y < L$:

$$V(y) = R_B - P \qquad (A.7)$$

$$M(y) = R_B y - P y - M_B + P b \qquad (A.8)$$

The plots of the shear force and bending moment in the vertical beam are illustrated in figure A.3 and figure A.4.

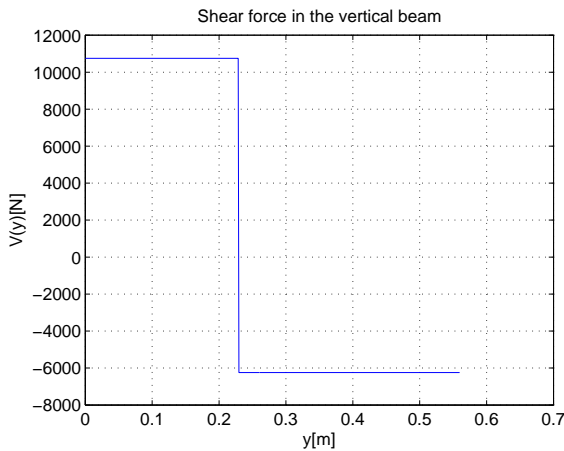


Figure A.3: Shear force in the vertical beam.

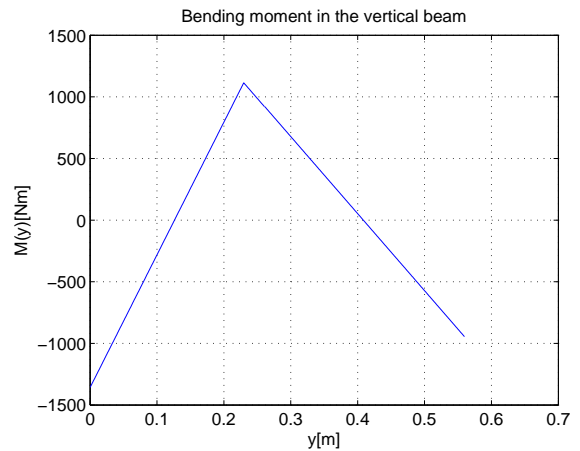


Figure A.4: Bending moment in the vertical beam.

As the bending moment and shear force have been determined the vertical beam is ready to be analysed with regards to stresses.

A.2 Lower beam

The lower beam is statically indeterminate as well, and the reactions are found easily as they are given by the reactions of the vertical beam. The free-body diagram of the lower beam is shown in figure A.5.

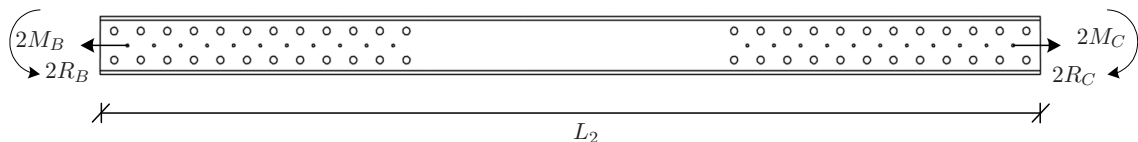


Figure A.5: The free-body diagram of the lower beam. The reactions are double as there is a contribution from the vertical beam on each side.

As shown on figure A.5 the reactions are double as there is a contribution from the vertical on each side of the lower beam.

As mentioned earlier the reactions in point A are equal in size but opposite those in point D. The same is the case for point B and C. The reaction of the lower beam are therefore given by:

$$R_B = R_C = 10750N \tag{A.9}$$

$$M_B = M_C = 1360Nm \tag{A.10}$$

As there are no external forces acting on this element, the shear force is zero, while the normal force and bending moment are given directly by the reactions as:

A Load analysis

$$N = 2R_B \quad (\text{A.11})$$

$$M = -2M_B \quad (\text{A.12})$$

As the forces and moments have been determined, it is possible to calculate the stresses in the beam.

Hydraulic eigenfrequency of a differential cylinder

B

This appendix contains the derivation of the hydraulic eigenfrequency of a differential cylinder.

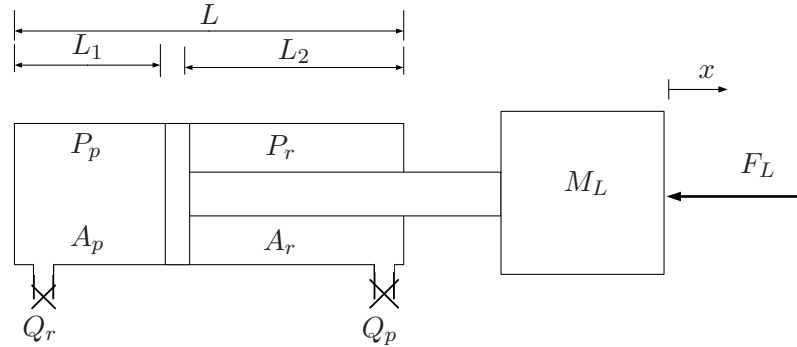


Figure B.1: Sketch for deriving the expression for the eigenfrequency of a hydraulic differential cylinder.

$$M_L \ddot{x} = P_p A_p - P_r A_r - F_L \quad (\text{B.1})$$

$$V_r \hat{=} V_{r0} + (L - x) A_r \quad (\text{B.2})$$

$$V_p \hat{=} V_{p0} + A_p x \quad (\text{B.3})$$

$$(\text{B.4})$$

$$K \hat{=} \beta \left(\frac{A_r^2}{V_r} + \frac{A_p^2}{V_p} \right) \quad (\text{B.5})$$

$$\omega_n = \sqrt{\frac{K}{M_L}} \quad (\text{B.6})$$

$$Q_p = A_p \dot{x} - \frac{V_p}{\beta} \dot{P}_p = 0 \quad (\text{B.7})$$

$$Q_r = A_r \dot{x} + \frac{V_r}{\beta} \dot{P}_r = 0 \quad (\text{B.8})$$

$$\dot{P}_p = \frac{A_p \dot{x} \beta}{V_p} \Rightarrow \quad (\text{B.9})$$

$$s P_p = \frac{A_p \beta}{V_p} s x \quad (\text{B.10})$$

B Hydraulic eigenfrequency of a differential cylinder

$$P_p = \frac{A_p \beta}{V_p} \cdot x(s) \quad (\text{B.11})$$

$$P_r = -\frac{A_r \beta}{V_r} \cdot x(s) \quad (\text{B.12})$$

$$M_L s^2 x(s) = \frac{A_p^2 \beta}{V_p} \cdot x(s) + \frac{A_r^2 \beta}{V_r} \cdot x(s) - F_L(s) \quad (\text{B.13})$$

$$F_L(s) = \left(\frac{A_p^2 \beta}{V_p} + \frac{A_r^2 \beta}{V_r} - M_L s^2 \right) x(s) \quad (\text{B.14})$$

$$\frac{x(s)}{F_L(s)} = \frac{1}{-M_L s^2 + \frac{A_p^2 \beta}{V_p} + \frac{A_r^2 \beta}{V_r}} \quad (\text{B.15})$$

$$= \frac{1}{-\left(\frac{A_p^2 \beta}{V_p} + \frac{A_r^2 \beta}{V_r}\right) \left(\frac{M_L}{\frac{A_p^2 \beta}{V_p} + \frac{A_r^2 \beta}{V_r}} s^2 + 1\right)} \quad (\text{B.16})$$

$$\frac{1}{\omega_n^2} = \frac{M_L}{\frac{A_p^2 \beta}{V_p} + \frac{A_r^2 \beta}{V_r}} \quad (\text{B.17})$$

$$\omega_n = \sqrt{\frac{\frac{A_p^2 \beta}{V_p} + \frac{A_r^2 \beta}{V_r}}{M_L}} \quad (\text{B.18})$$